Analysis of cyclic di-GMP signaling components in *Caulobacter crescentus* behavior and cell cycle control

Inauguraldissertation

zur

Erlangung der Würde eines Doktors der Philosophie

vorgelegt der

Philosophisch-Naturwissenschaftlichen Fakultät

der Universität Basel

von

Elvira Friedrich

aus Deutschland

Basel, 2013

Genehmigt von der Philosophisch-Naturwissenschaftlichen Fakultät auf Antrag von

- Prof. Dr. Urs Jenal
- Prof. Dr. Tilman Schirmer

Basel, den 16. Oktober 2012

Prof. Dr. Jörg Schibler

Dekan

Summary

Cell cycle progression and polar morphogenesis in *Caulobacter crescentus* are coordinated by the interplay of multiple proteins in time and space. One major regulatory factor is the second messenger cyclic di-GMP (c-di-GMP) therefore especially the activities of enzymes that are responsible for synthesis and breakdown of this small molecule are tightly regulated. The swarmer cell specific population in the early phase of the cell cycle contains low levels of c-di-GMP due to the action of the phosphodiesterase PdeA. During the course of cell cycle progression, PdeA is degraded and thereby the activity of the diguanylate cyclase (DGC) DgcB is released. At the same time a second DGC, PleD, is activated by a phosphorylation relay, to elevate c-di-GMP levels necessary for cell development. The two proteins DgcB and PleD are the main cyclases in *C. crescentus* contributing to the intracellular c-di-GMP pool. Cells lacking both DGCs have severe defects affecting cell morphology and cell cycle progression. However, a residual c-di-GMP concentration is still detectable in the *pleD dgcB* double mutant presumingly due to the activity of other DGCs of *C. crescentus*.

This work addressed the question, which additional GGDEF domain proteins reveal DGC activity and contribute to the c-di-GMP content in *C. crescentus* cells. This work presented here shows that two additional cyclases, BipB and CC0857, are involved in c-di-GMP signaling. Both enzymes belong to the group of so-called composite proteins harboring a GGDEF and EAL domain, encoding for opposing catalytic activities, respectively. Single deletions of either *bipB* or *CC0857* showed no phenotype. However, in combination with the deletion of *pleD* and *dgcB,* no c-di-GMP could be detected. The lack of c-di-GMP resulted in miss-localization of the effector protein PopA that is involved in the degradation of the replication inhibitor CtrA. Therefore, CtrA is stabilized in those cells leading to elongated cell morphology. These phenotypes resemble the phenotypes of a strain lacking all predicted DGCs (gutted strain, GS). To measure specifically low levels of c-di-GMP a strain was used lacking DGCs and in addition all PDEs (really gutted strain, rGS) to avoid immediate degradation in the GS. Introduction of either *bipB* or *CC0857* in the rGS reverted the strain to a wild-type phenotype, e.g. motility and popA localization, indicating a DGC phenotype *in vivo*. However, in the presence of different PDEs like in the GS neither *bipB* nor *CC0857* were able to revert the phenotype to wild-type suggesting weak DGC activity of both enzymes.

For BipB bifunctional enzyme activity could be demonstrated *in vitro* and *in vivo,* whereas the DGC and the PDE activities were present at the same time. The cyclase activity of BipB is substrate inhibited via c-di-GMP binding to the inhibitory site motif RxxD. Based on these finding we propose that BipB is a bifunctional protein contributing under the applied conditions with CC0857, PleD and DgcB to intracellular c-di-GMP levels in *C. crescentus*.

The c-di-GMP signaling circuit involves not only cyclases and phosphodiesterases, which produce c-di-GMP upon an environmental stimulus but also effector proteins that bind c-di-GMP and therefore transmit the signal into an intracellular response. Knowing different c-di-GMP binding proteins would allow understanding c-di-GMP output systems. Therefore, a biochemical screen was carried out using c-di-GMP linked to a capture compound to specifically isolate c-di-GMP binding proteins. Among the novel identified proteins a group clusters next to chemotaxis genes. One of the hits is CC3100, a single domain response regulator lacking the conserved phosphorylation site (aspartate) necessary for the function of a RR. Deletion of *CC3100* results in an increase in motility. To transmit the chemotactic signal CheY proteins interact directly with the flagellar apparatus. Therefore, the localization pattern of CC3100 in different flagellar mutants was determined showing polar localization dependent on the MS-ring forming protein FliF. This localization pattern is missing in c-di-GMP deficient cells. From these results, we concluded that CC3100 regulates motility in a c-di-GMP dependent manner.

Index

1 INTRODUCTION ..... - 1 -

1.1 INTRACELLULAR SIGNALING VIA NUCLEOTIDE BASED SECOND MESSENGERS ..... - 1 -
1.2 C-DI-GMP METABOLISM: GGDEF AND EAL DOMAIN PROTEINS ..... - 2 -
1.3 C-DI-GMP EFFECTOR PROTEINS ..... - 4 -
1.4 *CAULOBACTER CRESCENTUS* – A MODEL ORGANISM FOR C-DI-GMP SIGNALING ..... - 6 -
1.5 REGULATORY NETWORK CONTROLLING CELL CYCLE PROGRESSION AND POLE MORPHOGENESIS IN *C. CRESCENTUS* ..... - 9 -
1.6 DIMINISHED C-DI-GMP LEVELS IN *CAULOBACTER CRESCENTUS* ..... - 12 -
1.7 DIVERSE GGDEF-EAL DOMAIN COMPOSITIONS IN *CAULOBACTER CRESCENTUS*: GLOBAL *VS.* LOCAL POOL ..... - 13 -
1.8 COMPOSITE PROTEINS ..... - 15 -
1.9 THE DIFFERENT WAYS TO CONTROL BACTERIAL SWIMMING VELOCITY ..... - 18 -

2 AIM OF THE THESIS ..... - 22 -

3 RESULTS ..... - 23 -

3.1 CHARACTERIZATION OF BIFUNCTIONAL GGDEF AND EAL DOMAIN COMPOSITE PROTEINS IN *CAULOBACTER CRESCENTUS* - 23-

3.2 AN UNORTHODOX RESPONSE REGULATOR BINDS C-DI-GMP TO CONTROL MOTILITY IN *CAULOBACTER CRESCENTUS* ..... - 71 -
3.2.1 Supplementary material and methods ..... - 103 -

4 BIBLIOGRAPHY ..... - 118 -

5 CURRICULUM VITAE ..... - 127 -

6 ACKNOWLEDGMENTS ..... - 129 -

1 Introduction

1.1 Intracellular signaling via nucleotide based second messengers

Rapid transmission of signals and modulation of bacterial behavior is achieved by small molecules since they have the capacity to freely diffuse and rapidly bind to specific effectors. Many of those so called bacterial second messengers are versatile nucleotides which mediate appropriate cellular responses[1]. They differ in the nucleobase they use and in diverse cyclic forms. To nutrient poor environments, bacteria adapt by down-regulation of gene expression required for growth and division and up-regulate amino acid synthesis in order to promote survival until nutrient conditions improve[2]. For induction of this process known as the stringent response the linear effector molecule guanosine tetraphosphate, **ppGpp**, is produced[2–4].

Many second messengers originated from intramolecular nucleotide cyclisation like cyclic AMP (**cAMP**). In fact it was the first monocyclic nucleotide to be discovered in 1957 and functions as a second messenger in both pro- and eukaryotes[5]. In Bactria it is involved in the positive regulation of the lac operon[6], virulence[7], cell division and motility[8]. Another monocyclic representative is cyclic GMP (**cGMP)**. It was originally believed to have importance only in eukaryotic cells because in prokaryotes it was less abundant than cAMP. But merely 10 years ago it was proved that in *Synechocystis* PCC 6803 cGMP and cAMP levels are in the same order of magnitude and there cGMP controls adaptation of cells to UV-B stress[9,10]. In addition, in the α-proteobacterium *Rhodospirillum centenum* cGMP is involved in the regulation of cyst formation[11].

Its di-cyclic relative cyclic di-GMP (**c-di-GMP**) is present in the majority of all bacterial species[12,13]. This completely symmetric molecule was discovered in the late 80ies by the group of Benziman as a molecule controlling glucose polymerization into cellulose in *Glucon-*

acetobacter xylinus[14]. Since then this compound has remained obscure for almost 2 decades until its broad significance for bacterial growth and behavior was recognized. By defining the genes and enzymes involved in the synthesis and breakdown of c-di-GMP and by defining their cellular function[15], it turned out that c-di-GMP plays an important role in bacterial adaptation to changing environment[16,17]. More precisely, c-di-GMP controls bacterial community behavior and growth on surfaces by regulating the switch from planctonic to sessile lifestyles and therefore biofilm formation[18]. In pathogens, low levels of c-di-GMP lead to acute stage of virulence by expressing virulence factors and high levels lead to a persistent stage of virulence[19]. Recently, even in the mammalian protein STING (stimulator of interferon genes) a structure bound c-di-GMP molecule was found indicating that also eukaryotes sense the bacterial second messenger and therefore activate their immune response[20,21]. The di-cyclic analog **c-di-AMP** plays a crucial role in e.g. *Bacillus subtilis* during sporulation[22] and in host response during infection in *Listeria monocytogenes*[23].

1.2 c-di-GMP metabolism: GGDEF and EAL domain proteins

Synthesis and degradation of the ubiquitous second messenger c-di-GMP are regulated by diguanylate cyclases (DGCs) and phosphodiesterases (PDEs), respectively (Fig. 1). DGCs catalyze the synthesis of c-di-GMP and the corresponding enzymatic activity is encoded by the GGDEF sequence motif that is referred to as the active site (A-site)[24,25]. Many DGCs have an additional conserved amino acid motif RxxD that is located five amino acids upstream of the A-site. Binding of one molecule of c-di-GMP to this site results in product inhibition (called inhibitory site, I-site) and avoids excessive GTP consumption and c-di-GMP accumulation[25,26]. The GGDEF domain was first described in detail in the response regulator PleD that controls cell differentiation in the swarmer-to-stalked cell transition in *Caulobacter crescentus*[27]. PleD and all described DGCs form dimers for condensation of two identical GTP substrate molecules to create a two-fold symmetrical product. Structurally, they are related to the well-characterized class III adenylyl and guanylyl cyclases and type I DNA polymerases. Although they share a weak sequence identity, the structural conservation resembles the similarity of the chemical reactions catalyzed by this class of enzymes[28,29].

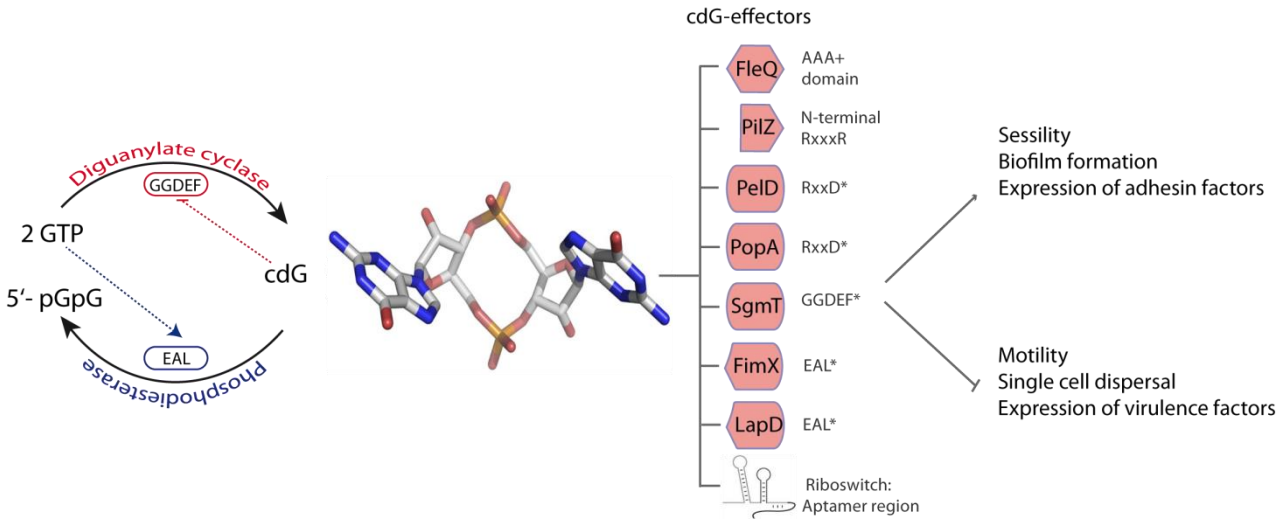

Figure 1: Components of c-di-GMP signaling pathways. Cellular c-di-GMP is produced from two GTP by diguanylate cyclases harboring a catalytic GGDEF domain (red) and degraded by phosphodiesterases carrying a catalytic EAL domain (blue) into linear 5'-pGpG. Dashed lines indicate substrate inhibition (red) and activation (blue) reactions. The different effector proteins (light red squares) are indicated with their c-di-GMP binding motifs. Proteins containing a degenerated sequence motif are marked with an asterisk. Cellular c-di-GMP bound to effector proteins transmit different input signals into physiological responses. Adapted from[13,30].

C-di-GMP is hydrolyzed by the enzymatic activity of PDEs into the linear degradation product 5'-phosphoguanylyl-(3'-5')-guanosine (pGpG)[26,31,32]. Subsequent hydrolysis of pGpG to GMP does take place in some cases but at much lower rate and therefore it is likely to be irrelevant *in vivo*[14]. The core domain of PDEs is the EAL signature motif, or more precise the EXL motif because mutation of glutamate (E) abolishes phosphodiesterase activity[26]. PDEs are highly specific for their substrate in the presence of Mg^{2+} or Mn^{2+} with a K_m in the sub-micromolar range, whereas Zn^{2+} and Ca^{2+} likely inhibit this process by replacing the Mg^{2+} or Mn^{2+} ion from the A-site[32]. Some PDEs are allosterically activated by GTP, actually the substrate of DGCs[26]. Like DGCs, PDEs also form dimers in their active state to embrace the c-di-GMP molecule for optimal nucleophilic attack on the 5'-phosporyl group. This was proven by different structures of the crystalized EAL domain proteins tdEAL from *Thiobacillus denitrificans* and YkuI from *Bacillus subtilis* revealing a dimer interface[33]. Dimerization is often induced by accessory N-terminal domains like the light sensitive BLUF (sensor of blue-light using FAD) domain from

BrlP1 in *Klebsiella pneumonia*[34] or by the PAS domain (Per-Arnt-Sim, named after the three proteins in which it occurs) of PdeA from *C. crescentus*[35].

Another class of c-di-GMP specific phosphodiesterases, even though less common, belongs to the HD-GYP family, named after the amino acid sequence of the active site[36]. These are metal dependent phosphohydrolases involved in c-di-GMP degradation. Although the EAL and HD-GYP domain catalyze the same reaction, both motifs are structurally unrelated. It remains a mystery why two different domains that are even found in the same organisms, albeit the HD-GYP domain is less abundant[12], have the same activity. One explanation may be derived from the recent structure of the HD-GYP domain from *Bdellovibrio bacteriovorus*[37]*.* There, a different mechanism of c-di-GMP hydrolysis was proposed implying the use of a binuclear iron center.

1.3 c-di-GMP effector proteins

C-di-GMP production is stimulated by different unknown environmental signals. To transmit this signals c-di-GMP interacts as a second messenger with different effectors like promoters[38], protein RNA in the form of riboswitches[39] and proteins to generate a specific readout that interferes with the cellular process including flagellar rotation[40], exopolysaccharide (EPS) biosynthesis[41] and excretion machineries[42]. As it turned out, c-di-GMP signaling includes a complicated and extensive network of effector molecules that directly bind c-di-GMP with a wide range of different affinities and thus initiate specific outputs (Fig. 1). The effector proteins are subdivided according their c-di-GMP binding-site. One large family of bacterial c-di-GMP effectors are PilZ domain proteins named after the PilZ protein in the opportunistic human pathogen *Pseudomonas aeruginosa* where it was first discovered[43,44]. PilZ proteins can be single domain proteins or are found together with the c-di-GMP metabolizing GGDEF, EAL or HD-GYP domains. C-di-GMP binding to the PilZ protein YcgR from *Escherechia coli* controls motility by interacting directly with the flagellar basal

body[40]. Also in *C. crescentus* the PilZ proteins DgrA and DgrB are involved in regulation of motility at elevated c-di-GMP levels[45].

Quite often c-di-GMP effectors contain an RxxD motif similar to the I-site in DGCs, while the overall sequence does not have further similarity to GGDEF domain of the active site. One archetype is PelD from *P. aeruginosa* that mediates c-di-GMP induced PEL polysaccharide biosynthesis[41]. A very prominent example for a regulatory protein that uses the I-site motif as an effector modul is PopA from *C. crescentus***.** PopA is an essential protein involved in cell cycle regulation. Upon binding of c-di-GMP PopA is sequestered to the pole and induces a whole cascade of interactions and localizations to finally result in degradation of the cell cycle regulator CtrA[46]. PopA was the first protein that directly linked cell cycle progression and pole morphogenesis (Fig. 3).

In addition to the RxxD motif, c-di-GMP also binds to PDE domains with degenerated EAL motifs. These domains have lost their original activity, but retained their ability to bind c-di-GMP. One such protein is FimX, a regulator for twitching motility and biofilm formation in *P. aeruginosa*[47]. This protein was initially described as a putative active phosphodiesterase because deletion of this gene abolished biofilm formation as predicted for PDEs[48]. But recent data clearly proved that this effect is not due to its PDE activity, in fact no PDE activity could be ever observed *in vitro*, but due to its role as a c-di-GMP effector[47]*.* Localization of FimX to a single pole in cells relies on intact GGDEF and EAL motifs, suggesting that both domains are important for molecular interactions. A similar binding motif is found in LapD, a protein involved in surface attachment of *P.fluorescens*[42,49,50]. LapD senses intracellular c-di-GMP levels in the cytoplasm and thereby controls biofilm formation by transmitting this information to the membrane-localized attachment machinery in the periplasm.

One substitute for a c-di-GMP effector, where the binding site could not be determined yet because it has no resemblance with the described motifs, is FleQ from *P. aeruginosa*. FleQ is a regulatory protein with homology to the NtrC group of bacterial transcription factors[51]. The specific feature is its bifunctional role due to different affinities for c-di-GMP. It is a

transcriptional regulator of flagellar gene expression[52] at low levels of c-di-GMP but at high levels of the second messenger it controls EPS production[53]. Binding of c-di-GMP to FleQ inhibits its association with the pel promoter and leads to de-repression of the pel operon and thus to biofilm formation.

These examples are only a selection of c-di-GMP effectors and in the future, this list will be surely prolonged by additional effectors, because the involvement of c-di-GMP signaling in bacteriais not fully exploited, yet.

1.4 *Caulobacter crescentus* – a model organism for c-di-GMP signaling

Caulobacter crescentus is a gram-negative, crescentoid-shaped α-proteobacterium that lives in freshwater environments, including streams and lakes[54]. Its hallmark, and one of the reasons why it is a model organism, is its asymmetric cell division (Fig. 2). In this developmental process *C. crescentus* produces two genetically identical, but morphologically and physiologically distinct progenies, the motile swarmer (SW) and the sessile stalked (ST) cell. The smaller SW cell is equipped with a flagellar motor, a chemotaxis apparatus and adhesive pili. During G1-to-S-phase the SW cell develops into a ST cell by shedding its flagellum, retracting pili and synthesizing a polar extrusion of the cytoplasm, called stalk. The end of the stalk contains the holdfast, an exopolysaccharide matrix that is a strong adhesion attaching to surfaces[55]. The strongest attachment to surfaces is reached when all three polar appendages, flagellum, pili and holdfast, are present at the same time during the motile-to-sessile-phase transition[56]. After formation of the ST cell, maturation of the predivisional cell begins during G2-phase including cell division and compartment engulfment bearing a new SW and ST cell. While the ST cell can immediately reinitiate a new round of cell division the SW has a replication block and remains in the G1-phase for a defined period before it differentiates into a ST cell and initiates DNA replication and cell division.

Another advantage *of C. crescentus* is its small genome size that can be easily manipulated for genetic and biochemical approaches. Since the cell cycle of *C. crescentus* is strictly regulated and chromosome duplication is coupled, cells contain only one chromosome. Due to capsule

formation in cells with high c-di-GMP levels, i.e. in ST and PD cells, these cells can be isolated from the newborn swarmer cells by density gradient centrifugation. This allows to follow a synchronized progression of *C. crescentus* cell cycle and to spot cell populations at any time point during cell cycle in regard to gene expression, subcellular protein localization and chromosome segregation[57]. The replication time in faster growing prokaryotes like *E. coli* exceeds the generation time leading to several chromosomes which makes it difficult to study single cell cycle regulated protein features or for example senescence[58,59,60].

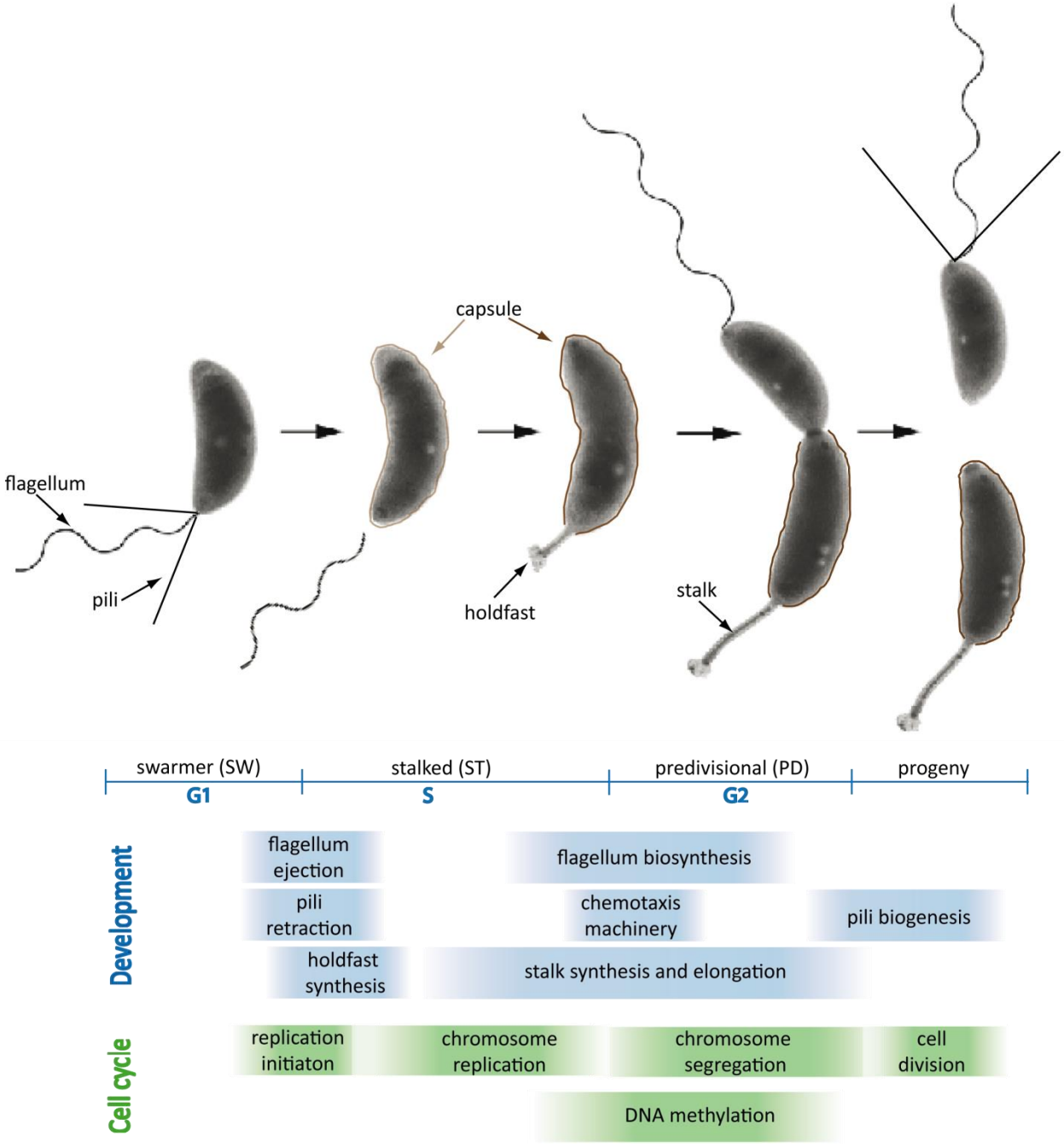

Figure 2: Asymmetric cell cycle progression and polar development of *C. crescentus*. Within one round of cell differentiation, the swarmer cell (G1-phase) retracts pili and loses flagellum to maturate into a surface attached predivisional cell (S- and G2-phase). Finally, cell division gives rise for a new swarmer cell and a stalked, capsulated progeny. Developmental processes are indicated in blue and cell cycle events in green. Adapted from[61] with the electron micrograph of *C. crescentus* cell cycle from the lab of Yves Brun.

1.5 Regulatory network controlling cell cycle progression and pole morphogenesis in *C. crescentus*

Pole development and cytokinesis require regulated fluctuations of c-di-GMP levels. The balance of low c-di-GMP levels in SW cells and high levels in ST cells is achieved by antagonistic actions of the phosphodiesterase PdeA and the cyclase DgcB[62]. PdeA reduces c-di-GMP levels in the SW cell by repressing the activity of DgcB. In the G1-to-S-phase transition PdeA is degraded by the protease complex ClpXP. This event releases DgcB activity resulting in the upshift of c-di-GMP levels. Simultaneously, the DGC PleD is activated by phosphorylation of its receiver-domain as an additional player to enhance c-di-GMP concentrations. PleD and DgcB are both required for optimal attachment and holdfast biogenesis. The deletion of both DGCs showed drastically reduced c-di-GMP levels resulting in a complete failure of stalk elongation, holdfast synthesis and attachment to surfaces[62]. C-di-GMP regulation represents one part of the regulation circuit of pole morphogenesis and cell cycle control. The asymmetric cell division in *C. crescentus* requires in addition a tight control of gene expression to relay gene information to the two different progenies with specialized developmental programs. This difficult task is performed by the global transcriptional regulator CtrA that controls multiple events in the *Caulobacter* cell cycle, including the initiation of DNA replication, DNA methylation and cell division[63,64]. Due to its important role, CtrA activity is tightly regulated in several ways[65]. Not only transcription and phosphorylation events, but also subcellular localization and regulated proteolysis belong to the complicated network of CtrA control (Fig. 3).

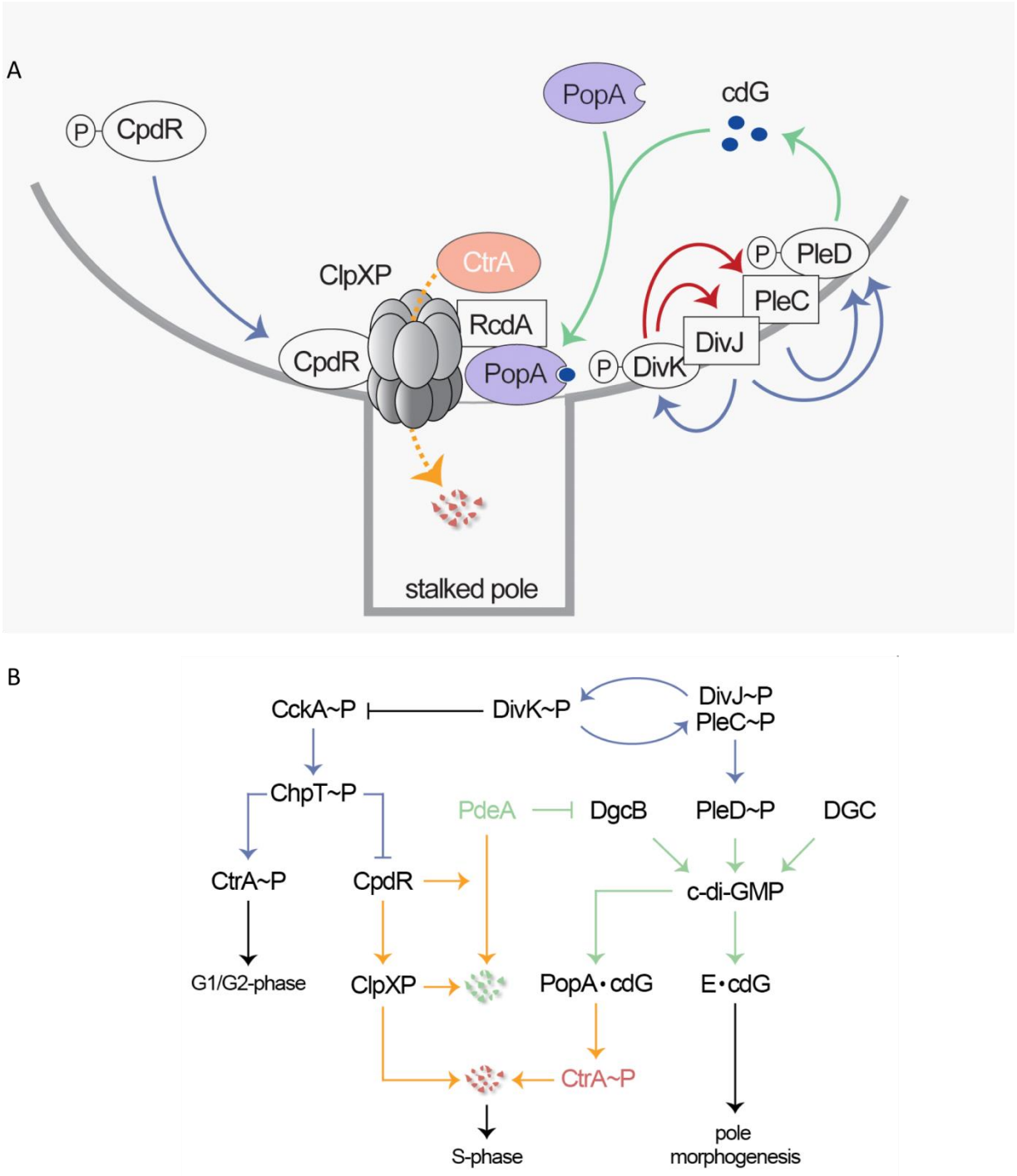

Figure 3: Modell for the regulatory network controlling cell cycle progression and pole morphogenesis in *C. crescentus*. Blue arrows indicate phosphorelays for CpdR and PleD activation, green c-di-GMP metabolic pathways and orange proteolytic processes for the ClpXP substrates PdeA (green) and CtrA (red). Additional unknown diguanylate cyclases (DGCs) and c-di-GMP effector proteins (E) contributing to this network are indicated. Adopted from[66].

In its phosphorylated form (CtrA~P) is present in the SW cell to block the origin of replication. The histidine kinase CckA phosphorylates CtrA using the mediator ChpT. The CckA-ChpT phosphorelay is also responsible for the dephosphorylation of CpdR that leads to its localization and recruitment of the AAA_+ protease complex ClpXP to the incipient stalked pole. At the same time, upon binding of c-di-GMP, PopA sequesters cell cycle dependent, to the same pole where it recruits the mediator protein RcdA and then in turn CtrA. These converging pathways result in ClpXP dependent CtrA degradation, thereby freeing the origin and permitting the initiation of DNA replication[67].

Subcellular localization of PopA has two addresses in the cell whereas only one is c-di-GMP specific. PodJ, a cell polarity determinant, directs PopA c-di-GMP-independent to the new cell pole. Whereas binding of c-di-GMP to the PopA I-site is responsible for its localization at the stalked pole (Fig. 4).

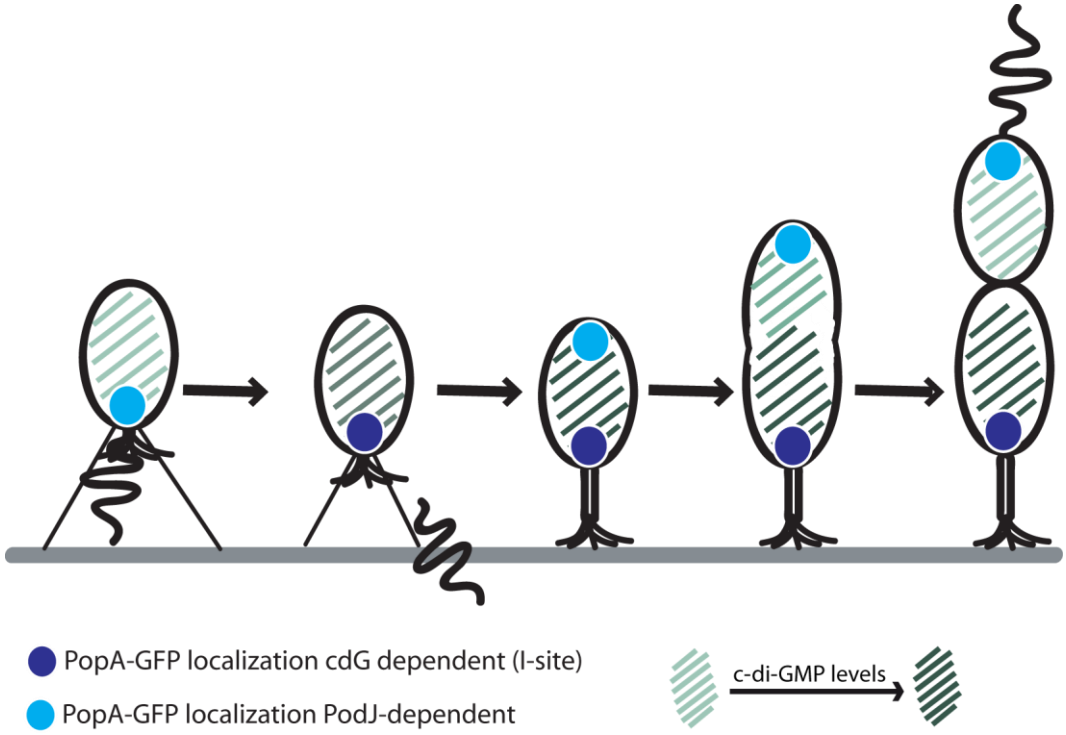

Figure 4: PopA cell cycle dependent localization in *C. crescentus*. Increasing c-di-GMP levels (light green to dark green stripes) induce popA localization to the stalked pole (dark blue circle). PodJ dependent localization takes place at the swarmer cell compartment (light blue circle).

1.6 Diminished c-di-GMP levels in *Caulobacter crescentus*

Investigating the activities of single DGCs or PDEs *in vivo* is complicated due to the redundancy of these enzyme families in bacteria[12]. To analyze contributions of specific enzymes, a strain lagging DGCs or PDEs is needed. Such a strain was engineered for *Salmonella enteritidis*, where all GGDEF proteins were deleted resulting in a so called "gutted strain" (GS), in which the c-di-GMP levels dropped below the detection limit[68]. Introduction of single DGCs restored c-di-GMP dependent phenotypes, indicating that c-di-GMP produced by different cyclases can influence the same downstream targets. In analogy to *S. enteritidis* a *Caulobacter* GS was generated in our group to enable the investigation of weak DGCs. We further constructed a strain in which all DGCs and PDEs were deleted, the so-called really gutted strain (rGS). While generating this strain, we observed that already the deletion of *dgcB* and *pleD* causes severe defects in pole morphogenesis and cell cycle control. Accordingly, the complete loss of c-di-GMP in the GS and rGS caused defects that are even more pronounced. This includes cell division defects, a wrong septum placement leading to elongated cell formation and the cells lose their crescentoid form (Fig. 5). Although low levels of c-di-GMP promote motility, the absence of c-di-GMP disrupts flagellum biosynthesis due to CtrA stabilization which renders the cells non-motile[69]. The reason for the stabilization of CtrA is the miss-localization of PopA in cells lagging c-di-GMP[70]. All other polar appendages like pili and stalk are also absent (Fig. 5), therefore both the GS and the rGS strain do not attach to surfaces. In addition, the capsule production is blocked in these strains, which renders them non-synchronizable. Taken together, *C. crescentus* cell cycle and development are severely disturbed in a c-di-GMP depleted (c-di-GMP^0) strain arguing for multiple c-di-GMP affected pathways.

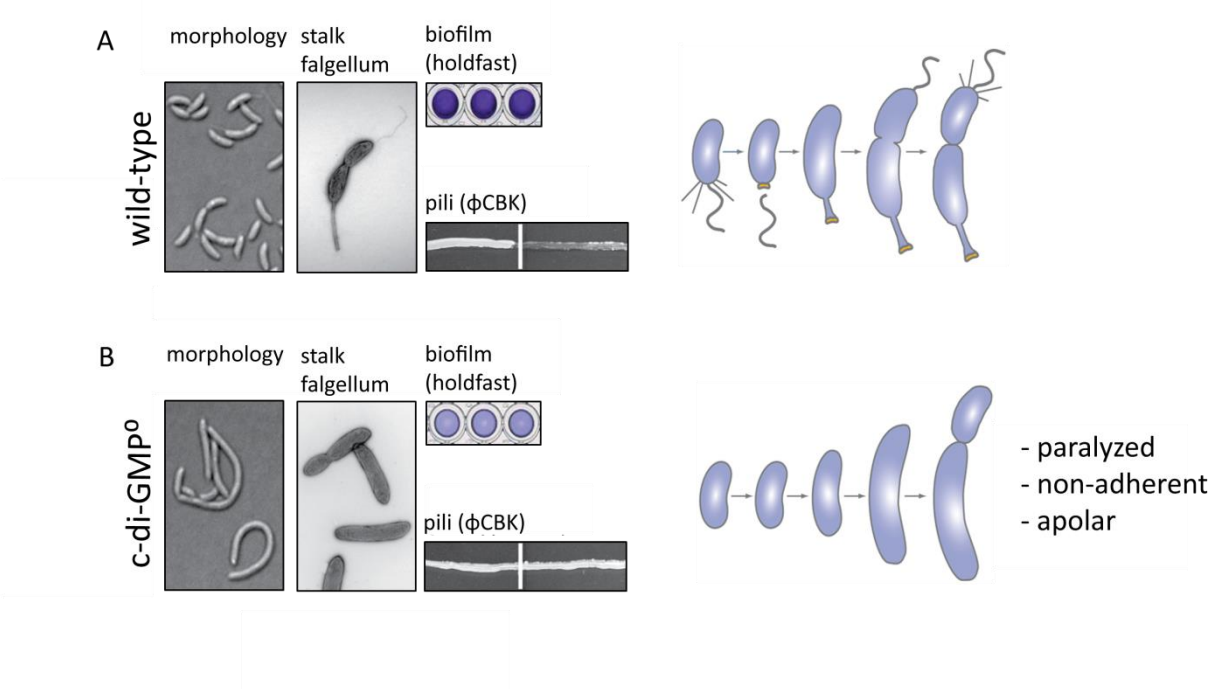

Figure 5: Phenotypes of wild-type and c-di-GMP^0 strain. A. WT cells are crescentoid shaped and harbor all three polar appendages (stalk, flagellum, pili) providing either attachment to surfaces (biofilm stain with crystal violet) or motility during the cell cycle. They are sensitive to the pili acceptor phage ϕCBK. B. Cells lacking c-di-GMP (c-di-GMP^0) have an elongated cell morphology due to wrong septum formation, deficiency in attachment, absence of polar organelles such as stalk, flagellum, pili, and are not sensitive to the bacteriophages ϕCBK and phage ϕCR30 (not shown). Adopted from[69].

1.7 Diverse GGDEF-EAL domain compositions in *Caulobacter crescentus*: Global *vs.* Local pool

Considering the important role of c-di-GMP in *C. crescentus* cell cycle and pole morphogenesis, the amount of c-di-GMP regulating proteins might be not impressive. Notwithstanding, *C. crescentus* encodes for a total of 14 c-di-GMP metabolizing proteins: 4 single GGDEF and 3 single EAL domains and 7 genes encoding for both domains. Regarding the number of those proteins, the question arises why such diversity is needed. Since in other organisms even more of these enzymes are encoded in the genome, one has to ask if this is a general phenomenon[12,71]. Do all proteins contribute to the same c-di-GMP pool or does each enzyme act on a separate, local pool? And if so, which are the underlying mechanisms

between different c-di-GMP dependent regulatory pathways? Looking at the domain architecture, most GGDEF and EAL domains are fused to known or hypothetical N-terminal signal input domains. These domains may determine the spatial destination of the corresponding proteins. This behavior called micro-compartmentalization describes a potential mechanism of separation between different temporal and spatial c-di-GMP dependent pathways. Multiple examples of proteins, localizing to specific cellular structures upon a signal are known for *C. crescentus,* among them PleD, the main cyclase responsible for cell cycle progression. PleD moves upon phosphorylation of its N-terminal receiver domain from diverse cytoplasmic distribution to the pole to generate c-di-GMP[27]. This c-di-GMP is sensed by PopA, which in turn shows a cell cycle dependent localization pattern in response to c-di-GMP binding to its N-terminal I-site. Another pair of proteins, PdeA and DgcB, that antagonistically control c-di-GMP levels in *C. crescentus* and therefore cell cycle control, also localize to the stalked pole[62]. It seems that the biggest accumulation of localized proteins involved in c-di-GMP signaling takes place at this pole (Fig. 3). Nevertheless, also at the at the swarmer cell pole c-di-GMP dependent localization of the effector protein TipF is observed. TipF is required for the correct assembly and positioning of the flagellated pole[72].

The above-discussed signaling pathways require particular localization. One could speculate whether all c-di-GMP signaling proteins that do not localize contribute or profit from a global c-di-GMP pool. However, also in this case a local pool is accessible via proteins that harbor a GGDEF and EAL domain. Those proteins are called composite proteins, because one enzyme harbors two domains that encode for different catalytic activities. Therefore, the GGDEF-EAL composites led to the assumption that they are bifunctional enzymes, harboring the capacity to generate and degrade c-di-GMP. In the context of the discussion about local c-di-GMP pools, composite proteins have the advantages of spatial control. If both proteins are already together, this results in optimal coordination of two opposite activities and further in higher efficiency because they do not have to find each other beforehand and they are independent concerning other enzymes. In summary, they can form their own local c-di-GMP pool independent of the location.

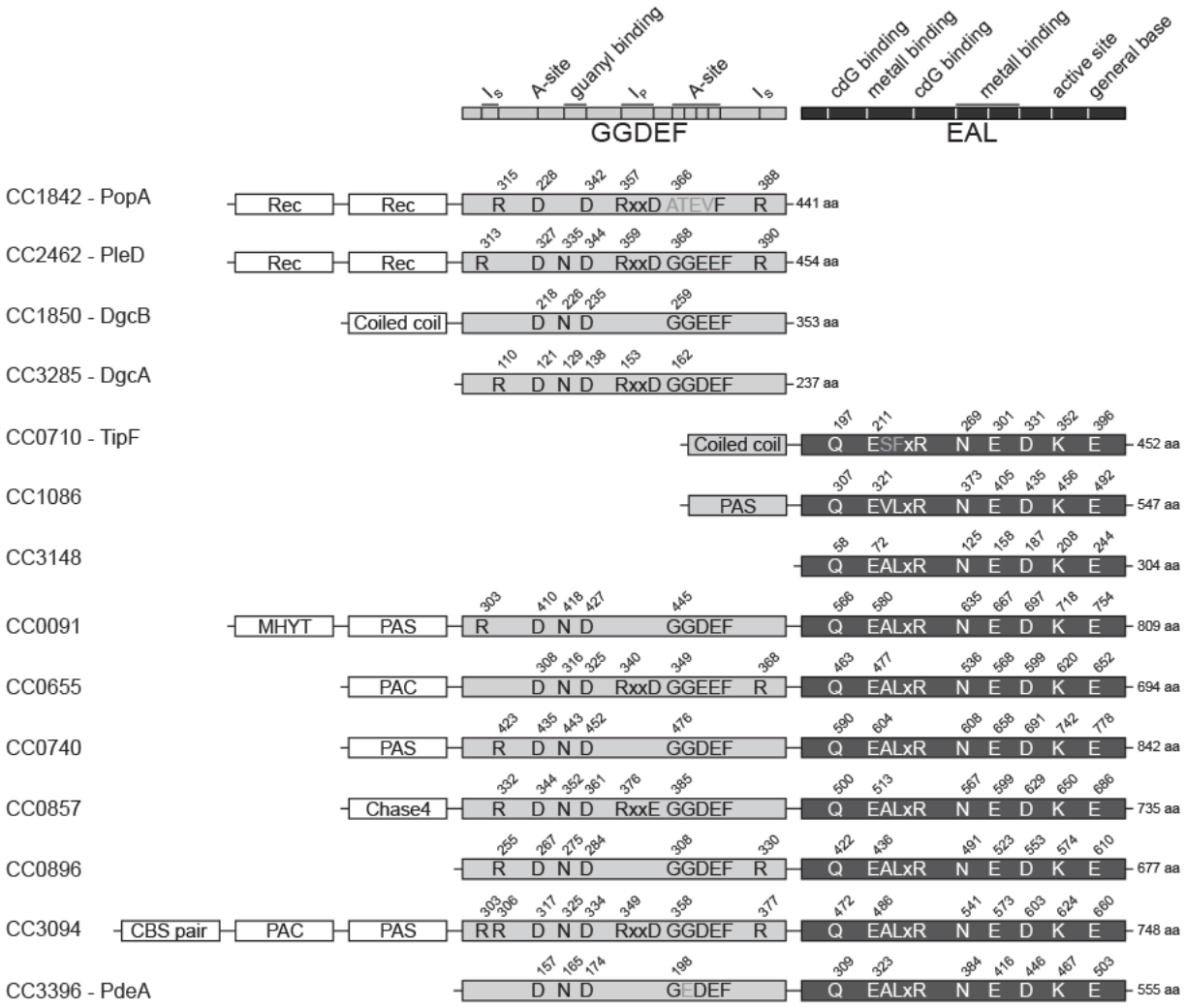

Figure 6: The different GGDEF and EAL domain compositions in *C. crescentus*. GGDEF domains with the conserved residues are depicted in light grey and the EAL domain and according conserved residues in dark grey. Additional N-terminal domains are represented in white boxes. Adopted from[73].

1.8 Composite proteins

Analyzing the GGDEF and EAL domain composition not only in *C. crescentus,* it becomes evident, that a large number of the GGDEF and EAL proteins contain the GGDEF-EAL dual domain[12]. The question arises what may be the advantage of having both domains within one protein. The advantage of spatial control was already discussed in chapter 1.7. Another advantage may be temporal control. Both proteins are always present but their activity

fluctuates during the cell cycle, according to c-di-GMP fluctuations. Changes between the activities may occur via coordinated crosstalk, as it is already known to exist in the RelA-SpoT homologs. This enzyme family regulates the synthesis and hydrolysis of another bacterial second messenger, ppGpp[2,3]. Ligand binding to the hydrolyze domain triggers a signal amplification cascade to the adjacent synthetase domain. That means the intramolecular crosstalk between the opposing catalytic sites is an intrinsic property. In this case the advantage is allosteric control like in PdeA from C. crescentus[26] where the degenerate GGDEF domain has a regulatory function and controls the activity of its adjacent EAL domain[26]. As described for c-di-GMP effector proteins, both domains may be also inactive and serve as c-di-GMP binding domains like in FimX from *P. aeruginosa*[47] or LapD from *P. fluorescens*[42,49,50]. However, which activity do composite proteins have that harbor a conserved GGDEF-EAL domain? Are they indeed bifunctional as the domain composition implies? Meanwhile, a few cases of composite proteins with DGC as well as PDE activity were described. For example BphG1 from the phototrophic bacterium *Rhodobacter sphaeroides* was the first biochemically described bifunctional GGDEF-EAL composite protein[16]. BphG1 belongs to a group of bacterial photoreceptors that sense red/far red light via a biliverdin chromophore. The Apo- and holoprotein (with and without biliverdin) were incubated with GTP and c-di-GMP to test for DGC and PDE activity, respectively. No turnover of GTP was detected whereas c-di-GMP was degraded, indicating c-di-GMP specific phosphodiesterase activity. This activity seemed to be light independent and therefore decoupled from photoreception. Albeit, upon cleavage of the N-terminal GGDEF from the EAL domain, they could observe diguanylate cyclase activity in the presence of biliverdin that was strongly light activated. In this case, cleavage of both domains might be the switch between the opposite activities fine-tuned by light exposure. However, clear evidence is missing, since *in vivo* data do not exist confirming the physiologically relevance of these results. In addition, although *R. sphaeroides* can synthesize c-di-GMP also by another DGC *(RSP3513 called DgcA*[24]*)*, the role of c-di-GMP signaling in this organism is still unknown.

One other example for a composite protein is ScrC from *Vibrio parahemeolyticus* that controls its dual activity by interaction with two other proteins from the same operon ScrA and ScrB[74]. *In vivo*, it seems to be a PDE when co-expressed with its putative interaction partners because

deletion of ScrC leads to a biofilm induced and swarming decreased state. Astonishingly, when expressed alone, it leads to increased cellular c-di-GMP concentration. Accordingly, the presence of ScrA and ScrB favors PDE activity whereas their absence DGC activity. However, also in this case there is no evidence that the DGC activity is physiologically relevant. For that, evidence should exist that verifies ScrAB degradation during the cell cycle. Also, in this work Western-blot analysis is missing to confirm the stability of all active site mutants and domain deletions. Ferreira and co-workers could also show that mutation of the GGDEF domain to GGAEF altered PDE activity, which is comprehensible. Contradictory, this mutation did not alter DGC activity although this is an important active site residue. One could speculate that this result indicates the irrelevance of the DGC activity *in vivo*.

One of the few gram-positive examples with c-di-GMP involvement, MSDGC-1 from *Mycobacterium smegmatis,* exhibits also both enzymatic activities simultaneously *in vitro*. In contrast to BphG1, the isolated domains were shown to be inactive[75], indicating that both activities could not be uncoupled from each other physically and active site mutants are missing to check whether the loss of one domain renders the protein inactive or loss of one activity. MSDGC_1 is essential for long-term survival under limited carbon source conditions but not for biofilm formation. After 5 days, the knockout strain had 50 % reduction in viability and similarly the overexpressing strain grew at a slower rate compared to the wild-type. However, those were the only two *in vivo* experiments, and only performed with the deletion of the full-length protein and not the single domain deletions. The same group could identify another bifunctional protein in *Mycobacterium tuberculosis* (Rv 1354c named as MtbDGC)[76]. Nevertheless, for both proteins no *in vivo* data were presented.

One composite protein was described to regulate its two opposing activities by phosphorylation of the N-terminal receiver domain via its neighbouring histidine kinase *in vitro.* The bifunctional protein Lpl0329 in the pathogen *Legionella pneumophila* decreases its DGC activity in the phosphorylated state without affecting the PDE activity. Whereas in the unphosphorylated state both activities are present[77].

The diversity and complexity of c-di-GMP specific composite proteins is compelling and not yet fully explored. They can be effectors, can be mono- or bifunctional and one type has evolved that has no influence on c-di-GMP signaling at all[78].

1.9 The different ways to control bacterial swimming velocity

Bacteria adjust their motility behavior in response to changes in the environment. In the presence of chemoattractants they swim towards this source by simultaneously rotating their flagella counterclockwise (CCW). To change directions flagellar filaments rotate clockwise (CW) so that the flagella bundle falls apart resulting in a random reorientation of the cells known as tumble events. Tumble events are initiated by transferring a phosphoryl group form the histidin kinase CheA to the response regulator CheY (CheY~P), which in turn diffuses to flagellar motors and modulates their CW rotation[79,80]. Dephosphorylation of CheY is catalyzed by the phosphatase CheZ leading to CCW rotation. Methyl-accepting chemotaxis proteins (CheR and CheB) of the receptor's kinase control module are able to sense and adapt to chemical gradients by reversible methylation (Fig. 7).

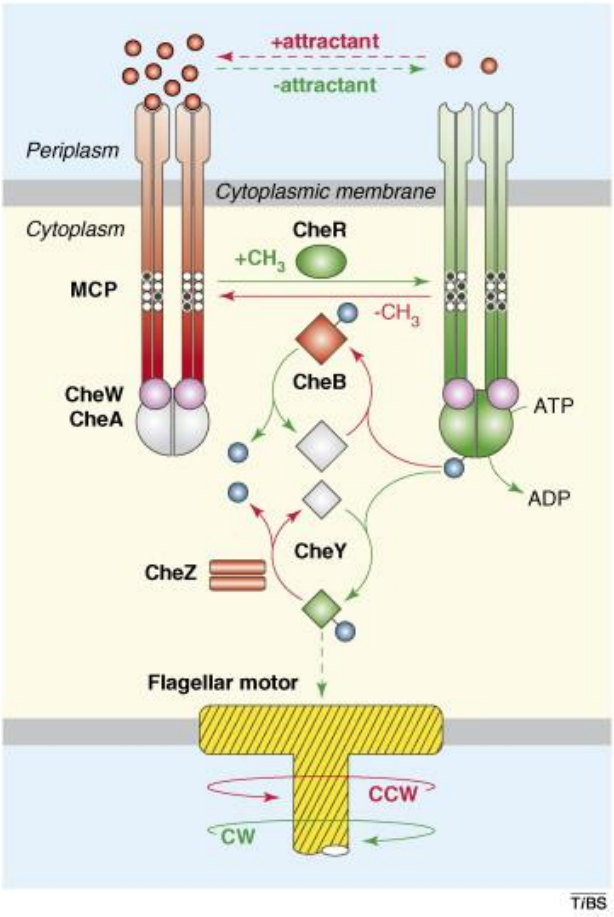

Figure 7: Components of the chemoreceptor signaling pathway in *E. coli.* CCW rotation is initiated by red and CW flagellar rotation by green reaction pathways. Inactive forms of CheA, CheB and CheY are represented in grey whereas the active forms are colored. The methyl-accepting chemotaxis proteins (MCP) are depicted in red in the de-methylated state and in red in their methylated state. Phosphoryl-groups are shown as blue and the receptor modification sites as white (de-methylated) and black (methylated) circles[79].

The driving force for the flagella rotation is a proton flux across the inner membrane channels composed of a complex of MotA and MotB, two stator proteins of the flagellar motor (Fig. 8).

Recent results revealed that bacteria even have different velocities due to varying chemoattractant concentrations. For example, when nutrient sources decrease during biofilm formation *Bacillus subtilis* stops its motility by disabling its flagella via a the protein EpsE[81]. EpsE, an enzyme that is involved in extracellular polysaccharide production, interacts with FliG

to alter FliG-MotA interactions and to abolish flagella rotation via a clutch-like mechanism (Fig. 8).

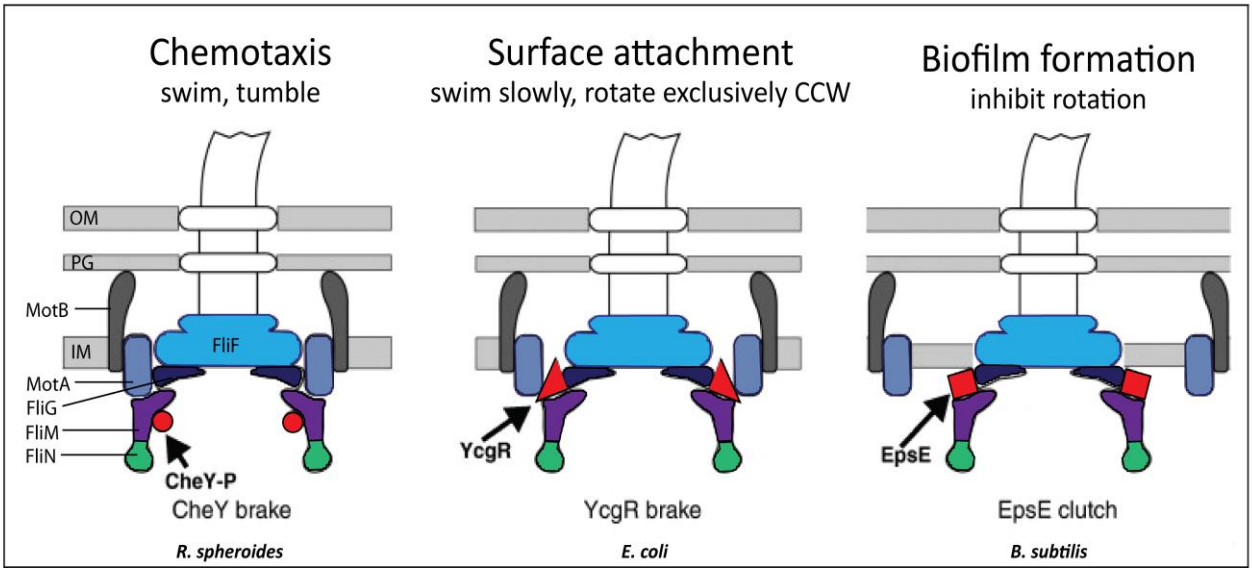

Figure 8: Different organisms adapt to diverse lifestyles by interference with the flagellar motor. In *R. sphaeroides* chemotaxis the motor is stopped by a CheY-P-induced brake (red circle) that binds to FliG (dark blue object) and causes a CCW to CW rotation switch. In *E. coli* the PilZ domain protein YcgR (red triangle) interacts upon c-di-GMP-binding with the falgellar stator protein MotA (blue square) to reduce flagellar speed in stationary phase. In order to attach to surfaces *B. subtilis* inhibits its rotation by binding of EpsE (red square) to the flagellar motor resulting in an interruption of the FliG/FliM (dark blue/violet objects) interaction. Adapted from[82].

For other organisms, a somewhat different speed control mechanism was described. For instance, the α-proteobacterium *R. sphaeroides* uses a brake-like mechanism to stop its single unidirectional driven flagellum hence in this case via the binding of CheY~P. The binding of CheY~P may induce conformational changes that alter the rotor-stator interface and stop the *R. sphaeroides* motor[83].

Similarly, *E. coli* modulates its swimming speed in liquid culture upon entry into stationary phase[84]. Recently, our group showed that *E. coli* moderates its swimming velocity from higher to lower speed via a molecular brake (YcgR) that directly interacts with the motor protein MotA to curb flagellar motor output by binding c-di-GMP[40]. YcgR is one of two PilZ domain proteins in *E. coli* that binds c-di-GMP specifically with a K_d in the low µM range known for c-

di-GMP effectors (as discussed in chapter 1.3)[85]. This c-di-GMP induced brake-like mechanism interrupts electrostatic interactions between MotA and the rotor protein FliG to reduce flagella rotation. The speed decline correlates with nutrient depletion and c-di-GMP decrease at stationary phase.

These findings indicate that bacteria make use of different alterations regarding the bacterial flagellar rotation. However, whether these mechanisms function as a break or a clutch, in common for all is a conformational change next to the stator-switch complex FliG-MotA induced by environmental signals.

2 Aim of the thesis

The second messenger c-di-GMP is a key signaling molecule involved in important bacterial processes like community behavior, growth on surfaces, biofilm formation and virulence. The genome of *Caulobacter crescentus*, the organism used in this study, encodes seven GGDEF domain proteins predicted to have diguanylate cyclase activity (DGCs). Two of the seven DGCs, PleD and DgcB, were known to be the main cyclases producing the major part of intracellular c-di-GMP. However, in a *pleD dgcB* double mutant c-di-GMP is still detectable, leading to the hypothesis that among the five remaining DGCs active cyclases exist.
In the first part of the thesis, the aim was to determine the minimal set of cyclases contributing to the c-di-GMP pool in *C. crescentus*. These cyclases were further characterized and their biological roles in cell cycle control and polar development were investigated. To determine their individual roles in c-di-GMP signaling, single DGCs were analyzed in a strain lacking all other cyclases of *C. crescentus*.

In the second part of this work, a biochemical screen was carried out to find other proteins that are involved in c-di-GMP signaling. In this assay a c-di-GMP bound capture compound was used for specific isolation of c-di-GMP binding proteins within *C. crescentus* cell lysates. The role of a c-di-GMP binding protein (CC3100) with an unsusual response regulator domain was found with this biochemical approach and was further characterized regarding its role in motility control of *C. crescentus* cells. The aim was to elucidate the mechanism CC3100 is using to interfere with the flagellar motor and consequential identify the interaction partners.

3 Results

3.1 Characterization of bifunctional GGDEF and EAL domain composite proteins in *Caulobacter crescentus*

Elvira Friedrich[1], Claudia Massa[1], Tilman Schirmer[1], Annette Garbe[2], Volker Kaever[2] and Urs Jenal[1]

Affiliations:

[1]Biozentrum of the University of Basel, Klingelbergstrasse 50, CH-4054 Basel, Switzerland

[2]Institute of Pharmacology, Hannover Medical School, D-30625 Hannover, Germany

For correspondence: urs.jenal@unibas.ch

Statement of my work

All plasmids and strains used in this study have been generated by me, unless otherwise stated in table 2, 3 and 4. I also performed the following assays of this study: motility (Figure 1.A; 2.B; 4.A; 5.A), attachment (Figure 1.A; 4.A; 5.A), phage-spotting analysis (Figure 1.C-D; 2.D-E; 4.C-D; 5. C-D), cell density gradient centrifugation (Figure 1.E; 3.A; 4.B; 5.B) and Western-blot analysis (Figure 1.B; 2.C; 3.B-C; S2). Phase-contrast/-fluorescence microscopy (Figure 1F; 4.E; 5.E; S1) including evaluation of popA-GFP localization using matlab, ImageJ, and the MicrobeTracker software. Furthermore, I prepared cell extracts for LC-MS/MS (4.A; 5.A), whereas the c-di-GMP measurements itself on LC-MS/MS were performed from Annette Garbe from the Kaever lab in Hannover. All *in vitro* data were performed and analyzed by Claudia Massa from the Schirmer lab at the Biozentrum Basel.

Abstract

In *Caulobacter crescentus* cell cycle progression and polar morphogenesis are spatially and temporally intimately linked. Recently we showed that both processes are directly controlled by the bacterial second messenger c-di-GMP signaling network[1]. The main c-di-GMP producing enzymes that contribute to this second messenger pool are the diguanylate cyclases (DGCs) DgcB and PleD. The deletion of both cyclases have clear phenotypes affecting pole morphogenesis and cell cycle control. However, there is a clear difference compared to a strain lacking c-di-GMP indicating that other enzymes supply c-di-GMP to the cellular pool. This work addresses the question, how many and which DGCs are active and therefore contribute to the c-di-GMP levels in *C. crescentus*. We found two additional active cyclases, CC0655 and CC0857 that according to their phenotypes provide intracellular c-di-GMP as expected for DGCs. Interestingly, both proteins are so-called composite proteins, i.e. they harbor a GGDEF and an EAL domain, which usually encode antagonistic catalytic activities. Whereas single deletions of *CC0655* or *CC0857* exposed no phenotype, the deletions of the four DGCs genes *pleD*, *dgcB*, *CC0655* and *CC0857* showed the same phenotypes like the strain containing no c-di-GMP indicating that these four proteins constitute the minimal set of cyclases in *C. crescentus* under the used conditions. Chromosomal reinsertion of *CC0655* and *CC0857* in the strain background without c-di-GMP reverted the phenotypes associated with increased c-di-GMP concentrations. Furthermore, detailed *in vivo* and *in vitro* characterization of CC0655 revealed that this enzyme is also a phosphodiesterase and that its DGC activity is controlled by substrate inhibition *via* an RxxD motif and we thus renamed this protein to BipB (bifunctional composite protein).

Introduction

Many bacteria employ the second messenger c-di-GMP to adapt to changing environmental conditions and to regulate changes in their life-style. It is well known that c-di-GMP controls bacterial community behavior and growth on surfaces by regulating the switch from planktonic to sessile lifestyle and therefore biofilm formation[2]. C-di-GMP is generated by the condensation of two GTP molecules by a protein family called diguanylate cyclases (DGCs) containing the conserved GGDEF motif (Gly-Gly-Asp-Glu-Phe)[3,4]. Active DGCs form dimers like the structurally related class III adenylyl and guanylyl cyclases and type I DNA polymerases, although they share weak sequence homology[5,6]. Many DGCs harbor an additional conserved amino acid motif RxxD for product inhibition, called inhibitory site (I-site)[4,7]. The cleavage of c-di-GMP into the linear dinucleotide 5'-pGpG[7,8] is catalyzed by phosphodiesterases (PDEs) that contain a conserved protein domain named EAL (Glu-Ala-Leu)[7,8]. Similar to DGCs, PDEs tend to form dimers like BrlP1 from *Klebsiella pneumonia*[9], which shows light-induced dimerization, or PdeA from *C. crescentus*, that dimerizes via its N-terminal PAS domain[10]. A substantial fraction (about one third) of all GGDEF/EAL proteins contain both domains, raising the important question of their enzymatic identity. The N-terminal domains of DGCs, PDEs and composite proteins are often associated with accessory domains such as REC, PAS, GAF, BLUF and helix-turn-helix or coiled coil domains that may serve as dimerization[10,11] or sensory[12] domains for signal input.

The GGDEF and EAL encoding domains are present throughout the bacterial kingdom, usually with several members of these protein families encoded within a single organism. Such redundancy might indicate the need of a differential modulation of c-di-GMP level in a well-defined cell compartment during the occurrence of a biological process. A good example of such spatial and temporal control is the asymmetrical cell division of *C. crescentus*. This α-proteobacteria divides asymmetrically giving rise to two morphologically different progenies: a motile swarmer cell (SW) containing pili and one flagellum and a sessile stalked cell (ST) attaching to surfaces. While the stalked cell can immediately reinitiate a new round of cell division, the swarmer cell is blocked for DNA replication by the phosphorylated form of the cell cycle regulator CtrA. As it has been extensively studied, the transition from swarmer to

stalked cell requires high levels of c-di-GMP at the incipient stalk pole. Such levels are achieved with the degradation of the main PDE PdeA and the concurrent activation of the two main DGCs, DgcB and PleD. DgcB gets activated by the release of PdeA inhibition, while PleD requires phosphorylation of its N-terminal receiver-domain to be activated and to further enhance c-di-GMP levels[13–15]. Elevated amounts of c-di-GMP prompt also the activation of the c-di-GMP effector protein PopA. PopA is a GGDEF domain protein that has a degenerated signature motif. Therefore, the protein is catalytically not competent but can still bind c-di-GMP to its I-site. Upon c-di-GMP binding PopA is sequestered to the incipient stalk pole and recruits other proteins, like the mediator protein RcdA that is essential for PdeA degradation.

The main *C. crescentus* DGCs DgcB and PleD that have been well studied, being are both required for CtrA degradation, optimal attachment and holdfast biogenesis[1]. Interestingly, the *dgcB pleD* double mutant show only reduced c-di-GMP levels, which still reach up to 40 % compared to the wild-type. This raises the question about the presence of additional cyclases that contribute to the total c-di-GMP pool in *C. crescentus.* The genome of *C. crescentus* contains 11 GGDEF domain proteins, four of them consisting of GGDEF domains associated with regulatory domains and the left seven being composite proteins. Beside the already mentioned proteins DgcB, PleD and PopA, the other GGDEF protein, DgcA, has been previously characterized and it was shown to display a very weak enzymatic activity *in vivo* due to a strong feedback inhibition[16]. Therefore, the additional DGCs have to be identified within the class of composite proteins. Sequence analysis of these seven composite proteins revealed that they possess all the residues necessary for substrate binding and catalysis and intact signature motifs, excluding CC3396 (pdeA), which displays only PDE activity as extensively studied. This implies that these proteins may be bifunctional enzymes, enabling to generate and degrade c-di-GMP. Until now, the first composite protein reported as bifunctional was found in the phototrophic α-proteobacterium *Rhodobacter sphaeroides* (BphG1)[17]. Light-independent PDE activity was observed *in vitro*, however after tryptic cleavage of the C-terminal EAL domain, the GGDEF domain exposed light activated DGC activity. In this case proteolysis and exposure to light may be the switch between the opposing activities. Though, for a photochromic protein, light-independent activity is unusual and it is questionable if the PDE activity is real *in vivo*.

In this work we identified two composite proteins, BipB (bifunctional protein, CC0655) and CC0857, which contribute with PleD and DgcB to the c-di-GMP levels in *C. crescentus*. In order to understand if and how they can contribute to c-di-GMP homeostasis and if they have opposing activities we investigated in detail the molecular properties of both proteins.

Furthermore we have elucidated their role in cellular processes like flagellum synthesis and motility, pili synthesis, holdfast formation and popA localization.

Results

1. PleD, DgcB, BipB and CC0857 constitute the minimal set of cyclases in C. crescentus

To identify additional DGCs that contributes to the c-di-GMP pool in *C. crescentus*[1], different genes coding for GGDEF domain proteins were deleted individually in a Δ*pleD* Δ*dgcB* strain background. Using motility as readout, we identified two composite proteins enabling to affect motility on semi-solid agar plates, BipB and CC0857 (Figure 1.A). While the deletion of *bipB* or *CC0857* alone did not affect motility on swarmer plates, the deletion of both *dgcs* in the Δ*pleD* Δ*dgcB* background further impaired motility. Moreover, the deletion of all four *dgcs* in the same strain completely abolished motility in liquid culture (data not shown). Additional studies were performed using a strain that totally lacks c-di-GMP. Such a strain was generated deleting all the DGCs from the genome (gutted strain, GS)[18]. In order to be able to detect c-di-GMP produced by cyclases with weak activity, a second version of the GS strain was generated, deleting all predicted PDEs (really gutted strain, rGS). In such strains, all processes that directly or indirectly depend on the second messenger were affected (cell morphology, pili and stalk formation, ability to form capsule, PopA localization) (Abel et al., in preparation). Comparing the swarming colony of the quadruple mutant and of the rGS mutant on semi-solid agar, a difference in size was observed, even though both colony types showed a typically sprinkled shape often associated with non-motile strains. To investigate if the size difference is due to residual motility we looked for FlgH protein levels, a flagellar class III protein used as marker for flagellar biosynthesis. No protein levels were observed, neither for the deletion of the four DGCs nor for the rGS (Figure 1.B).

Attachment

In addition to motility, the ability to attach to surfaces - a key c-di-GMP regulated process - was also tested in these strains. When comparing the ability to form biofilms in an attachment assay, the ability to attach to surfaces was already lost in the *pleD* and *dgcB* double mutant and did not change with the deletion of either *bipB* or *CC0857* or both (Figure 1.A).

Morphology

Cell morphology is another c-di-GMP regulated feature. While wild-type cells have a crescentoid shape and a detectable stalk, cells lacking c-di-GMP are elongated, straighter and lack the stalk. Cells lacking *pleD* and *dgcB* exhibited no stalk formation, as known from previous results[1]. A deletion of either *bipB* or *CC0857* in a Δ*pleD* Δ*dgcB* strain rendered cells more elongated and thicker (triple deletion strains). The elongation was even more pronounced in a strain lacking all four DGCs (quadruple deletion strain) and this strain phenocopied the rGS strain (Figure 1.A), again arguing that the four DGCs are the main c-di-GMP sources in the cell under the experimental conditions. To define if the morphology change affected the crystalline surface S-layer and its accessibility, we tested for bacteriophage ϕCR30 susceptibility (Figure 1.D). All strains were susceptible to ϕCR30 to the same dilution rate, but the Δ*pleD* Δ*dgcB* Δ*CC0857* strain and the quadruple strain had plaques that were much clearer and therefore hypersensitive to the phage like the rGS strain[19]. In a *ΔpleD ΔdgcB* strain, stalk and holdfast are not synthesized and a rGS strain is missing all polar appendages. From the microscope and the attachment assay, the triple and the quadruple strains also do not exhibit a stalk or a holdfast, respectively. To gain information about pili synthesis, another phage related assay was performed using the pili-acceptor ϕCBK. Compared to the wild-type the quadruple deletion and the rGS strain were insensitive to the ϕCBK (Figure 1.C), while the Δ*pleD* Δ*dgcB* Δ*bipB* mutant was less susceptible.

Capsule formation

We analyzed if the different mutant strains were capable of capsule formation. In a cell density centrifugation, *C. crescentus* cells separate in two bands. The upper band correlates with cells of lower density expressing a capsule around their membrane (predivisional and stalked cells) and the lower band correlates with a cell population of higher density, like swarmer cells. Cells with no c-di-GMP, like the GS and the rGS strain, are incapable to build a capsule and thus the different cell populations cannot be distinguished. Analyzing the density gradient centrifugation it was observed that the Δ*pleD* Δ*dgcB* mutant and the two triple mutant strains were hardly capable to form two bands in the gradient (Figure 1.E). By dissecting the lower band, it turned out that the swarmer cell population was contaminated with stalked and predivisional cells (data not shown). The picture was clearer in the density

gradient of the quadruple and rGS strain. There, only one band was visible that contains mixed cell populations.

PopA localization

The examination of subcellular localization of PopA is a sensitive assay for quantitative determination of c-di-GMP levels in the cell. Due to a c-di-GMP specific and unspecific localization pattern of PopA at both poles, different numbers of PopA-GFP foci can be detected upon GFP exposure. One foci refers to c-di-GMP independent binding in a swarmer cell or c-di-GMP-dependent localization at the stalked cell. Two foci are detectable in a predivisional cell whereby only the foci at the old pole is c-di-GMP specific. Finally, no foci can be detected in ST cells in the absence of c-di-GMP. Due to different c-di-GMP levels, the ratios of detected foci vary.

Micrographs of a Δ*pleD* Δ*dgcB* mutant strain revealed that the signals for two foci decreased in favor to zero foci. The same was observed for the triple deletion strains. A drastic decrease for detected foci was observable in the quadruple and in the rGS strain comparable to the PopA I-site mutant that lacks c-di-GMP dependent foci at the stalked poles (Figure 1.F; Figure S1).

In vivo characterization of Bip and CC0857 in a rGS strain

The fact that single deletions of *bipB* and *CC0857* had no phenotype, except when deleted together with *dgcB* and *pleD*, led us to elucidate their individual roles in a rGS strain background. The *bipB* and accordingly the *CC0857* encoding genes were inserted in the chromosome of the rGS strain, downstream of their native promoter so that native gene expression was obtained. For both reinsertions, a morphotype not distinguishable from wild-type cells was observed (Figure 2.A). When a motility assay on semi solid agar plates was performed, the rGS_ *bipB* mutant strain formed bigger colonies compared to the rGS, indicating that this strain is motile although not to the wild-type extent. Surprisingly, the rGS_*CC0857* mutant formed colonies comparably the size of the rGS strain (Figure 2.B), indicating that it is either not involved in motility or CC0857 catalyzes c-di-GMP production in excess blocking flagella rotation. In that case, the flagella protein FlgH should be detectable in

a Western-blot. Immunoblot analysis revealed FlgH protein levels in the rGS_*bipB* and in the rGS_*CC0857* mutants (Figure 2.B). To elucidate the reason for the medium motility, cell extracts were prepared to measure c-di-GMP levels on LC-MS/MS. The GS_*bipB* strain produced one quarter of the wild-type c-di-GMP levels (Figure 4.A). This result indicated that BipB produces not enough c-di-GMP to reach wild-type motility levels due to a weak cyclase activity or the lack of input signals. Further, the ability of ϕCBK susceptibility was tested to gain information about pili synthesis in the wild-type, the rGS and the reinsertions of *bipB* and *CC0857* (Figure 2.D). Different dilutions (1:10) of phage lysates were tested on the corresponding strains. In contrary to the rGS, the wild-type, the rGS_*bipB* and rGS_*CC0857* mutant strains revealed the same pattern of phage sensitivity indicating that chromosomal reinsertion of *bipB* and *CC0857* restored pili biosynthesis. Another phage related assay was used to test for integrity of the S-layer, a two-dimensional crystalline cluster on *C. crescentus* surface. A dilution series of the bacteriophage ϕCR30 lysates were analyzed according to plaque size and clearance in the corresponding strains. All the strains exhibited the same plaque size and were susceptible to the same dilution rate except that the plaques in the rGS were much clearer (Figure 2.E).

BipB and CC0857 alone cannot restore all cell cycle regulated functions

To ensure that the reinsertion of both enzyme genes can restore proper CtrA distribution throughout the cell cycle, a small-scale density centrifugation was performed. We could observe for both mutants two bands, indicating proper capsule formation (Figure 3.A). Therefore, we separated the SW cell corresponding band from an up-scaled density gradient and followed CtrA levels during one round of cell cycle (Figure 3.B-C). CcrM was used as a stalked cell specific marker protein to characterize the quality of the synchronized cells. Immunoblots of CtrA and CcrM protein levels in the wild-type, rGS_*bipB* and rGS_*CC0857* revealed that only the wild-type exposed a proper protein distribution of CtrA and CcrM throughout the cell cycle. In the mutant strains both proteins were stabilized. A second conclusion we can draw from the Western-blot analysis with specific antibodies against BipB, is that BipB is present during the whole cell cycle in the wild-type and in the rGS strain background (Figure 3.B). These results are reminiscent of DgcB that is also present during the

cell cycle but antagonized by PdeA[1]. The fact that many interaction partners of PdeA localize to the cell pole during the SW to ST cell transition, led us to dissect the cellular localization of BipB. A functional C-terminal *bipB*-GFP fusion protein under the control of the vanillate promotor was constructed, but no localization could be observed (data not shown).

These results indicate that under the used conditions, in addition to PleD and DgcB, BipB and CC0857 are the main source of c-di-GMP production and they can restore c-di-GMP epistasis phenotypes in a strain background containing no other DGCs or PDEs.

2. In vivo characterization of BipB mutants

I-site mutant

To test a possible role for feedback inhibition of BipB in a c-di-GMP free background *in vivo*, the I-site motif was chromosomally exchanged from RxxD to AxxA. A motility assay performed in the GS, showed similar swarm sizes of GS_*bipB* and GS_*bipB*^{AxxA}, indicating no feedback control (Figure 4.A). However, measurements of c-di-GMP levels from the cell extracts on LC-MS/MS revealed nearly twice as much c-di-GMP as the wild-type. In the rGS, no increase in swarm size in a motility assay could be detected whereas c-di-GMP level measurements revealed more than 10 times c-di-GMP increase compared to wild-type levels (Figure 5.A). These results confirmed that the BipB DGC activity is regulated by feedback inhibition via c-di-GMP binding to the I-site. Upon mutation of the I-site, c-di-GMP levels increased and assumingly blocked partially the flagellar motor resulting in medium motility in the GS and loss of motility in the rGS. To confirm that the flagellum biosynthesis is not altered immunoblotting analysis of the rGS_ *bipB*^{AxxA} was performed to detect the flagellar protein FlgH. The assay confirmed FlgH expression indicating that this strain has a polar flagellum (Figure S2).

Concerning the attachment, even if GS_*bipB*^{AxxA} has high levels of c-di-GMP, this strain is unable to attach to surfaces (Figure 4.A). One explanation might be that BipB is unable per se to restore attachment because this protein is not involved in this pathway. Another explanation is that attachment, like motility, decreases upon excess of c-di-GMP and GS_*bipB*^{AxxA} has twice as much c-di-GMP as the wild-type (Figure 4.A). One argument for this

theory would be the results obtained in the rGS (Figure 5.A). There, the strain rGS_*bipB* attached 40 % compared to wild-type levels, because it has also c-di-GMP levels comparable to the wild-type.

PDE mutant

To investigate the physiological relevance of the BipB PDE activity a PDE mutant was constructed by changing the amino acids for the general base catalyst Glu652 into Ala. It was shown that this residue unrecoverly abolishes PDE activity without affecting protein stability[20]. Accordingly, several assays were performed employing the PDE mutant BipB^{E652A} (Figure 4 and 5). At first, mobility and morphology were analyzed. The swarm size of the BipB^{E652A} in the GS were tested and showed a comparable size to the colony size of a GS_*bipB.* The c-di-GMP levels measured in the GS_*bipB*^{E652A} mutant lay within the same range like in the GS containing the full-length protein (Figure 4.A). These data suggested that the EAL domain has no influence on the DGC activity of BipB. In addition, these data indicated that the mutation in the EAL domain did not interfere with DGC activity under the used conditions because the same c-di-GMP levels were detected in the GS_*bipB*. C-di-GMP concentration measurements of the rGS_*bipB*^{E652A} revealed higher c-di-GMP levels compared to rGS_*bipB* (Figure 5.A). As all PDEs were deleted in the rGS, the only candidate accountable for such difference in c-di-GMP levels is the BipB EAL domain itself. Indeed, nearly wild-type c-di-GMP levels were reached in the rGS_bipB^{E652A} strain. However, the colony size decreased in a motility assay and the question why motility decreased and not as expected increased is undefinable so far. Immunoblot analysis for FlgH protein levels indicated that in this mutants the flagellum biosynthesis is unaffected (Figure S2).

Another c-di-GMP-based assay that showed an effect of PDE activity of BipB was the cell density gradient centrifugation. Comparing rGS_*bipB* and rGS_*bipB*^{E652A} a change in the density gradient became apparent (Figure 5.B). The PDE mutant showed only one band, however opposite the band that would correspond to a c-di-GMP free strain. We assume that the mutation of the EAL domain resulted in overproduction of c-di-GMP and induced uncontrolled capsule formation in every cell type resulting in an upshift of the populations in

the gradient centrifugation. This hypothesis may be confirmed by the fact that the I-site mutant with high c-di-GMP content showed the same phenotype in the cell density gradient centrifugation. In the GS, where also other PDEs are present, only the I-site mutant changes the phenotype of the c-di-GMP free strain (Figure 4.B).

The results indicate that BipB controls its own c-di-GMP production not only by an inhibitory site but in addition by the action of its own EAL domain.

BipB and its I-site and PDE mutant can restore ϕCBK susceptibility

A wild-type strain is sensitive to the bacteriophage ϕCBK that uses pili to invade bacteria. Because a strain depleted of c-di-GMP lacks pili, this phage cannot attach and the strain is insensitive. To further test if BipB and its mutants in the GS and the rGS strains are phage sensitive, a phage-spotting assay using different dilutions of the phage lysate was performed (Figure 4.C and 5.C). BipB could restore ϕCBK susceptibility in both strain backgrounds, as also did its I-site and PDE mutant. One difference was detected in the I-site mutant in the rGS. There it seemed that rGS_*bipB*^{AxxA} was only partially sensitive to ϕCBK. Because this strain overproduced c-di-GMP this might interfere with pili susceptibility. It was reported that successful ϕCBK infection requires flagellar rotation for a first contact with *C. crescentus* cells to increase the likelihood of interactions between the phage tail and polar receptors[21]. Immunoblotting analysis of the rGS_*bipB*^{AxxA} confirmed that the flagellar protein FlgH is expressed indicating that this strain has a polar flagellum (Figure S2). However rotation might be blocked due to elevated c-di-GMP levels leading to decreased ϕCBK infection rate. The DGC mutant retained insensitive, suggesting that no pili are made and thus no c-di-GMP is produced.

The *bipB* DGC mutant is hypersensitive to bacteriophage ϕCR30

The S-layer of *C. crescentus* is the receptor for another bacteriophage ϕCR30. A phage-spotting assay was performed to compare phage susceptibility of a wild-type, a c-di-GMP depleted strain and the *bipB* mutants in the GS and rGS (Figure 3.D and 4.D). The results showed that the BipB DGC mutant is hypersensitive to ϕCR30 like the c-di-GMP reduced strains resulting in clearer plaques compared to the wild-type. Interestingly, although the

GS_*bipB* and its PDE and I-site mutant showed no change in ϕCR30 susceptibility the very same proteins had an effect in the rGS. There, they seemed to be less sensitive towards ϕCR30. It looks like there is a correlation between susceptibility and c-di-GMP content in the mutant strains. The more c-di-GMP a strain contains the less susceptible it is towards ϕCR30.

PopA localization as a tool for qualitative c-di-GMP measurements

The localization of PopA during the cell cycle is c-di-GMP dependent[22]. Therefore, PopA localization can be used as a tool to evaluate c-di-GMP levels in different strains. We followed PopA localization pattern in the GS and rGS and compared it to the corresponding strains with chromosomal reinsertion of the BipB full-length protein and different active site mutants. In both strain backgrounds PopA could be localized, except in the DGC mutant where no c-di-GMP could be observed (Figure 4.E and 5.E), again indicating that DGC activity was abolished by mutations in the GGDEF domain.

For all strains, Western-blot analysis confirmed that all described phenotypes were reliant on stable protein expression. The strains used in this work expressed BipB and its different mutants at levels similar to that for wild-type BipB. Additionally, FlgH protein levels were detected in the GS and the rGS to confirm flagellar biosynthesis (Figure S2).

3. In vitro BipB characterization

To determine whether *in vitro* BipB displays DGC, PDE or both enzymatic activities, BipB was heterologously expressed in *E. coli* and purified to homogeneity. As resulted from analytical size exclusion chromatography, the protein is a dimer in solution (data not shown). This finding agrees well with the detection of a physiological DGC activity, which requires dimerization[23,15]. To estimate enzymatic activities, the BipB was incubated with GTP and c-di-GMP, respectively. As shown in the product progression profile (Figure 6.A) the end product of the reaction upon GTP incubation was pGpG, indicating that the enzyme is bifunctional. Moreover, the intermediate species of the reaction (c-di-GMP) was not detected, implying that the second enzymatic activity is faster than the first one. In addition, the end product was also pGpG upon c-di-GMP incubation (Figure 6.B). In order to quantify the DGC and the PDE enzymatic activities, BipB was incubated with different amounts of GTP and c-di-GMP,

respectively, and the initial velocities were estimated (Figure 6.C). The analysis of the saturation curves upon incubation with GTP and c-di-GMP revealed k_{cat} values of 0.039 sec^{-1} and 0.13 sec^{-1} for the DGC and PDE activity, respectively. On the other hand, BipB showed K_m values of 38 and 10 µM, for GTP and for c-di-GMP, respectively. These values are comparable with those obtained for other DGCs and PDEs, like YdeH from *C. crescentus*[24] and RocR from *P. aeruginosa*[25].

To further investigate how and if the communication between the two domains interfere on their respective enzymatic activity, active site mutants of GGDEF (GGAQF) and EAL (E652A) domains were analyzed *in vitro*. The DGC mutant $BipB^{GGAQF}$ displayed no DGC activity (data not shown) while a 25-fold increase in the PDE specific activity (k_{cat} = 3.20 sec^{-1}) was observed. The purification of $BipB^{E652A}$ revealed a feature not observed during the purification of the wild-type protein: the mutant co-purified together with a nucleotide, which has been proven to be c-di-GMP by the means of FPLC analysis (data not shown). $BipB^{E652A}$ loaded with c-di-GMP displayed no PDE activity, as expected, whereas it exhibited only a residual DGC activity (k_{cat} < 0.01 sec^{-1}, data not shown). Such reduction in DGC activity suggests that as the PDE activity is abolished, c-di-GMP accumulates in the reaction solution and can bind to the I-site, imposing a feedback control to the DGC activity. To confirm the role of the I-site in the regulation of the DGC activity, the enzymatic activities of the I-site mutant were measured. Changes of the I-site motif from RxxD to AxxA resulted in a 10-fold increase in specific activity (k_{cat} = 3.20 sec^{-1}), confirming the role of the feedback inhibition mechanism in the control of DGC activity. $BipB^{AXXA}$ also retains PDE activity, showing kinetic constants unchanged if compared with the wild-type. Taken together, these data suggest that BipB is a bifunctional enzyme *in vitro*, displaying a DGC activity that is modulated by a feedback inhibition mechanism via c-di-GMP binding to the I-site.

Discussion

C-di-GMP is an important second messenger whose levels control a wide range of cellular functions in bacteria e.g. motility, biofilm formation, virulence and host colonization[2–4]. Modulation and homeostasis of c-di-GMP levels are provided by the opposing actions of two enzymatic activities, provided by the GGDEF and the EAL domain that are responsible for its synthesis and degradation, respectively. Many bacterial species encode for a number of such domains, suggesting their involvement in different cellular pathways. In the *C. crescentus* genome 11 GGDEF domain encoding genes were found. So far two DGCs, DgcB and PleD, were identified as the main cyclases responsible for the production of c-di-GMP during cell cycle[1]. However, activities and biological function of the other DGCs remain unknown to date. In this work we have identified and characterized two additional DGCs, BipB and CC0857. The influence of BipB and CC0857 DGC activity seemed to be moderate because single deletions of both genes showed no phenotypes distinguishable from wild-type. In addition, both enzymes in triple deletions strains (*pled*, *dgcB* and *bipB* or *CC0857*) had a minor effect compared to the double deletion strains (*pleD dgcB*). However, the quadruple deletion strains (*pled*, *dgcB* and *bipB* and *CC0857*) showed phenotypes already observed in a *C. crescentus* strain lacking all DGCs and hence non-detectable c-di-GMP levels (S. Abel, in preparation;[18,19]). In order to address the biological role of a DGC in a cellular environment containing other DGCs or PDEs, a strain background lacking all DGCs (GS) and in addition all PDEs (rGS) was employed. Our data have shown that both proteins exhibit DGCs activity in a rGS background and they reverted the rGS-phenotypes concerning morphology, flagellum synthesis and motility, pili and holdfast formation (Figure 2). The finding that both DGCs could restore different phenotypes indicates that c-di-GMP produced by different GGDEF proteins can activate the same targets. Moreover, CC0857 seemed to produce more c-di-GMP because the effect on motility in the triple deletion strain with *CC0857* was more prominent compared to the triple deletion with *bipB*. In addition, the swarmer colony of the rGS_*CC0857* appeared smaller than the one of rGS_*bipB*. Detection of FlgH protein levels in the rGS_*CC0857* cells indicated that the flagellum is formed but its rotation is blocked, probably due to c-di-GMP excess in the strain. The elevated c-di-GMP production by CC0857 compared with BipB can be rationalized

considering that CC0857 has a partially degenerate I-site, which renders the enzyme insensitive to the environmental c-di-GMP levels (Figure S2). Our results concerning the reinsertion of *bipB* and *CC0857* genes in the rGS strains agree well with the ones observed in similar studies in *Salmonella enteritidis,* where single reinsertions of different DGCs restored cellulose synthesis in a c-di-GMP-dependent manner[29]. On the other hand, in the rGS_*bipB* and rGS_CC0857 strains CtrA levels were stabilized during the cell cycle. A similar behavior was observed also by the reinsertion of the strong DGCs, PleD or DgcB, in the rGS (unpublished data, S. Abel and coworkers). These findings can be explained keeping in mind that CtrA degradation requires fluctuation of c-di-GMP levels during the cell cycle[22,30], which cannot occur in the rGS due to the absence of all PDEs. Abel and coworkers have indeed shown that the insertion of a PDE whose activity is cell cycle controlled, like PdeA, leads to cell cycle regulated CtrA levels in the rGS. The same effect can be achieved by the re-insertion of a constitutive active PDE and a cell cycle regulated DGC like PleD. Thus, these results indicate that the cell cycle progression in *C. crescentus* requires a modulation of c-di-GMP level, which is provided by its abundant system of GGDEF and EAL domain proteins.

Interestingly, BipB and CC0857 are composite proteins containing a GGDEF and EAL domain. This raises the important question of how these antagonistic activities are coordinated within the same polypeptide. A well-studied example of a composite protein is PdeA, which shows only phosphodiesterase activity[1,7,10]. PdeA PDE activity is activated upon binding of GTP to the degenerate and therefore inactive GGDEF domain[7]. Some composite proteins actually lost both activities and act as c-di-GMP effector proteins like FimX from *P. aeruginosa*[31] or LapD from *P. fluorescens*[32–34]. Here we report for the first time a detailed *in vivo* and *in vitro* characterization of a bifunctional composite protein. Our study revealed that the DGC activity is slightly slower than the PDE, being the k_{cat} value for DGC activity (0.039 sec-1) 3.5 fold lower than the k_{cat} value for the PDE activity (0.13 sec-1). However, considering that the DGC activity requires protein dimerization, the two enzymatic rates seem comparable. On the other hand, the comparison of the K_m values for GTP (37.7 ± 4.6 µM) and for c-di-GMP (9.5 ± 1.5 µM) raises the question why only the DGC activity seems to have a physiological relevance. In fact, since the intracellular concentration of GTP in exponentially growing bacterial cells is in the submillimolar range[28], the BipB DGC activity is expected to be fully induced under

physiological conditions. On the other hand, since the BipB K_m value for c-di-GMP (9.5 ± 1.5 µM) is much higher than the intracellular c-di-GMP concentration (1.2 ± 0.11 µM)[27], the BipB PDE activity may be physiologically not relevant (unless in the context of high local c-di-GMP concentrations).

In order to verify if the two domains interfere on their respective enzymatic activity, active site mutants of GGDEF and EAL domains were generated and their activities were studied *in vivo* and *in vitro*. The mutation of the GGDEF active site mutant revealed that DGC activity was abolished in the GS and the rGS background, as expected. This was confirmed by different assays testing the motility, synchronization ability, phage ϕCBK susceptibility and finally by c-di-GMP concentration measurements on LC-MS/MS where no c-di-GMP could be detected (Figure 4 and 5). On the other hand, *in vitro* characterization revealed that $BipB^{GGAQF}$ displays a 25-fold increase in the PDE activity. This finding led us to suggest that GGDEF domains exhibit an inhibitory effect on the PDE activity. We speculate that global changes in BipB quaternary structure might take place, leading to an optimization of the EAL dimer interface and thus to an enhancement of PDE activity. In fact, the finding that $BipB^{GGAQF}$ shows virtually the same K_m value (12.1 ± 1.1 µM) as the wild-type protein indicates that the local conformation of the substrate-binding pocket remains unchanged.

Furthermore, the mutation within the EAL domain showed that BipB has indeed PDE activity that became apparent in the *in vivo* assays performed in the rGS background (Figure 5). In addition, c-di-GMP level measurements on LC-MS/MS show elevated levels in the rGS_$bipB^{E652A}$ strain compared to the rGS_*bipB*. These results indicate that the PDE activity resides in the EAL domain and the loss of PDE activity does not interfere with the adjacent DGC activity, as the same c-di-GMP levels were measured on LC-MS/MS in GS_*bipB* and GS_$bipB^{E652A}$ (Figure 4). The *in vitro* data showed also that $BipB^{E652A}$ was co-purified with bound c-di-GMP and displayed only a residual DGC activity. In fact, in the absence of a PDE activity, c-di-GMP produced by the GGDEF domain accumulates in the reaction solution and its concentration can reach levels that trigger its binding to I-site of the GGDEF domain. However, in a physiological context, the c-di-GMP produced from the intrinsic BipB DGC activity diffuses quickly away and can be sequestered by specific c-di-GMP binders with binding affinities in the pico- or nanomolar ranges (e.g. ribozymes or PilZ domains)[35,36,37]

preventing that the local concentration of c-di-GMP reaches the level needed for the c-di-GMP binding to the I-site.

In order to verify if c-di-GMP binding to the I-site had a physiological relevance or if it was an artifact of the *in vitro* experiments, a BipB I-site mutant was characterized. The assays performed (motility, capsule formation, attachment and phage ϕCR30 and ϕCBK susceptibility) showed that mutations in the I-site lead to an excess of c-di-GMP levels. The measurements with LC-MS/MS in the rGS containing the BipB I-site mutant showed c-di-GMP accumulation by a factor of ten compared to wild-type levels. This value is even higher than the one in the PDE mutant, indicating that c-di-GMP levels regulation is rather I-site controlled. This is confirmed by the DGC k_{cat} value measured for the I-site mutant *in vitro*, which is 25 fold higher than the value found for the wild-type enzyme. From previous studies on feedback inhibition of cyclases it was reported that the substitution of the arginine and glutamic acid of the RxxD motif into alanines interfered with DGC activity of DgcA and PleD in *C. crescentus* and only a subfraction of I-site mutations were found to increase c-di-GMP turnover[38,14,15]. This may either suggest a different allosteric control mechanism in BipB as mutations at the I-site enhance DGC activity or indicate that I-site mutations cause partially structural instabilities as also seen for BipB (data not shown) and for DgcA (P. Wassman, personal communication) proteins *in vitro*. The DgcA and PleD I-site mutants with enhanced DGC activity in addition showed a 100 fold increase in c-di-GMP levels compared to the wild-type proteins, however the BipB I-site mutant exhibits only a 10 fold increase of c-di-GMP. The difference may be explained by the additional PDE activity of BipB.

Therefore, our results indicate that BipB is a bifunctional composite protein, which *in vivo* displays an I-site controlled DGC activity. The associated PDE activity might serve as a second control level, allowing a fine-tuned c-di-GMP homeostasis. On this line, we propose a model according to which BipB displays a DGC or PDE activity in response to c-di-GMP environmental concentration (Figure 7). In fact, at low c-di-GMP levels BipB would work as a DGC. However, if the local c-di-GMP concentration would increase beyond a threshold value, the DGC activity would be turned off by the c-di-GMP binding to the I-site motif and at the same time the PDE activity would come in place. The difference in the PDE activity of BipB wild-type and $BipB^{GGAQF}$ may suggest that the GGDEF domains display an inhibitory effect on the PDE

activity, which seems relieved when the GGDEF loop located at the dimer interface is mutated. Structural rearrangements occurring upon intramolecular crosstalks were already reported for another class of bifunctional proteins, RelA-SpoT homologs[39,40]. This enzyme family regulates the synthesis and hydrolysis of the small nucleotide ppGpp, a bacterial alarmone. RelA-SpoT crystal structures revealed that the enzyme exists in two different conformations, corresponding to known reciprocal activity states. The switch between the two states is a consequence of conformational changes triggered by nucleotide binding to the hydrolase domain[23,24]. Our data support a similar mechanism for the switch between the two enzymatic activities, suggesting that the regulation resides in the c-di-GMP binding to the I-site and in the subsequent conformational changes. Crystal structures of a bifunctional GGDEF-EAL composite protein are not known yet, leaving open many questions about domain cross-talks and activity regulation. In addition, the effect of a second protein that serves as an interaction partner of BipB controlling its activities cannot be ruled out. In *C. crescentus* c-di-GMP levels dynamically change from low levels in the swarmer cell compartments to high levels in stalked cells implicating that PDE and DGC activities are differently controlled during cell cycle progression. For example PdeA activity is regulated by the ClpXP protease and DgcB activity in turn by PdeA[1]. However BipB protein levels could be detected throughout the cell cycle (Figure 3.B) excluding direct control by a protease, yet an interaction partner may regulate PDE and DGC activity in the course of a cell cycle.

Material and Methods

Strains, Plasmids, and Media

The bacterial strains and plasmids used in this work are summarized in Table 2, 3 and 4. For markerless deletions or allelic mutations a two-step recombination sucrose counter-selection procedure based on pNPTS138-derivatives was used. Plasmids were constructed in *E. coli* DH10B or S17.1 strains and transferred by conjugation into *C. crescentus* strains[41]. *E. coli* was grown in Luria Broth (LB) media at 37 °C and *C. crescentus* was grown in rich medium (peptone yeast extract; PYE)[41]. For synchronization experiments cells were grown at 30 °C in minimal medium containing 0.2% glucose and swarmer cells were isolated after Ludox gradient centrifugation[42]. For plasmids with Vanillate inducible promotor a concentration of 1mM was used. All media were supplemented with the according antibiotics for selection. If not otherwise stated, for assays in liquid media cells in exponential growth phase were analyzed.

Motility Assay

To score motility, single *C. crescentus* colonies were inoculated onto PYE soft agar plates (0.3 % agar) and incubated for 72 h at 30 °C. After scanning (SilverFast®-SE i800 Scanner; Microtek International, CA, USA) the swarm size was analyzed using Photoshop CS3 (Adobe, CA, USA) and ImageJ (NIH, USA) software. For all motility experiments the mean of at least six independent colonies was shown with error bars calculated by standard deviation.

Attachment Assay

For attachment experiments *C. crescentus* strains were grown in PYE in 96-well microtiter plates (Falcon, USA) under shaking conditions (200 rpm) for 24 h at 30 °C. After crystal violet staining (0.3 % crystal-violet, 5 % isopropanol, 5 % methanol), the attached biofilm was dissolved with 20 % acetic acid. The optical density was measured at 660 nm in a photospectrometer (Genesys6, Thermo Spectronic, USA). For each tested strain a mean of at least seven independent colonies was shown with error bars calculated by standard deviation.

Phage Sensitivity Assay

C. crescentus overnight cultures (350 µL) were mixed with 2.5 mL of molten 0.5 % PYE top agar and immediately distributed on 1.5 % PYE agar. According to the phage spot assay phage lysates were diluted 10^{-1}-10^{-8} and spotted on the plated bacteria/top agar mixture[43]. Plates were incubated at 30 °C for 24 h, until small plaque-forming units (pfu) were visible.

C-di-GMP extraction for LC-MS/MS

Overnight cultures of *C. crescentus* strains grown in PYE were diluted twice in M2G to finally reach an OD_{660} ~ 0.3 next morning. A total amount of 10 mL liquid culture was used for c-di-GMP extraction. After centrifugation (4 °C, 5 min, 4.300 rpm) the pellets were washed with 1 mL dH_2O (4 °C, 1 min, 13.000 rpm) and resuspended in 300 µL Acetonitril/Methanol/dH_2O (40/40/20 v/v). The suspension was incubated for 15 min at RT, then for 10 min at 95 °C and cooled on ice for 1 min. After a centrifugation step (4 °C, 1 min, 13.000 rpm), the supernatant was collected, the pellet resuspended in 200 µL Acetonitril/Methanol/ dH_2O (40/40/20 v/v) and incubated again for 15 min at RT. This procedure was repeated by collecting the supernatant to a final volume of 700 µL and the extractions were stored at -20 °C.

Microscopy

Fluorescence and phase contrast (PH) microscopy were performed on a DeltaVision Core (Applied Precision, USA)/Olympus IX71 microscope equipped with an UPlanSApo 1003/1.40 Oil objective (Olympus, Japan) and a coolSNAP HQ-2 (Photometrics, USA) CCD camera. Cells were placed on a PYE pad solidified with 1 % agarose (Sigma, USA). Images were processed and analyzed with softWoRx version 5.0.0 (Applied Precision, USA) and Photoshop CS3 (Adobe, USA) software. For the evaluation of popA localization data, the MicrobeTracker command in MATLAB (matrix laboratory) was used[44]. In this assay, at least 200 cells were counted and all data were normalized to the corresponding wild-type. Error bars represent the standard deviation of at least two independent experiments.

Antibody Production and Immunoblotting

Purified His-BipB was was injected into rabbits for polyclonal antibody production (Josman, LLC™, Californien, USA). The serum was adsorbed against a whole cell lysate of the BipB

deletion mutant. According to standard Western-blot methods proteins were detected with a 1:500 dilution of α-CtrA, 1:5000 of α-CcrM, 1:10000 of α-FlgH and 1:1000 of α-BipB. The secundary HPR-conjugated swine α-rabbit antibodies were used with a 1:10000 dilution. Western-blots were developed with ECL detection reagents (Western Lightning, Perkin Elmer, MA, USA) and exposed on medical X-ray films (Fujifilm Corporation).

BipB Expression and Purification

C-terminally His-tagged BipB was expressed in the *E. coli* BL21 (DE3) pGroESL by adding 0.4 mM isopropyl-β-d-thiogalactopyranoside (IPTG) at an OD_{600} of 0.7 and incubation at 26 °C for 4 h. Cells were harvested by centrifugation (6.800×*g*, 10 min, 4 °C) and were resuspended in Ni-A buffer (50 mM Tris-HCl, pH 8.0, 300 mM NaCl, 20 mM imidazole, 50 mM L-glutamic acid, 50 mM L-arginine, 2.5 µg/mL DNAse; 100 ug/mL lysozyme, EDTA-free protease-inhibitor cocktail (Roche, 1 tablet/50 mL buffer)). Cells were disrupted with a Sonicator (Thermo Spectronic) at 15.000 psi, lysates were cleared by centrifugation (28.000×*g*, 45 min, 4 °C), filtered (0.22 µm) and loaded onto a 5 mL HisTrap column (GE Healthcare). After washing the column with Ni-A buffer (10 column volumes (CV)), the protein was eluted with a linear gradient of imidazole from 20 to 500 mM in 10 CV. The pooled fractions were concentrated to 1 mL and further purified by size-exclusion chromatography using a Superdex 200 26/60 column (GE Healthcare) and SEC buffer (20 mM Tris–HCl, pH 8.0, 150 mM NaCl, 50 mM L-glutamic acid, 50 mM L-arginine). Analytical size-exclusion chromatography runs were carried out using a Superdex 200 10/30 column (GE Healthcare) connected to an Äkta Purifier FPLC unit and monitored with Unicorn software. Protein purity was verified by SDS-PAGE followed by Coomassie blue R-250 staining. Protein concentrations were estimated from the measurement of the optical density at 280 nm (ε_{280} = 56,755 $M^{-1}cm^{-1}$).

Enzymatic Activity

BipB enzymatic activity was measured by following the substrate consumption using ion exchange chromatography[24]. Briefly, BipB at a concentration of 2 µM or 1 µM was employed, using different concentrations of substrates, GTP or c-di-GMP to estimate DGC or PDE activity, respectively. For BipB mutants, protein concentrations of 0.1 µM ($BipB^{GGAQF}$) and of 0.5 µM ($BipB^{AxxA}$) were used. The total reaction volume was 600 µL and in both cases the reaction mixtures were supplemented with 5 mM $MgCl_2$. Aliquots of 100 µL were taken at regular time intervals and the reaction was stopped by adding $CaCl_2$ at a final concentration of 1 mM. Subsequently, the samples were diluted 1:10 in 5 mM NH_4HCO_3, pH 8.0, filtered (0.22 µm) and loaded on an ion-exchange column (ResourceQ 1 mL, GE Healthcare). The nucleotides were separated with a gradient from 0.005 to 1 M NH_4HCO_3, pH 8.0, in 14 CV. The amount of substrate and reaction product was determined by integration of the UV absorption (253 nm) peaks. The procedure was calibrated with GTP (Sigma) and c-di-GMP (Biolog, Bremen) standards of known concentrations. Kinetic data consisting of initial enzymatic rates at each substrate concentration were fitted to the Michaelis-Menten equation using the ProFIT program (QuantumSoft) to estimate K_m and k_{cat} values.

Acknowledgements

We thank Fabienne Hamburger for her help in plasmid preparation and Dr. Sören Abel for critical reading of this manuscript. This work was supported by the Deutsche Forschungsgemeinschaft grant FOR929; JE 442/1-1.

References

1. Abel, S. *et al.* Regulatory cohesion of cell cycle and cell differentiation through interlinked phosphorylation and second messenger networks. *Molecular Cell* **43**, 550–60 (2011).

2. Boehm, A. *et al.* Second messenger signalling governs *Escherichia coli* biofilm induction upon ribosomal stress. *Molecular Microbiology* **72**, 1500–16 (2009).

3. Ryjenkov, D. A., Tarutina, M., Moskvin, O. V. & Gomelsky, M. Cyclic diguanylate is a ubiquitous signaling molecule in bacteria: insights into biochemistry of the GGDEF protein domain. *Journal of Bacteriology* **187**, 1792–8 (2005).

4. De, N., Navarro, M. V. a S., Raghavan, R. V. & Sondermann, H. Determinants for the activation and autoinhibition of the diguanylate cyclase response regulator WspR. *Journal of Molecular Biology* **393**, 619–33 (2009).

5. Pei, J. & Grishin, N. V. GGDEF domain is homologous to adenylyl cyclase. *Proteins* **42**, 210–6 (2001).

6. Sinha, S. C. & Sprang, S. R. Structures, mechanism, regulation and evolution of class III nucleotidyl cyclases. *Reviews of Physiology, Biochemistry and Pharmacology* **157**, 105–40 (2006).

7. Christen, M., Christen, B., Folcher, M., Schauerte, A. & Jenal, U. Identification and characterization of a cyclic di-GMP-specific phosphodiesterase and its allosteric control by GTP. *Journal of Biological Chemistry* **280**, 30829–37 (2005).

8. Schmidt, A. J., Ryjenkov, D. A. & Gomelsky, M. The ubiquitous protein domain EAL is a cyclic diguanylate-specific phosphodiesterase: enzymatically active and inactive EAL domains. *Journal of Bacteriology* **187**, 4774–81 (2005).

9. Barends, T. R. M. *et al.* Structure and mechanism of a bacterial light-regulated cyclic nucleotide phosphodiesterase. *Nature* **459**, 1015–8 (2009).

10. Rood, K. L., Clark, N. E., Stoddard, P. R., Garman, S. C. & Chien, P. Adaptor-dependent degradation of a cell-cycle regulator uses a unique substrate architecture. *Structure* **20**, 1223–32 (2012).

11. Paul, R. *et al.* Cell cycle-dependent dynamic localization of a bacterial response regulator with a novel di-guanylate cyclase output domain. *Genes & Development* **18**, 715–27 (2004).

12. Tschowri, N., Busse, S. & Hengge, R. The BLUF-EAL protein YcgF acts as a direct anti-repressor in a blue-light response of *Escherichia coli*. *Genes & Development* **23**, 522–34 (2009).

13. Aldridge, P. & Jenal, U. Cell cycle-dependent degradation of a flagellar motor component requires a novel-type response regulator. *Molecular Microbiology* **32**, 379–91 (1999).

14. Aldridge, P., Paul, R., Goymer, P., Rainey, P. & Jenal, U. Role of the GGDEF regulator PleD in polar development of *Caulobacter crescentus*. *Molecular Microbiology* **47**, 1695–708 (2003).

15. Wassmann, P. *et al.* Structure of BeF3- -modified response regulator PleD: implications for diguanylate cyclase activation, catalysis, and feedback inhibition. *Structure* **15**, 915–27 (2007).

16. Christen, B. *et al.* Allosteric control of cyclic di-GMP signaling. *Journal of Biological Chemistry* **281**, 32015–24 (2006).

17. Tarutina, M., Ryjenkov, D. a & Gomelsky, M. An unorthodox bacteriophytochrome from *Rhodobacter sphaeroides* involved in turnover of the second messenger c-di-GMP. *Journal of Biological Chemistry* **281**, 34751–8 (2006).

18. Nicollier, M. The influence of the bacterial second messenger c-di-GMP on cell cycle and pole development in *Caulobacter crescentus*. *Master Thesis, University of Basel, Faculty of Science* (2009).

19. Bucher, T. C-di-GMP is a key regulator of *Caulobacter crescentus* flagellum biosynthesis. *Master Thesis, University of Basel, Faculty of Science* (2011).

20. Minasov, G. *et al.* Crystal structures of YkuI and its complex with second messenger cyclic Di-GMP suggest catalytic mechanism of phosphodiester bond cleavage by EAL domains. *Journal of Biological Chemistry* **284**, 13174–84 (2009).

21. Guerrero-Ferreira, R. C. *et al.* Alternative mechanism for bacteriophage adsorption to the motile bacterium *Caulobacter crescentus*. *Proceedings of the National Academy of Sciences* **108**, 9963–8 (2011).

22. Duerig, A. *et al.* Second messenger-mediated spatiotemporal control of protein degradation regulates bacterial cell cycle progression. *Genes & Development* **23**, 93–104 (2009).

23. De, N. *et al.* Phosphorylation-independent regulation of the diguanylate cyclase WspR. *PLoS Biology* **6**, e67 (2008).

24. Zähringer, F., Massa, C. & Schirmer, T. Efficient enzymatic production of the bacterial second messenger c-di-GMP by the diguanylate cyclase YdeH from *E. coli*. *Applied Biochemistry and Biotechnology* **163**, 71–9 (2011).

25. Rao, F., Yang, Y., Qi, Y. & Liang, Z.-X. Catalytic mechanism of cyclic di-GMP-specific phosphodiesterase: a study of the EAL domain-containing RocR from *Pseudomonas aeruginosa*. *Journal of Bacteriology* **190**, 3622–31 (2008).

26. Feazel, L. M. *et al.* Opportunistic pathogens enriched in showerhead biofilms. *Proceedings of the National Academy of Sciences* **106**, 16393–9 (2009).

27. Shikuma, N. J., Fong, J. C. N. & Yildiz, F. H. Cellular Levels and Binding of c-di-GMP Control Subcellular Localization and Activity of the *Vibrio cholerae* Transcriptional Regulator VpsT. *PLoS pathogens* **8**, e1002719 (2012).

28. Bordeleau, E., Brouillette, E., Robichaud, N. & Burrus, V. Beyond antibiotic resistance: integrating conjugative elements of the SXT/R391 family that encode novel diguanylate cyclases participate to c-di-GMP signalling in *Vibrio cholerae*. *Environmental Microbiology* **12**, 510–23 (2010).

29. Solano, C. *et al.* Genetic reductionist approach for dissecting individual roles of GGDEF proteins within the c-di-GMP signaling network in *Salmonella*. *Proceedings of the National Academy of Sciences* **106**, 7997–8002 (2009).

30. Christen, M. *et al.* Asymmetrical distribution of the second messenger c-di-GMP upon bacterial cell division. *Science* **328**, 1295–7 (2010).

31. Navarro, M. V. A. S., De, N., Bae, N., Wang, Q. & Sondermann, H. Structural analysis of the GGDEF-EAL domain-containing c-di-GMP receptor FimX. *Structure* **17**, 1104–16 (2009).

32. Newell, P. D., Monds, R. D. & O'Toole, G. A. LapD is a bis-(3',5')-cyclic dimeric GMP-binding protein that regulates surface attachment by *Pseudomonas fluorescens* Pf0-1. *Proceedings of the National Academy of Sciences* **106**, 3461–6 (2009).

33. Newell, P. D., Boyd, C. D., Sondermann, H. & O'Toole, G. A c-di-GMP effector system controls cell adhesion by inside-out signaling and surface protein cleavage. *PLoS Biology* **9**, e1000587 (2011).

34. Navarro, M. V. a S. *et al.* Structural basis for c-di-GMP-mediated inside-out signaling controlling periplasmic proteolysis. *PLoS Biology* **9**, e1000588 (2011).

35. Lee, E. R., Baker, J. L., Weinberg, Z., Sudarsan, N. & Breaker, R. R. An allosteric self-splicing ribozyme triggered by a bacterial second messenger. *Science* **329**, 845–8 (2010).

36. Smith, K. D. *et al.* Structural basis of ligand binding by a c-di-GMP riboswitch. *Nature Structural & Molecular Biology* **16**, 1218–23 (2009).

37. Pratt, J. T., Tamayo, R., Tischler, A. D. & Camilli, A. PilZ domain proteins bind cyclic diguanylate and regulate diverse processes in *Vibrio cholerae*. *Journal of Biological chemistry* **282**, 12860–70 (2007).

38. Christen, M. *et al.* DgrA is a member of a new family of cyclic diguanosine monophosphate receptors and controls flagellar motor function in *Caulobacter crescentus. Proceedings of the National Academy of Sciences* **104**, 4112–7 (2007).

39. Mechold, U., Murphy, H., Brown, L. & Cashel, M. Intramolecular regulation of the opposing (p)ppGpp catalytic activities of Rel(Seq), the Rel/Spo enzyme from *Streptococcus equisimilis*. *Journal of Bacteriology* **184**, 2878–88 (2002).

40. Hogg, T., Mechold, U., Malke, H., Cashel, M. & Hilgenfeld, R. Conformational antagonism between opposing active sites in a bifunctional RelA/SpoT homolog modulates (p)ppGpp metabolism during the stringent response. *Cell* **117**, 57–68 (2004).

41. Ely, B. Genetics of *Caulobacter crescentus. Methods in Enzymology* **204**, 372–84 (1991).

42. Jenal, U. & Shapiro, L. Cell cycle-controlled proteolysis of a flagellar motor protein that is asymmetrically distributed in the *Caulobacter* predivisional cell. *The EMBO Journal* **15**, 2393–406 (1996).

43. Lillehaug, D. An improved plaque assay for poor plaque-producing temperate lactococcal bacteriophages. *Journal of Applied Microbiology* **83**, 85–90 (1997).

44. Sliusarenko, O., Heinritz, J., Emonet, T. & Jacobs-Wagner, C. High-throughput, subpixel precision analysis of bacterial morphogenesis and intracellular spatio-temporal dynamics. *Molecular Microbiology* **80**, 612–27 (2011).

45. Evinger, M. & Agabian, N. Envelope-associated nucleoid from *Caulobacter crescentus* stalked and swarmer cells. *Journal of Bacteriology* **132**, 294–301 (1977).

46. Poindexter, J. S. Biological properties and classification of the *Caulobacter* group. *Bacteriological Reviews* **28**, 231–95 (1964).

47. Thanbichler, M., Iniesta, A. & Shapiro, L. A comprehensive set of plasmids for vanillate- and xylose-inducible gene expression in *Caulobacter crescentus*. *Nucleic Acids Research* **35**, e137 (2007).

Figure Legends

Figure 1: Deletions of PleD, DgcB, BipB and CC0857 lead to phenotypes associated with low c-di-GMP levels in *C. crescentus*.

Analysis of *C. crescentus* strains lacking the cyclases PleD, DgcB, BipB and CC0857 in different combinations. The rGS was used as control for c-di-GMP concentrations under the detection limit. The results of all assays were normalized to the wild-type (WT).

A. The effect of several DGC deletions in *C. crescentus* in regard to motility (dark grey bars on the left) and attachment to surfaces (light grey bars on the right). For some deletion mutants the swarmer colony was indicated for colony morphology comparisons.

B. Immunoblot analysis for quantification of FlgH protein levels in the different mutants in regard to the ability to synthesize a functional flagellum.

C. The susceptibility towards phage ϕCBK that uses pili as a receptor was tested to confirm intact pili formation and flagellum rotation. The plaques refer to different dilutions of the phage lysates (1:10 ratio).

D. The susceptibility of different DGC deletion mutants towards phage ϕCR30 (1:10 ratio) that uses the crystalline S-layer of *C. crescentus* as a receptor was tested.

E. The ability to separate different cell populations (swarmer cells from stalked and predivisional cells) in a cell density gradient centrifugation due to proper capsule formation was analyzed.

F. Statistical distribution of PopA localization within the different mutants. Due to the diverse localization behavior of PopA, different amounts of intracellular foci can be distinguished (0, 1, 2 foci). To differentiate between PodJ and c-di-GMP dependent foci distribution an I-site mutant of PopA was used as a control that exhibits only a PodJ dependent localization pattern.

Figure 2: BipB and CC0857 enzyme activities can complement phenotypes caused by the absence of c-di-GMP

A. Reinsertion of *bipB* or *CC0857* into the rGS under their native promotor changed cell morphology from an elongated form that was found in the rGS to a normal shaped form comparable to wild-type-like cell morphology exhibiting a stalk (left micrograph).

B. Motility analysis showed that insertion of *bipB* in the rGS resulted in an increase on the swarming size on semi-solid agar plates compared to the rGS although not to wild-type extent. However, reinsertion of *CC0857* did not change colony size.

C. Immunoblot assay for determination of FlgH protein levels in the rGS_*bipB* or rGS_*CC0857* strains revealed that both strains expose FlgH levels like the wild-type. To rule out loading mistakes a loading control was indicated.

D. and E. The susceptibility towards phage ϕCBK and ϕCR30 was tested using different dilutions of the phage lysates (1:10 ratio).

Figure 3: Synchronization of cells harboring a copy of BipB or CC0857 in a c-di-GMP free background

A. The ability to separate swarmer and stalked cells of the rGS_ *bipB* and rGS_ *CC0857* strains in a cell density gradient centrifugation due to proper capsule formation was analyzed.

B. An immunoblot of synchronized rGS_ *bipB* cultures was performed to follow BipB levels during the cell cycle. The α-CtrA and α-CcrM immunoblots were used as positive controls and served as indication for the performance of cell synchronization.

C. rGS cells containing a copy of *CC0857* were separated in a cell density gradient centrifugation and α-CtrA and α-CcrM levels were followed on immunoblots to define the performance of cell synchronization.

Figure 4-5: BipB is a bifunctional composite protein with DGC and PDE activity that is substrate inhibited

Phenotypic characterization of cells harboring a copy of BipB and different active site mutants in a GS (Figure 4) and in an rGS background (Figure 5) in *C. crescentus*.

A. Behavior of wild-type and c-di-GMP signaling mutants of BipB in regard to motility (dark grey bars), attachment (middle grey bars) and intracellular c-di-GMP synthesis (light grey bars).

B. The ability of the c-di-GMP free strains containing BipB and its mutants to produce two different populations (SW and ST cells) that are separable in a cell density gradient centrifugation was tested.

C. The sensitivity to the bacteriophage ϕCBK in the c-di-GMP free strains containing BipB and its mutants was tested in a phage-spotting assay using different dilutions of the phage lysates (1:10).

D. The sensitivity to the bacteriophage ϕCR30 in the GS and rGS strains containing BipB and its mutants was tested in a phage-spotting assay using different dilutions of the phage lysates (1:10).

E. Analysis of subcellular localization of PopA in a mixed population of c-di-GMP free strains containing BipB and its mutants in *C. crescentus*. The relative numbers of fluorescent foci at the poles depends on PodJ or c-di-GMP dependent PopA localization. The y-axis represents the number of cells used for microscopy in % and the x-axis indicates the number of foci detected in the cells.

Figure 6: BipB exhibits DGC and PDE activity

Product progression profiles of BipB incubated with GTP (A) and with c-di-GMP (B).

C. Saturation curves for BipB upon incubation with GTP (blue curve) and c-di-GMP (red curve), respectively. These data were fitted with the Michaelis-Menten equation in order to determine the kinetic parameter K_m and k_{cat}.

Figure 7: Proposed model for BipB bifunctional activities

A model suggesting a regulation for BipB DGC or PDE activity in response to c-di-GMP concentration.

A. Low c-di-GMP levels favor BipB DGC where the GGDEF domain (white ellipsoid representation) forms a dimer with the A-site of each monomer facing each other in a GTP bound conformation.

B. High c-di-GMP concentrations promote an inactive DGC conformation where the I-sites of each monomer face each other leading to a spatial separation of the the A-sites. Two c-di-GMP molecules are bound to each I-site leading to a PDE active state where the EAL domains are in close proximity to each other forming a dimer. Each EAL domain binds a c-di-GMP molecule leading to hydrolysis into the linear product pGpG.

Figure S1: Deletions of PleD, DgcB, BipB and CC0857 lead to low c-di-GMP levels and misslocalization of popA at the stalked pole in C. crescentus

Micrographs of the strains used in 1.F to see the difference in popA localization and fluorescence intensity in the mutant strains. The micrographs observed in the GFP channel are shown on the left and on the right the same view with phase contrast.

Figure S2: Protein level quantification of BipB and BipB mutant strains in the GS and rGS strains

Quantification of cellular BipB and FlgH protein levels in *C. crescentus* wild-type and mutant strains determined by immunoblot assay (upper lane).

Figure 1

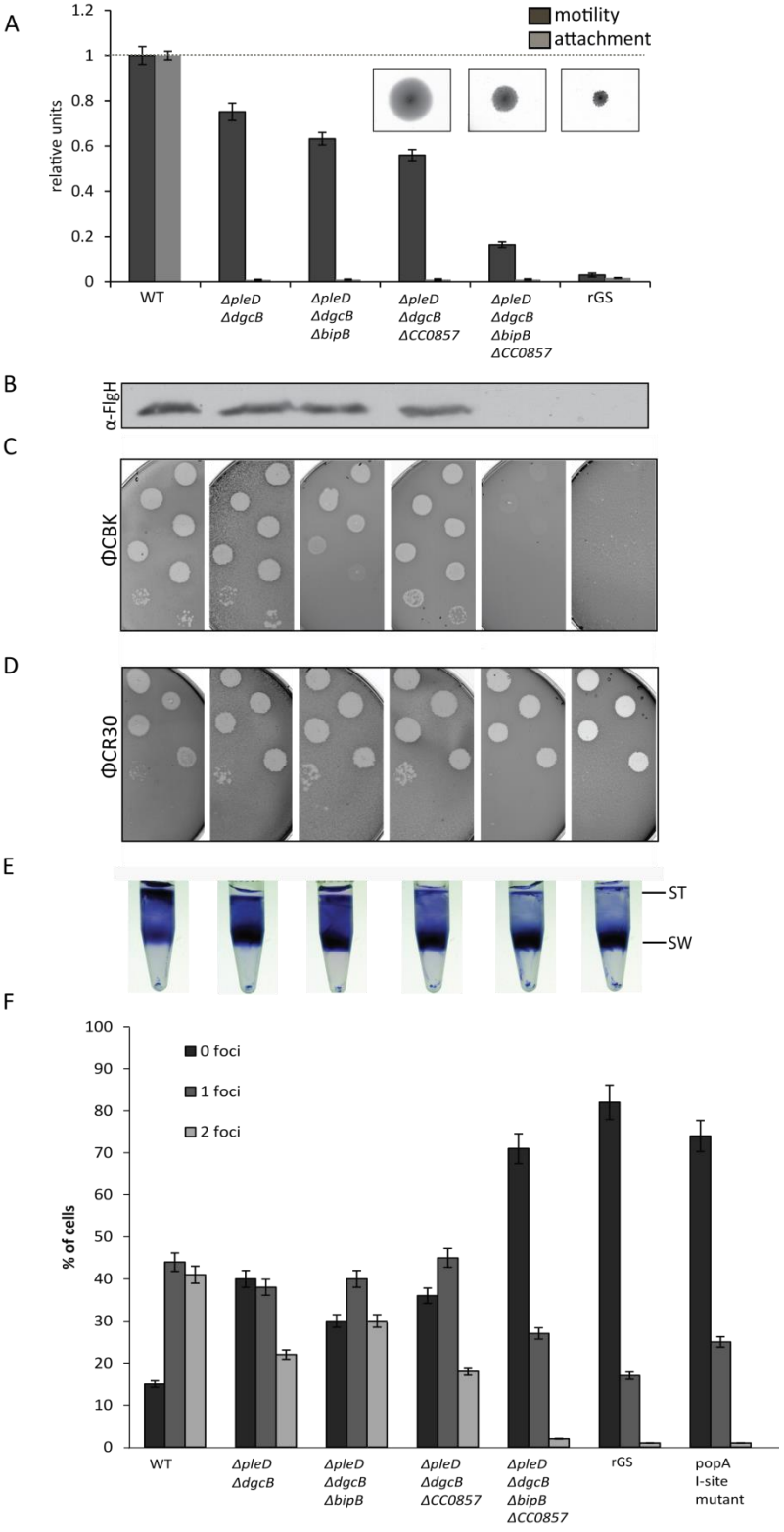
A
motility
attachment
relative units
1.2
1
0.8
0.6
0.4
0.2
0
WT
ΔpleD ΔdgcB
ΔpleD ΔdgcB ΔbipB
ΔpleD ΔdgcB ΔCC0857
ΔpleD ΔdgcB ΔbipB ΔCC0857
rGS
B
α-FlgH
C
ΦCBK
D
ΦCR30
E
ST
SW
F
0 foci
1 foci
2 foci
% of cells
100
90
80
70
60
50
40
30
20
10
0
WT
ΔpleD ΔdgcB
ΔpleD ΔdgcB ΔbipB
ΔpleD ΔdgcB ΔCC0857
ΔpleD ΔdgcB ΔbipB ΔCC0857
rGS
popA I-site mutant

Figure 2

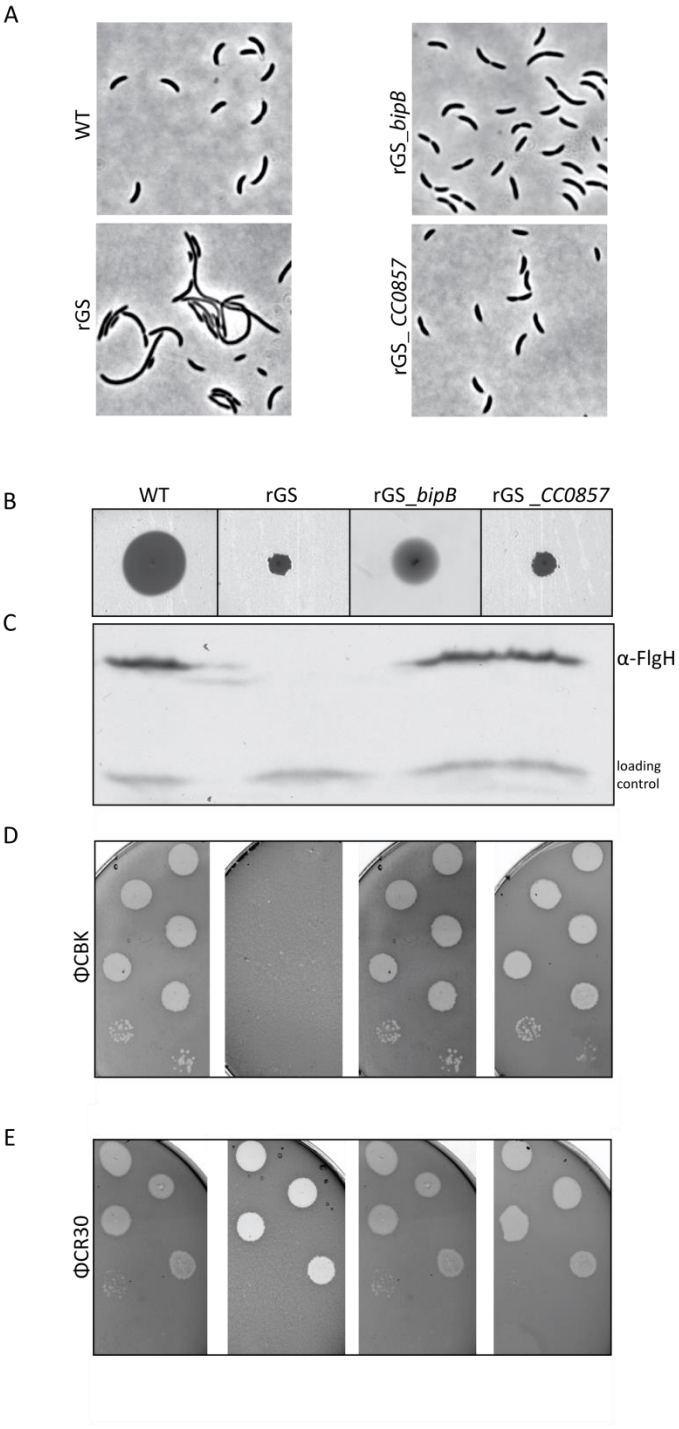
A
WT
rGS
rGS_bipB
rGS_CC0857
B
WT
rGS
rGS_bipB
rGS _CC0857
C
α-FlgH
loading control
D
ΦCBK
E
ΦCR30

Figure 3

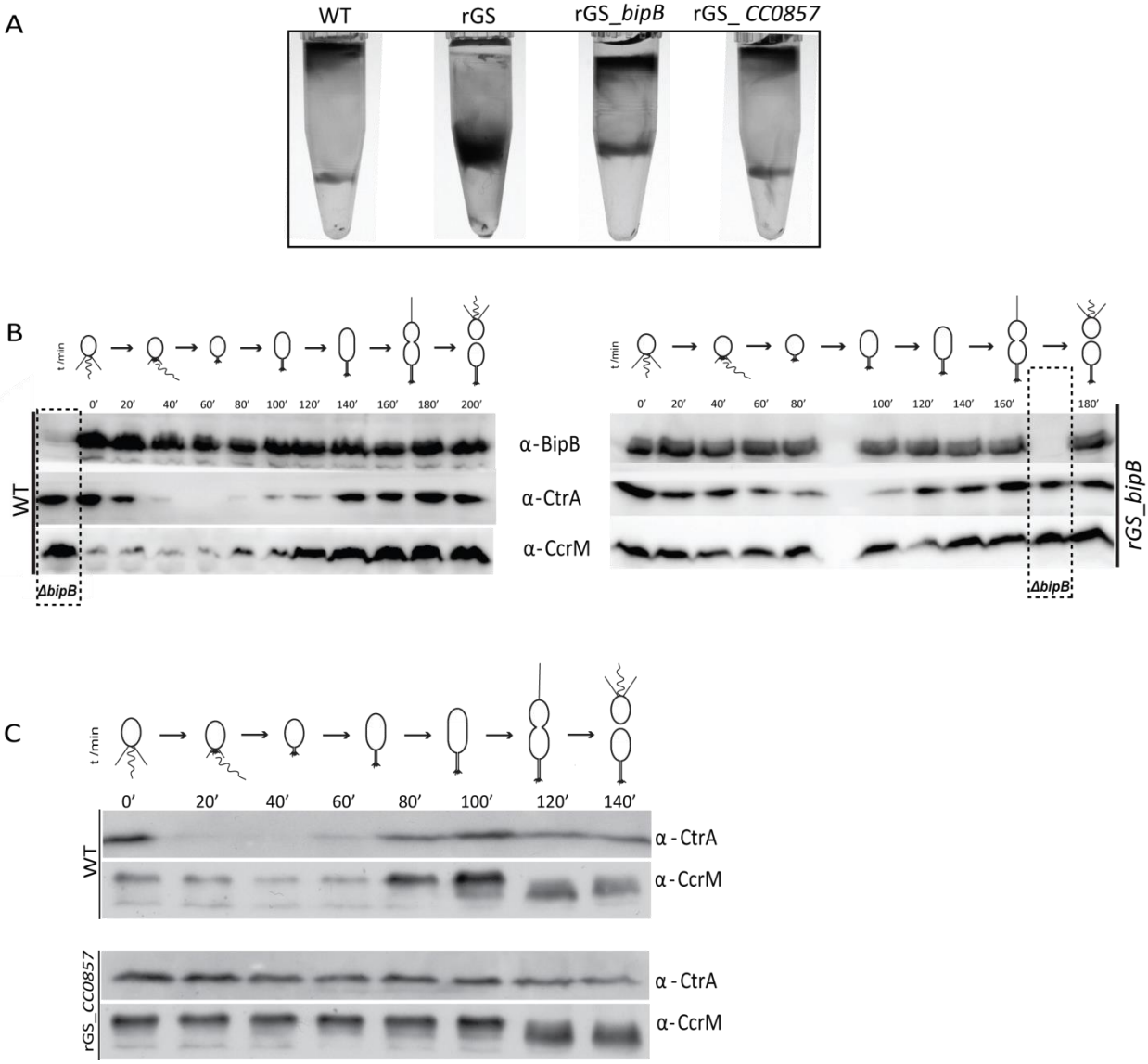
A
WT
rGS
rGS_bipB
rGS_ CC0857
B
t /min
0′ 20′ 40′ 60′ 80′ 100′ 120′ 140′ 160′ 180′ 200′
WT
ΔbipB
α-BipB
α-CtrA
α-CcrM
0′ 20′ 40′ 60′ 80′ 100′ 120′ 140′ 160′ 180′
rGS_bipB
ΔbipB
C
t /min
0′ 20′ 40′ 60′ 80′ 100′ 120′ 140′
WT
α-CtrA
α-CcrM
rGS_CC0857
α-CtrA
α-CcrM

Figure 4

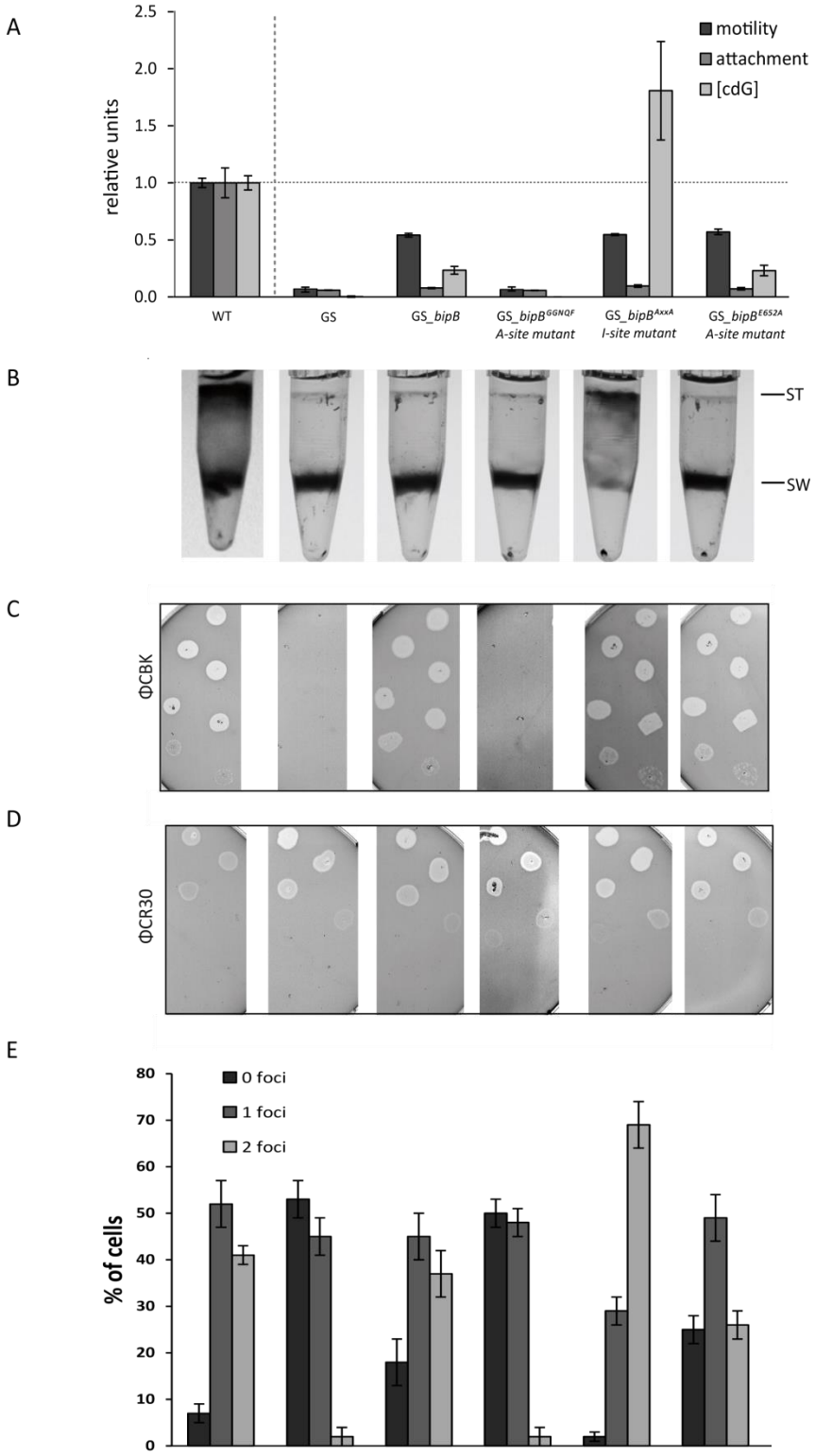
A
relative units
2.5
2.0
1.5
1.0
0.5
0.0
motility
attachment
[cdG]
WT
GS
GS_bipB
GS_bipB^GGNQF
A-site mutant
GS_bipB^AxxA
I-site mutant
GS_bipB^E652A
A-site mutant
B
ST
SW
C
ΦCBK
D
ΦCR30
E
% of cells
80
70
60
50
40
30
20
10
0
0 foci
1 foci
2 foci

Figure 5

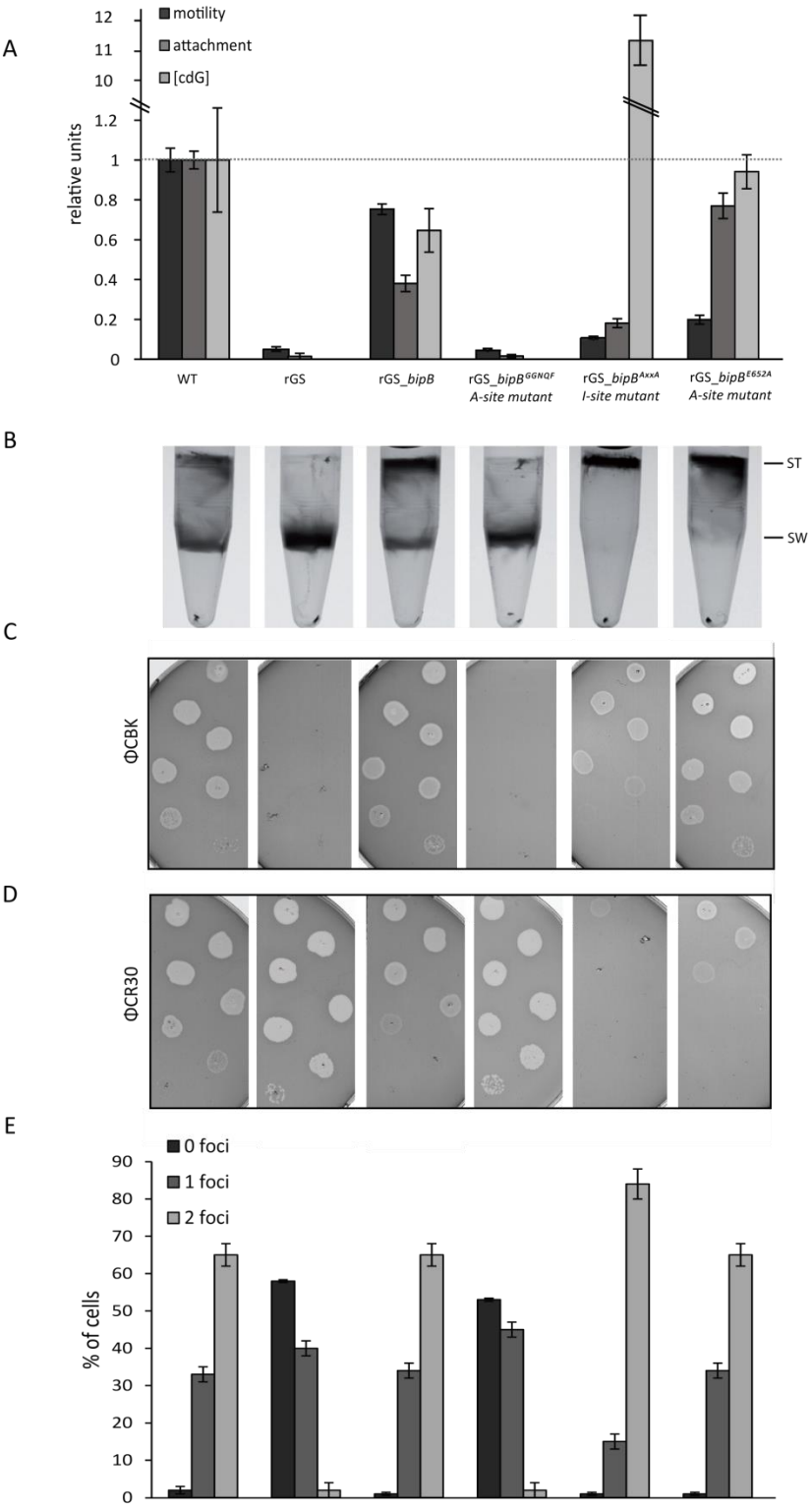
A
motility
attachment
[cdG]
relative units
12
11
10
1.2
1
0.8
0.6
0.4
0.2
0
WT
rGS
rGS_bipB
rGS_bipB^GGNQF
A-site mutant
rGS_bipB^AxxA
I-site mutant
rGS_bipB^E652A
A-site mutant
B
ST
SW
C
ΦCBK
D
ΦCR30
E
0 foci
1 foci
2 foci
% of cells
90
80
70
60
50
40
30
20
10
0

Figure 6

A

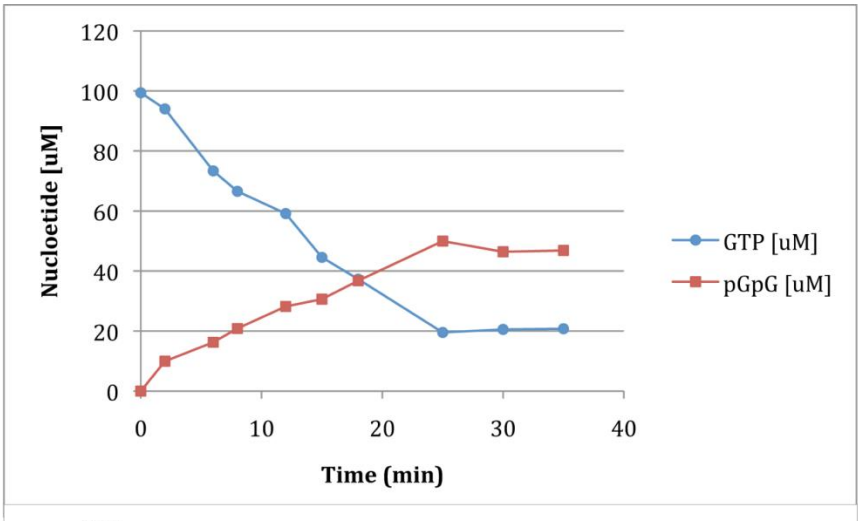
Nucloetide [uM]
120
100
80
60
40
20
0
0
10
20
30
40
Time (min)
GTP [uM]
pGpG [uM]

B

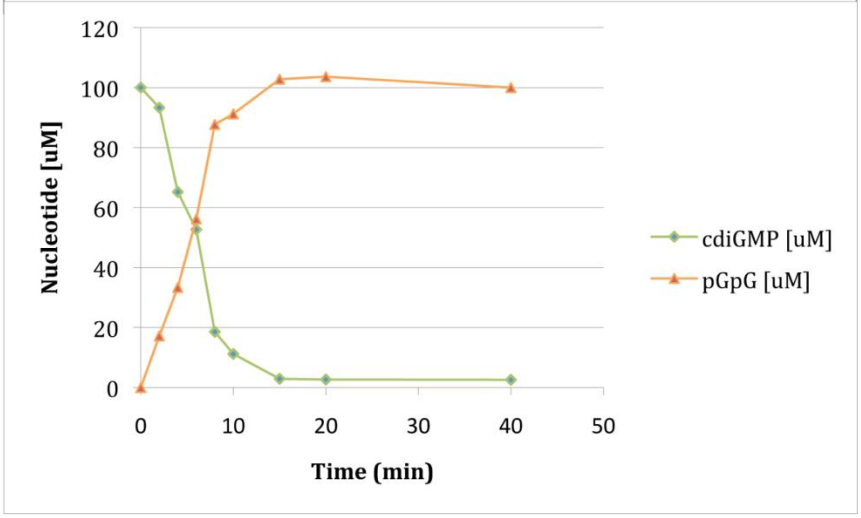
Nucleotide [uM]
120
100
80
60
40
20
0
0
10
20
30
40
50
Time (min)
cdiGMP [uM]
pGpG [uM]

C

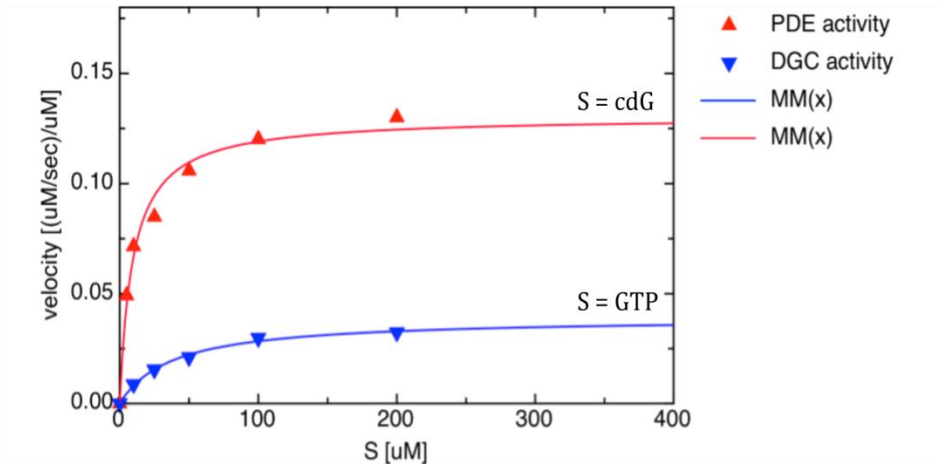
velocity [(uM/sec)/uM]
0.15
0.10
0.05
0.00
0
100
200
300
400
S [uM]
S = cdG
S = GTP
PDE activity
DGC activity
MM(x)
MM(x)

Figure 7

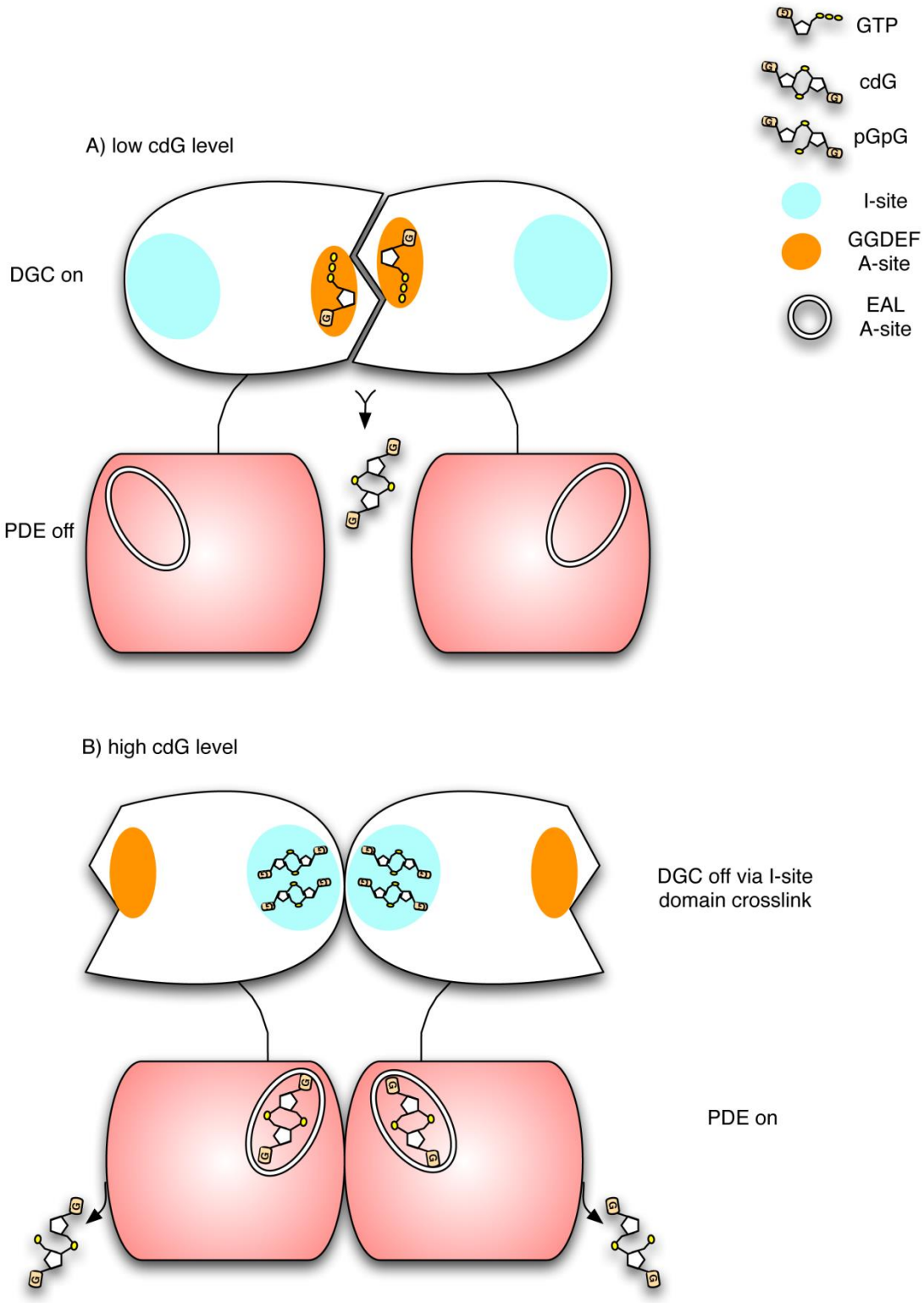
GTP
cdG
pGpG
I-site
GGDEF
A-site
EAL
A-site
A) low cdG level
DGC on
PDE off
B) high cdG level
DGC off via I-site
domain crosslink
PDE on

Figure S1

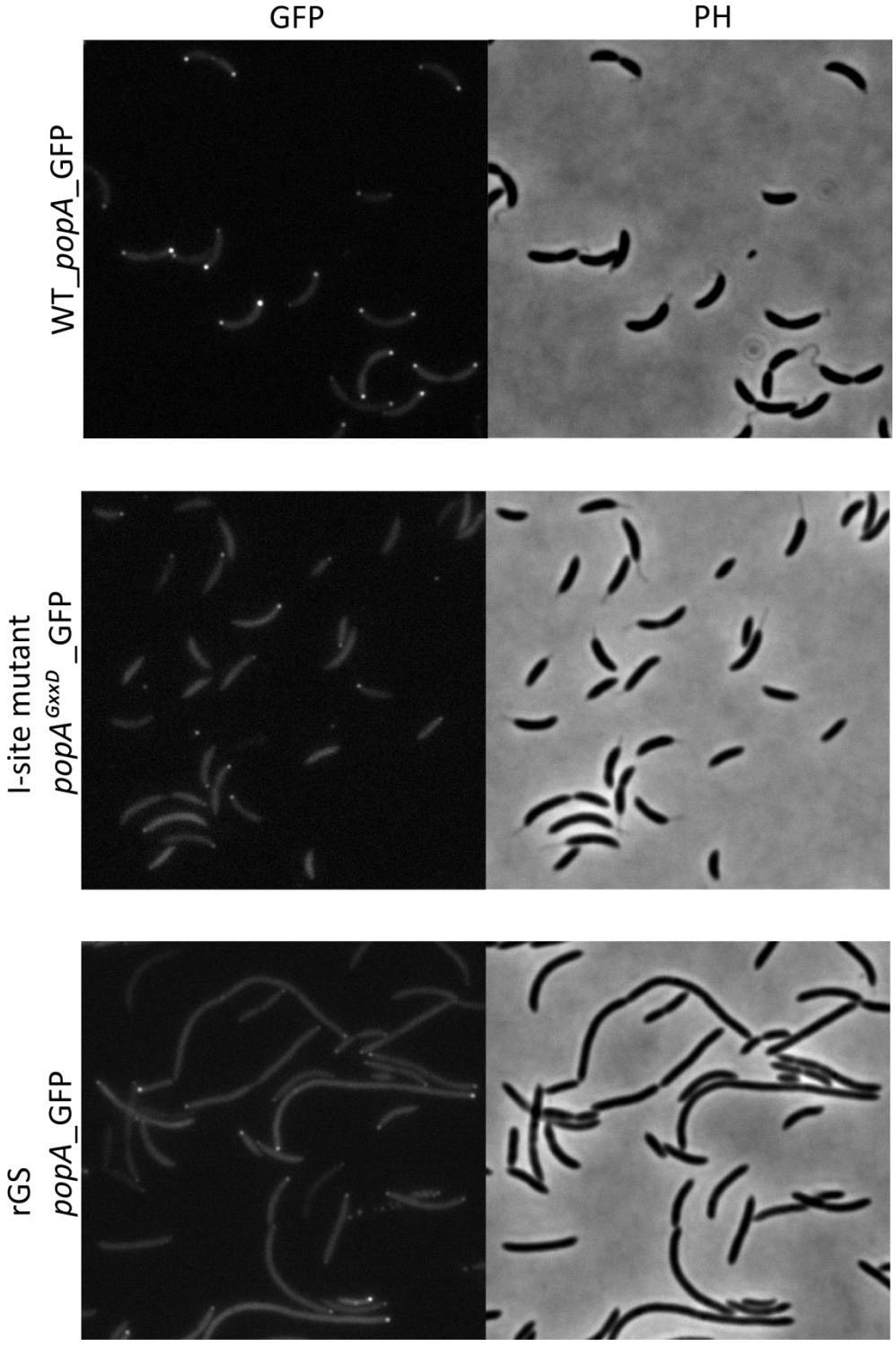

Figure S2

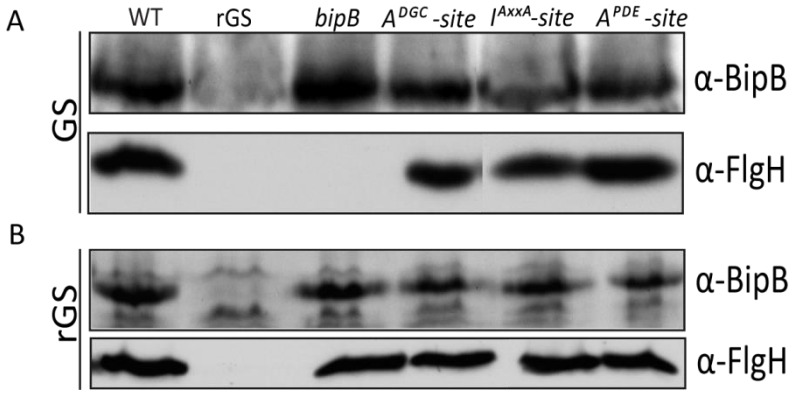
A
WT
rGS
bipB
A^DGC-site
I^AxxA-site
A^PDE-site
GS
α-BipB
α-FlgH
B
rGS
α-BipB
α-FlgH

Table 1: Enzymatic constants of BipB and its mutants

	K_m for GTP [µM]	K_m for c-di-GMP [µM]	DGC activity k_{cat} [sec^{-1}]	PDE activity k_{cat} [sec^{-1}]
BipB (WT)	37.7 ± 4.6	9.5 ± 1.5	0.039 ± 0.002	0.130 ± 0.005
$BipB^{GGAQF}$	-	12.1 ± 1.1	-	3.20 ± 0.08
$BipB^{E652A}$	-	-	inhibited (<0.01)	-
$BipB^{AxxA}$	65.8 ± 10.4	10.1 ± 1.1	1.0 ± 0.06	0.10 ± 0.005

Table 2: Strains used in this study

Caulobacter crescentus Strains

Name	Description	Reference
NA1000	WT; synchronizable laboratory strain of CB15 (CB15N)	[45]
NA1000_rGS	Markerless in frame deletions of *cc0091, cc0655, cc0740, CC0857, cc0896, cc1086, cc1850, cc2462, cc3094, cc3148, cc3285, cc3396* in NA1000	Abel, unpublished
UJ5934*	Holdfast positive strain of NA1000_rGS	This study
UJ6098*	NA1000 Δ*pleD* Δ*dgcB*	This study
UJ6100*	NA1000 Δ*pleD* Δ*dgcB* Δ*bipB*	This study
UJ6338*	NA1000 Δ*pleD* Δ*dgcB* Δ*CC0857*	This study
UJ6278*	NA1000 Δ*pleD* Δ*dgcB* Δ*bipB* Δ*CC0857*	This study
UJ6498*	NA1000 and plasmid pAD5	This study
UJ4254	NA1000 *popA* I-site^{GxxD} mutant and plasmid pAD5	[22]
UJ4445	NA1000 Δ*CC0857*	S. Abel
UJ6264	NA1000 rGS_ *CC0857* (NA1000 rGS::pLW151 *CC0857*$^{+}$)	This study
UJ6099*	NA1000 Δ*bipB*	This study
UJ5935*	NA1000 rGS_ *bipB*	This study
UJ5936*	NA1000 rGS_ *bipB*^{GGNQF} A-site mutant	This study
UJ5938*	NA1000 rGS_ *bipB*^{AxxA} I-site mutant	This study
UJ5939*	NA1000 rGS_ *bipB*^{E652A} A-site mutant	This study
CB15	WT; ATCC 19089	[46]
CB15_GS	Markerless in frame deletions of *cc1850, cc0740, CC0857, cc3285, cc3094, cc0655, cc0896, cc2462* in CB15	M. Nicollier
UJ5925	CB15 GS_ *bipB*	This study
UJ5883	CB15 GS_ *bipB*^{GGAQF} A-site mutant	This study
UJ5885	CB15 GS_ *bipB*^{AxxA} I-site mutant	This study
UJ5886	CB15 GS_ *bipB*^{E652A} A-site mutant	This study

* holdfast positive NA1000 strains

E. coli strains

Name	Description	Reference
DH10B	Tc::Mu-Tn7	[45]
S17.1	F-, lambda (-), thi, pro, recA, restriction (-) modification (+),RP4, derivative integrated into the chromosome with Tet::Mu, Km::T7	[45]
BL21 (DE3)	Expression host for pET21 vectors; genomic integrated T7-RNApolymerase under control of lac promoter; deficient in Lon and OmpT protease	Novagen

Table 3: Plasmids used in this study

pAD5	pMR20; popA-Gfp under the control of the native popA promotor		[22]
pNPTS138	Kan^R, suicide vector with sacB gene and oriT		D. Alley
pEF50	pNPTS138; $bipB^{AxxA}$ I-site mutant R340A and D343A	Template pEF49; 3383 (NheI) and 3386 (HindIII)	This study
pEF55	pNPTS138; $bipB^{GGNQF}$ A-site mutant	Template pEF57; 3424 (NheI) and 3425 (HindIII)	This study
pEF63	pNPTS138; $bipB^{E652A}$ A-site mutant	Template NA1000; 3427 (NheI) + 76 and 75 + 3426 (HindIII)	This study
pMT727	pRVGFPC_5; pGFP; Tet^R, Pvan low copy replicating plasmid		[47]
pEF73	pMT727 ; bipB_GFP	primer 3886 (NdeI) and 3887 (KpnI)	This study
pET21b	overexpression plasmid; AmpR		Novagen
pbipB-His	pET21b; bipB	Template NA1000; 48 (NdeI) + 49 (XhoI)	This study
pEF76	pET21b; $bipB^{GGAQF}$ A-site mutant	template pEF59; 48 (NdeI) + 49 (XhoI)	This study
pEF77	pET21b; $bipB^{E652A}$ A-site mutant	template pEF62; 48 (NdeI) + 49 (XhoI)	This study
pEF49	pET21b; $bipB^{AxxA}$ I-site mutant R340A and D343A	template NA1000; 48 (NdeI) + 3418 and 3419 +49 (XhoI)	This study

Table 4: Oligos used in this study

Oligo	Sequence	Description
3383	AAAAGCTAGCCGCTCAGCGGGTCTGGCG	pNPTS138 bipB IRxxD-site mutant R340A and D343A; pEF49 as template
3386	TTTTAAGCTTGACGTTCTCGGTGACCTCG	pNPTS138 bipB IRxxD-site mutant R340A and D343A; pEF49 as template
3424	AAAGCTAGCCGGGCGCTCAGCGGG	pNPTS138 bipB ADGC-site mutant; pEF57 as template
3425	TTTAAGCTTTCGCTGACCAGGTCAGAGC	pNPTS138 bipB ADGC-site mutant; pEF57 as template
3427	AAAGCTAGCGGGCCAAGGAGGCGG	pNPTS138 APDE-site mutant E652A; NA1000 as template; 1st PCR
76	CGTCCTCGACGCCGGCGGCCACCACCTTCATGC	pNPTS138 APDE-site mutant E652A; NA1000 as template; 1st PCR
75	GCATGAAGGTGGTGGCCGCCGGCGTCGAGGACG	pNPTS138 APDE-site mutant E652A; NA1000 as template; 2nd PCR
3426	TTTAAGCTTCGCCGCAAGCCGGCAGC	pNPTS138 APDE-site mutant E652A; NA1000 as template; 2nd PCR
3887	TTTTGGTACCGCCGCCAAAC	with oligo 3386 for pEF73; bipB_GFP
48	AATTACATATGAAGACTCAAGCCTTGGCTGTCCGA	pET21b bipB APDE-site mutant E652A (pEF77); pEF62 as template
49	TATATCTCGAGGCCGCCAAACCCCTTCAGGAAC	pET21b bipB APDE-site mutant E652A (pEF77); pEF62 as template
3418	CGCGACGGTGGCGCCGGTCGCGAAGGCGTGC	with oligo 48 for pEF49; bipB_I-site on pET1b;NA1000 as template; 1st PCR
3419	GCACGCCTTCGCGACCGGCGCCACCGTCGCG	with oligo 49 for pEF49; bipB_I-site on pET1bNA1000 as template; 2nd PCR

Oligo 48, 49, 75, 76 were designed by C. Massa.

3.2 An unorthodox response regulator binds c-di-GMP to control motility in *Caulobacter crescentus*

Jutta Nesper[1], Elvira Friedrich[1], Eric Hajjar[2], Thorsten Schwede[2] and Urs Jenal[1]

Affiliations:

[1] Biozentrum of the University of Basel, Klingelbergstrasse 50, CH-4054 Basel, Switzerland

[2] SIB Swiss Institute of Bioinformatics, Biozentrum University of Basel, CH-4054 Basel, Switzerland

For correspondence: urs.jenal@unibas.ch

Keywords: *Caulobacter crescentus*; c-di-GMP effector; Motility; Chemotaxis; Capture Compound mass spectrometry

Statement of my work

All plasmids and strains for bacterial two-hybrid and plasmid pEF84 used in this study have been generated by me. I also performed the following assays of this study: the phylogenetic tree analysis (S1B), phage-spotting analysis (Figure S2A), cell density gradient centrifugation (Figure S2C), motility (Figure S3A), Western-blot analysis (Figure 3, S3B). Phase-contrast/-fluorescence microscopy (Figure 4, 5, S4) and the bacterial two-hybrid assay (Figure S5).

Abstract

The second messenger c-di-GMP controls a variety of cellular processes of the motile-sessile transition in bacteria. Typically, high cellular concentrations of c-di-GMP promote surface adherence and biofilm formation, whereas low c-di-GMP levels promote single cell behavior and sanction flagellar-based motility. Recent studies in *Escherichia coli* have suggested that flagellar motors can be curbed through a c-di-GMP bound PilZ domain effector that directly interacts with motor proteins powering rotation. In *Caulobacter crescentus*, reduced levels of c-di-GMP are critical for the motile behavior of its swarmer cell progeny. Mutants that lack the swarmer cell specific phosphodiesterase PdeA, show poor motility, however the molecular basis for motor control is unknown.

Here we used the Capture Compound mass spectrometry proteomics approach to identify c-di-GMP binding proteins involved in *C. crescentus* motility control. We identified two members of an unusual subfamily of response regulators that share an arginine-rich stretch adjacent to their receiver domain. One of these proteins, CC3100, was shown to bind c-di-GMP specifically and with high affinity (K_d 212 nM). Deletion of the *CC3100* gene restored motility of a *pdeA* mutant, arguing that its product is responsible for motor obstruction at high c-di-GMP levels. We show that CC3100 is present only in flagellated swarmer cells and that components of the flagellar basal body are required for the dynamic polar localization of CC3100. This argues that CC3100 mediates motor performance in *C. crescentus* in response to fluctuating levels of c-di-GMP.

Introduction

Cyclic-di-GMP (c-di-GMP) is a ubiquitous second messenger that regulates several cellular processes in a wide range of gram-positive and gram-negative bacteria. In particular, it promotes the switch from a motile planktonic to a biofilm lifestyle. The synthesis of c-di-GMP is catalyzed by the GGDEF domains of diguanylate cyclases (DGC) and the degradation by EAL or HD-GYP domain containing phosphodiesterases (PDE). The cellular processes regulated by the c-di-GMP signaling pathway are modulated by c-di-GMP binding proteins or RNA. Several effectors are meanwhile characterized but as there is no common domain or c-di-GMPbinding site there is still a lack of knowledge[1-3]. Recently, progress was achieved, when two different chemical proteomics approaches were reported to be useful for the identification of novel c-di-GMP binding proteins[4,5].

In general, when cellular c-di-GMP levels are high bacteria form a biofilm, whereas at low physiological c-di-GMP concentrations they are in a motile planktonic state. Bacterial swimming behavior is promoted by rotating flagella that are driven by the flagellar motor. The driving force is powered by a proton flux across inner membrane channels composed of a complex of MotA and MotB. These are two stator proteins arranged around the MS- and C-rings, that span the inner membrane of the flagellar motor[6]. The MS-ring of the flagellar basal body consists of multiple copies of the transmembrane protein FliF[7]. The C-ring is composed of different copy numbers of three proteins: FliG, FliM and FliN[8]. The interaction of the soluble cytoplasmic protein FliG with FliF is responsible for both transmission of torque and control of the rotational direction of the flagellum[9].

Motility is both, positively and negatively, controlled by c-di-GMP effectors at different levels. The response regulator (RR) VpsT from *Vibrio cholerae* binds c-di-GMP via its non-canonical receiver domain and represses genes involved in motility[10]. TipF of *C. crescentus* binds c-di-GMP with its degenerate EAL domain (Cohen *et al*. unpublished) and promotes flagellar assembly[11]. *E. coli* adjusts its swimming speed *via* the molecular brake YcgR[12]. This effector protein contains a PilZ domain and binds c-di-GMP with high affinity[13]. C-di-GMP bound YcgR interacts with the motor protein MotA, leading to changes of the electrostatic interactions between MotA and the rotor protein FliG and hence curbs flagellar rotation[12].

Bacteria also make use of c-di-GMP independent mechanisms to control their motility behavior. The gram-positive bacterium *Bacillus subtilis* uses a molecular clutch, EpsE, to disable the rotation of its flagellar bundle during biofilm formation. EpsE, a putative family II glycosyltransferase, located within an operon encoding enzymes of extracellular polysaccharide production, alters the interaction between the switch protein FliG and the stator protein MotA to stop the rotation of the flagellum[14]. Flagellar rotation is controlled by the chemotaxis pathway, allowing bacteria to escape from less attractive places and swim towards and grow in nutrient-rich environments. Bacteria occupy different environmental niches and therefore, they dispose different amounts of flagella or show different swimming behaviors. Surprisingly, the genes required for chemotaxis are highly conserved[15]. The mediator between chemoreceptor and the output organelle, the flagellar switch, is a two-component regulatory system[15]. To reorient the direction, bacteria carrying bidirectional motors, like *E. coli*, activate tumbling via autophosphorylation of the histidine kinase (HK) CheA. The phosphoryl-group is then transferred to conserved aspartate residues in the receiver domains of the RRs CheB and CheY[16]. The phosphorylated CheY interacts strongly with the flagellar motor switch protein FliM and enables *E. coli* to change its direction by clockwise flagellar rotation. The antagonist of CheA is CheZ, a phosphatase responsible for dephosphorylation of CheY-P and therefore change to counterclockwise rotation[17]. The α-proteobacterium *Rhodobacter sphaeroides* exposes only a single unidirectional-driven flagellum, that periodically briefly stops its rotation, and due to Brownian motion, re-orientates the cell in a new direction[18]. Similar to *E. coli* this is controlled by the chemotaxis system and CheY-P binding to FliM. However, the binding induces a conformational change that alters the rotor-stator interface and stops the motor in a brake-like mechanism[19].

The aquatic α-proteobacterium *C. crescentus* has a dimorphic life cycle and divides asymmetrically. The stalked cell is sessile, while the swarmer cell is chemotactically active and motile due to rotation of its single polar flagellum[20]. *C. crescentus* encodes a large number of proteins putatively involved in chemotaxis. Some of the chemotaxis (che) genes are located in one of two che operons, but a large number is distributed over the whole chromosome[21]. Interestingly, not all of the annotated *che* genes are essential for chemotaxis and in fact only one of the two operons was linked so far to chemotaxis[20]. The flagellum is assembled at a

specific time point during the cell cycle and later on ejected into the medium and this programmed and cell cycle-dependent process is controlled by c-di-GMP[22]. Recently evidence was found that c-di-GMP also directly controls flagellar motility of *C. crescentus*. A strain lacking the swarmer cell-specific PDE PdeA possesses elevated levels of c-di-GMP in the swarmer cells. Despite the presence of a flagellum, cells are unable to spread on semi-solid agar plates. In a screen for spontaneous motile suppressors DGCs and PDEs were identified that re-adjusted the cellular c-di-GMP level[23]. Although predicted, neither flagellum proteins nor c-di-GMP effectors involved in this control could be identified in this screen.

We performed Capture Compound mass spectrometry (CCMS)[4] to identify novel c-di-GMP proteins of *C. crescentus*. Two receiver domain proteins belonging to an unusual subfamily of RRs bound specifically to the c-di-GMP Capture Compound. Within this family four proteins are annotated as CheYIII. In this study, we investigated in particular the fifth protein of this subfamily, CC3100. CC3100 is an unorthodox RR that presumably does not become phosphorylated because of a mutation in the receiver domain. Instead, CC3100 is linked to the c-di-GMP signaling pathway and we show here that CC3100 binds c-di-GMP specifically and with high affinity. Furthermore, we present evidence that CC3100 is involved in c-di-GMP-mediated motility control by binding to flagellar proteins.

Results

The unorthodox RR CC3100 is a novel c-di-GMP binding protein

To screen for novel effectors, we used the c-di-GMP Capture Compound in combination with mass-spectrometry[4] and identified specifically and repeatedly two RRs, CC1364 and CC3100 (Table 1). The two proteins are grouped with three other RR (CC0440, CC2249 and CC3155) in a subfamily ([24], http://www.ncbi.nlm.nih.gov/Complete_Genomes/SigCensus/RECalpha2010.html). In addition to the conserved amino acids (aa) of the receiver domain they share an arginine-rich region of 29 aa (Supplementary Figure 1A). All but CC3100 are annotated as CheYIII proteins and in a phylogenetic tree that is based on receiver domain residues only, and they cluster with 9 of 11 *C. crescentus* proteins annotated as CheY (Supplementary Figure 1B). The receiver domain of CC3100 is more related to the receiver domains of three OmpR-type RRs. However, instead of a DNA-binding motif CC3100 carries a domain of unknown function and with low structural homology to known proteins. In addition, not all residues of the active site of the receiver domains[25] are conserved in CC3100 (Supplementary Figure S1A). Notably, the predicted site of phosphorylation is exchanged from Asp to Glu suggesting that CC3100 cannot get phosphorylated. In contrast, the active-site residues of the receiver domain of the other four CheYIII proteins are intact.

To determine whether all five proteins of this specific subfamily of RR bind c-di-GMP, we expressed them with N-terminal StrepII- or N- and C-terminal His-tags. All but CC3100 were insoluble, therefore we focused on this unusual RR. In UV cross-linking experiments N-terminal StrepII-tagged CC3100 bound to increasing amounts of c-[^{33}P]-di-GMP (Figure 1A), with an apparent K_d of 212 nM. To confirm specific binding of c-[^{33}P]-di-GMP, UV cross-linking experiments in the presence of unlabeled nucleotides were performed. C-di-GMP competed very efficient with the binding of the radiolabeled nucleotide while the presence of 400- or 1000-fold more GTP or pGpG did not compete efficiently (Figure 1B), indicating that CC3100 specifically binds c-di-GMP.

CC3100 is solely involved in motility control

In a recent global analysis of all RR of *C. crescentus* it was observed that a CC3100 deletion mutant formed larger swarm sizes on semi solid agar plates[26]. To further investigate whether CC3100 is involved in motility control, we generated in-frame deletion mutants of *CC3100* in NA1000 and CB15 and constructed plasmids to express CC3100 under control of the xylose-inducible promoter. Deletion of *CC3100* and over-expression interfered with motility (Figure 2A and B), but it did not affect attachment, the ability to synchronize, the susceptibility to phages CR30 and CBK, which recognize pili and S-layer respectively (Supplementary Figure S2), and morphology (data not shown). The *CC3100*-deletion mutant showed improved swarming behavior (Figure 2A), which was not caused by a defective swarmer-to-stalk cell transition. Rather the opposite, the mutant proceeded normally through the cell cycle and was able to eject the flagellum (data not shown). The motility phenotype could be restored by mildly expressing CC3100 in trans from the plasmid (data not shown). When CC3100 was over-expressed, cells were unable to spread efficiently on semi-solid agar plates (Figure 2B). Taken together, these results suggest a function of CC3100 in motility control.

Cell cycle abundance and localization of CC3100

The dimorphic bacterium *C. crescentus* divides asymmetrically into a motile swarmer and a sessile stalked cell. Only the stalked cell can replicate and elongate the cell body to become a predivisional cell. To determine the abundance of CC3100 in the different cell types, we isolated swarmer cells of the wild-type strain and allowed them to synchronously proceed through one cell cycle. CC3100 was detected by immunoblot analysis using a CC3100-specific polyclonal antiserum. The protein was mainly present in swarmer and late pre-divisional cells (Figure 3). In line with this, *CC3100* is only transcribed at time points 100 – 180 minutes during the cell cycle (data not shown; RNA sequencing data of synchronized cells, unpublished). These results indicate that CC3100 is mainly present in flagellated cells and that it is degraded during the swarmer-to-stalk cell transition.

To investigate whether and where CC3100 is localized, we generated N- and C-terminal GFP fusions on a plasmid under control of a vanillate-inducible promoter. While the N-terminal

GFP-fusion protein could not complement the phenotype of a CC3100-deletion mutant, the C-terminal GFP-fusion protein was functional (Supplementary Figure S3A) and was therefore used for subsequent localization experiments using fluorescence microscopy. We found that 27 % of the cells expressing CC3100-GFP from the inducible vanillate promotor, which were induced with vanillate, showed polar foci; 32 % of the cells showed a diffuse, bright fluorescent signal distributed in the whole cell; and 41 % of the cells had no GFP signal (Figure 4B). In contrast, when only GFP was expressed from the vanillate-inducible promotor, no polar localization was detected (Figure 4A). CC3100 localized to both cell poles in predivisional cells and in stalked cells it mainly localized to the stalked pole, however localization opposite the stalked pole was also, albeit rarely, observed. We used immunoblotting to detect the presence of the GFP-fusion protein in a control experiment (Supplementary Figure S3B).

Since we found evidence that CC3100 is involved in motility control, we tested whether CC3100 localization is dependent on the presence of the flagellum. The assembly of the flagellum starts with the insertion of the transmembrane protein FliF into a structure called the MS-ring that forms the basis for further assembly of the export apparatus, the motor switch complex and the hook[27]. The absence of this protein abrogates the whole flagellar assembly[28]. In a *fliF* deletion mutant the fluorescent signal observed for CC3100-GFP was bright and diffuse with no visible foci, indicating that CC3100 does not localize in the absence of the flagellum (Fig. 4C) and that it interacts with a flagellar protein.

Several proteins are known to control motor function by binding either to the motor stator protein MotA[12], or the switch complex proteins FliG[14] and FliM[29]. To get more insights whether CC3100 also interacts with one of the three proteins, we tested localization of CC3100-GFP in *motA*, *fliG* and *fliM*-deletion mutants. In absence of *motA*, CC3100-GFP showed the same localization pattern as the wild-type (Supplementary Figure S4A). Also, in a bacterial two-hybrid assay CC3100 and MotA did not interact (Supplementary Figure S5A). This indicates that MotA is not the interaction partner of CC3100. In a *fliG* mutant CC3100 did localize, albeit with weak intensity (Supplementary Figure S4B). In contrast, no localization of CC3100 was observed in the absence of *fliM* (Figure 4D). To ensure that a flagellar protein is the target of CC3100, a *flbD* mutant was tested, which expresses only flagellar class II genes

but not class III and IV genes. CC3100 did indeed localize to the cell poles, however, because of the division defect of the *flbD* mutant, cells were elongated and additional auto-fluorescence signals were observed[30] (Supplementary Figure S4C). *FlbD* mutants expressing only GFP showed a diffuse signal and the same auto-fluorescence pattern observed for the fusion protein (data not shown).

Evidence that CC3100 is involved in the c-di-GMP mediated flagellar motility control

In a strain background where the swarmer cell-specific PDE PdeA is deleted, the flagellated cells are non-motile on semi-solid agar plates due to elevated c-di-GMP levels in the swarmer cell[23]. The effector(s) and target mediating this c-di-GMP-dependent output are currently unknown and therefore we investigated whether CC3100 might be involved. Deletion of *CC3100* in a *pdeA*-deletion mutant suppressed the *pdeA* mutant phenotype and cells were able to swarm as well as the wild-type (Figure 2A). The effect of the *CC3100* deletion was specific for motility, as the attachment phenotype of the *pdeA* mutant could not be suppressed by deletion of *CC3100* (Supplementary Figure S2D). In conclusion, these results support the view that CC3100 is the effector responsible for the c-di-GMP-mediated flagellar motility control of *C. crescentus* and blocks motility in its c-di-GMP-bound state.

To gain more insights how c-di-GMP binding interferes with CC3100 function, we measured the protein levels in a strain lacking c-di-GMP (rc-di-GMP^0 strain, Abel *et al*., unpublished). In immunoblot analysis CC3100 protein levels of the wild-type and rc-di-GMP^0 strain are comparable (data not shown), indicating that c-di-GMP binding does not interfere with protein stability. We observed that CC3100-GFP did not localize in the absence of c-di-GMP (Figure 5A). As this mutant is not flagellated (Abel *et al*., unpublished) and therefore the binding partner of CC3100 is absent, we currently cannot conclude that c-di-GMP binding is a prerequisite for polar localization. Our attempts to investigate localization in motile suppressors of the rc-di-GMP^0 strain (Abel *et al*., unpublished) failed due to problems with genetic manipulations of these mutant strains.

Discussion

Identification and characterization of effectors and their downstream targets is important to acquire a detailed understanding of the molecular mechanisms of c-di-GMP signaling. In this study we used a chemical proteomics approach and identified an unusual RR as a novel c-di-GMP-binding protein. To date only one other RR was described to bind c-di-GMP, the transcriptional regulator VpsT[10]. VpsT is likewise unusual, because it possesses an additional α–helix (α6) right after the conserved receiver domain. This helix is involved in dimerization, and this process is facilitated by c-di-GMP binding to a 4-residue-long conserved motif, W[F/L/M][T/S]R[10]. In contrast, CC3100 neither has this motif, nor a predicted 6th helix. In addition, CC3100 is most likely a monomer, since no dimerization of the purified protein in the absence or presence of c-di-GMP was observed (data not shown). Instead of a 6th helix, CC3100 has an arginine-rich 29-aa extension after the conserved receiver domain. This motif is shared with 4 other RR, all annotated as CheYIII. Arginines are associated with c-di-GMP binding and as one of the other RR CC1364 was also identified as a putative c-di-GMP binding protein in our CCMS experiments it is therefore tempting to speculate that the c-di-GMP binding site lies within this region. To elucidate this hypothesis, we currently analyze the residual CheYIII proteins of this group regarding their ability to bind c-di-GMP. However due to problems with protein solubility this was so far not successful. In addition, crystallization trials with c-di-GMP bound to CC3100 are currently ongoing.

Our experimental data favor a model in which CC3100 is involved in flagellar motor arrest upon c-di-GMP binding. Phenotypes solely interfering with motility were observed when the protein was absent or over-expressed. In the same line, our experiments revealed, that this RR required flagellar proteins to localize to the poles. For the localization studies a vanillate-inducible C-terminal GFP expression construct was used. The fusion protein was functional; however GFP expression was observed in only 60 % of the induced cells when analyzed by fluorescence microscopy. The same result was obtained when only GFP was expressed from the same promoter, suggesting that either vanillate was not taken up by all cells, the promoter was not active in all cells, or less likely, not all cells contained the plasmid. Localization of CC3100-GFP was not restricted to swarmer and pre-divisional cells. This is a rather surprising result considering that the native protein was found to be mainly present in

swarmer and late predivisional cells. The rapid degradation observed in immunoblot analysis during the swarmer-to-stalked cell transition and the aa sequence of the C-terminus indicate that CC3100 might be a substrate of ClpXP. This protease is localized during G1-S transition to the incipient stalked cell pole to degrade proteins, e.g. the master regulator CtrA or PdeA[23,31-33]. It is possible that the GFP-tag at the C-terminus of CC3100 prevents degradation and therefore the fusion protein stays at the stalked pole. Anyhow, this potential stabilization does not seem to interfere with function since the construct complemented the phenotypes of the *CC3100* deletion mutant. Meanwhile, we have constructed a C-terminal flag-tagged version that is functional, in contrast to an N-terminal fusion protein. This confirms that the possible stabilization of the protein does not interfere with protein function. The role of ClpXP in the degradation of CC3100 will be addressed in future studies.

So far the exact flagellar interaction partner of CC3100 is unknown. Our localization studies in different flagellar mutant strains excluded at least the motor protein MotA. Assembly of the flagellum is a sequential process and transcription and translation of these genes are hierarchical and tightly controlled[34]. The first checkpoint is the completion of the MS- and C-ring and only then the transcription of class III and IV genes by the transcriptional activator FlbD is initiated. In a *flbD* mutant CC3100 localizes, confirming that the basal body is the target. The other mutants we tested interfered with either the MS ring (*fliF* mutant) or the C-ring (*fliG* and *fliM* mutants) assembly. In a *fliM* mutant CC3100 did not localize, suggesting that neither FliF nor FliG are recognized by CC3100 assuming that they are assembled in this background. Furthermore, these data indicate that either FliM or FliN could be the interaction partner. For a detailed characterization, we will construct clean deletions in *fliN* and *fliM*, because the *fliM* mutant used in this study was a transposon mutant that could have polar effects on the three genes located downstream in this operon. We can exclude that *pflI*, the gene located next to *fliM*, is causing the phenotype, because CC3100 is localized in a *pflI* mutant (data not shown). Right now we cannot exclude the last two genes of the operon, CC2058 and CC2059, because both deletion mutants result in non-motile and non-flagellated cells[35,36]. In order to get more insights in a possible FliM-CC3100 binding, *in silico* analysis were performed to elucidate whether CC3100 could interact with FliM. This interaction was very well studied in *E. coli* on a structural level[37,38]. On the one hand, the aa of FliM, that are known

to be involved in the binding to CheY from *E. coli*, are conserved in *C. crescentus* (data not shown). On the other hand two important residues of CheY from *E. coli*, Tyr106 and Lys122, involved in interaction are not conserved in CC3100 (Supplementary Figure S1A,[37]) and this does not support our model of a possible interaction between the receiver domain of CC3100 and FliM. However, CC3100 has an additional C-terminal domain of around 100 aa, which could in principle also mediate the interaction. The structural homology of this domain to other proteins is quite low and a model can only be built with a low reliability using the histidine phosphotransferase (HPT) domain of the histidine phosphotransferase ShpA (2ooc) as a template. As none of the residues important for function are conserved in CC3100, it is unlikely that CC3100 is a histidine phosphotransferase.

Somehow puzzling is the localization of CC3100 in the *fliG* mutant although the signal intensity is very low. It is possible that this weak signal is due to localization of CC3100-GFP to another interaction partner, which is masked in a *fliM* and *fliF* mutant. This seems possible as we observe also diffuse GFP signals in wild-type cells, consistent with a model for a dynamic protein. Such a behavior is e.g. known for CheY proteins as they have to shuttle from the chemoarrays, where their cognate histidine kinase CheA is localized to their target protein FliM on the flagellum[39]. In order to identify the CC3100 interaction partner, co-immunoprecipitation experiments will be performed using our functional Flag-tagged CC3100 protein. In addition, this analysis should give information as to whether a HK, CC3102, which is encoded in close proximity to CC3100 is somehow linked to the function of CC3100. CC3100 has its own promoter whereas CC3102 lies in an operon together with CC3101. However, both promoters are active at the same time during the cell cycle (data not shown).

So far, it is unclear how CC3100 interferes with the flagellar motor function, for example via controlling the speed or the direction of the rotation of the flagellar motor. The latter is usually mediated by the chemotaxis system. It is not expected that CC3100 is controlled by the usual phosphorylation cascade, as known for CheY proteins since it has a mutation in the residue prone to phosphorylation by CheA. However, an alternative residue for phosphorylation in CC3100 cannot be excluded yet. That was observed in an *E. coli* CheY mutant, which harbored a mutation at the phosphorylation site[40]. To distinguish between chemotaxis and speed control, we are currently setting up dark-field video microscopy with *C.*

crescentus swarmer cells. With such trajectories the frequency of tumbling events and swimming velocities can be compared in wild-type and mutant strain. This technique will also be used to determine whether the other four CheIII proteins are involved in chemotaxis.

Finally, more experimental work is necessary to elucidate how c-di-GMP interferes with CC3100 function. So far we can exclude that c-di-GMP binding stabilizes the protein. This was for example observed for TipF, which is rapidly degraded in the absence of c-di-GMP (Yaniv Cohen, unpublished). Also, PopA cannot localize in the absence of c-di-GMP[41], and we observed a similar behavior for CC3100. However, this has to be tested in another strain background, because the rc-di-GMP^0 strain used in this study is missing the flagellar basal body and therefore the putative binding partner of CC3100.

Material and Methods

Strains, Plasmids, and growth conditions

The bacterial strains, plasmids and oligos used in this work are summarized in Tables 2, 3, and 4 respectivly. *E. coli* was grown in Luria Broth (LB) media at 37 °C and *C. crescentus* was grown in rich medium (peptone yeast extract; PYE) at 30 °C[42]. Marker-less deletions were generated using the standard two-step recombination sucrose counter-selection procedure based on pNPTS138-derivatives. *E. coli* S17.1 was used to transfer plasmids by conjugation into *C. crescentus* strains[42]. Motility of *C. crescentus* was scored on semi-solid (0.3 %) PYE agar plates. For synchronization experiments cells were grown at 30°C in minimal medium containing 0.2 % glucose[42] and swarmer cells were isolated after Ludox gradient centrifugation[43]. For induction of plasmids with a vanillate inducible promotor a concentration of 1 mM vanillate, and with a xylose inducible promoter 0.1 % xylose was added to the media. If not stated otherwise, exponentially growing cells were used for all experiments. Antibiotics were used at the following concentrations: Kanamycin 50 μg/ml (*E. coli*) and 5 μg/ml (*C. crescentus*); Chloramphenicol 30 μg/ml (*E. coli*) and 2 μg/ml (*C. crescentus*).

Microscopy

For microscope imaging, log phase cells were placed on a glass slide layered with a pad of 1% agarose (Sigma) dissolved in water. An Olympus IX71 microscope equipped with an UPlanFLN 100x/1.30 oil objective (Olympus, Germany) and a coolSNAP HQ (Photometrics, AZ, United States) CCD camera was used to take phase contrast (PH) and fluorescence images. For GFP fluorescence, FITC filter sets (Ex 490/20 nm, Em 528/38 nm) were used with an exposure time of 1.0 sec. Images were processed with softWoRx v3.3.6 (Applied Precision, WA, United States) and Photoshop CS2 (Adobe, CA, United States) software.

Protein Expression and Purification

N-terminally StrepII- or His-tagged CC3100 was expressed in *E. coli* BL21 (DE3) (Stratagen) by adding 0.5 mM IPTG at an OD_{600} of 0.6 and incubation for 3 h at 30 °C. Cells were collected by centrifugation, resuspended in lysis buffer and disrupted by a French pressure cell press

(Thermo, Elcetron corporation). Lysates were centrifuged for 1 h at 100.000 g and proteins were purified using affinity chromoatography. For purification of StepII-tagged protein Strep-Tactin Superflow Plus (Quiagen) was used and batch purification was carried out according to the manufactures protocol. His-tagged CC3100 was purified using a 1 mL HisTrap HP column (GE Healthcare) connected to an ÄKTA chromatography system. For lysis 20 mM Tris pH8, 500 mM NaCl, 10 mM Imidazole and 1 mM DTT, pH 8 was used and proteins were eluted with increased Imidazole concentration up to 500 mM. Tagged proteins were further purified by size exclusion chromatography on a HiLoad Superdex S200 16/60 column (GE Healthcare) equilibrated with 20 mM Tris-HCl pH 8.0, 200 mM NaCl, 1 mM DTT.

CCMS

CCMS using the c-di-GMP Capture Compound was carried out as described recently [4].

UV cross-linking

Synthesis of radiolabeled c-di-GMP using YdeH and UV light-induced cross-linking experiments in conical 96-well plates (Greiner Bio-One) were performed as described recently[44],[45]. Briefly, 2 μM protein was incubated for 10 min at room temperature with c-[^{33}P] -di-GMP in a total volume of 20 μl using PBS as buffer. As a control BSA was included. For competition experiments unlabeled nucleotides were incubated with the protein for 15 min prior the addition of c-[^{33}P] -di-GMP. The 96-well plates were then UV-irradiated at 254 nm for 20 min using a Bio-Link crosslinker (Vilber Lourmat, France). After addition of 5 μl loading dye and boiling for 5 min the samples were subjected to SDS-PAGE. Proteins were analyzed by Coomassie staining and autoradiography. Band intensities were quantified using the ImageJ64 software and the data were fitted using GraphPad Prism® version 5.04 for Windows (GraphPad Software, San Diego California USA). The K_d was calculated by non-linear regression using the “One site – Total binding” equation.

Antibody production and immunoblotting

Purified His-3100 was denatured by SDS-PAGE. After elution from the gel the protein was injected into rabbits for polyclonal antibody production (Josman, LLC^{TM}, Californien, USA). The serum was adsorbed against a whole cell lysate of the CC3100 deletion mutant. For immunoblots anti-CC3100 antiserum was diluted 1:1.000. Other antibodies were used in the following dilutions: CtrA 1:10.000 and HPR-conjugated swine α-rabbit antibodies 1:10.000. After incubation with ECL chemiluminescent substrate (Perkin Elmer, USA), X-ray films (Fujifilm Corporation) were used to detect luminescence.

Acknowledgments

We thank Fabienne Hamburger for help with cloning and strain constructions and Benoit-Joseph Laventie for help with data analysis. This work was supported by the Swiss National Science Foundation (SNF) Sinergia grant CRSII3_127433.

References

1. Schirmer, T. & Jenal, U. Structural and mechanistic determinants of c-di-GMP signalling. *Nature Publishing Group* **7**, 724–735 (2009).

2. Povolotsky, T. L. & Hengge, R. 'Life-style' control networks in *Escherichia coli*: Signaling by the second messenger c-di-GMP. *Journal of Biotechnology* 1–7 (2012).

3. Sondermann, H., Shikuma, N. J. & Yildiz, F. H. You've come a long way: c-di-GMP signaling. *Current Opinion in Microbiology* 1–7 (2012).

4. Nesper, J., Reinders, A., Glatter, T., Schmidt, A. & Jenal, U. A novel capture compound for the identification and analysis of cyclic di-GMP binding proteins. *Journal of Proteomics* **75**, 4874–4878 (2012).

5. Düvel, J. *et al.* A chemical proteomics approach to identify c-di-GMP binding proteins in *Pseudomonas aeruginosa*. *Journal of Microbiological Methods* 1–8 (2011).

6. Berg, H. C. The rotary motor of bacterial flagella. *Annu. Rev. Biochem.* **72**, 19–54 (2003).

7. Ueno, T., Oosawa, K. & Aizawa, S. Domain structures of the MS ring component protein (FliF) of the flagellar basal body of *Salmonella typhimurium*. *Journal of Molecular Biology* **236**, 546–555 (1994).

8. Francis, N. R., Sosinsky, G. E., Thomas, D. & DeRosier, D. J. Isolation, characterization and structure of bacterial flagellar motors containing the switch complex. *Journal of Molecular Biology* **235**, 1261–1270 (1994).

9. Levenson, R., Zhou, H. & Dahlquist, F. W. Structural Insights into the Interaction between the Bacterial Flagellar Motor Proteins FliF and FliG. *Biochemistry* **51**, 5052–5060 (2012).

10. Krasteva, P. V. *et al. Vibrio cholerae* VpsT Regulates Matrix Production and Motility by Directly Sensing Cyclic di-GMP. *Science* **327**, 866–868 (2010).

11. Huitema, E., Pritchard, S., Matteson, D., Radhakrishnan, S. K. & Viollier, P. H. Bacterial Birth Scar Proteins Mark Future Flagellum Assembly Site. *Cell* **124**, 1025–1037 (2006).

12. Boehm, A. *et al.* Second Messenger-Mediated Adjustment of Bacterial Swimming Velocity. *Cell* **141**, 107–116 (2010).

13. Ryjenkov, D. A., Simm, R., Romling, U. & Gomelsky, M. The PilZ Domain Is a Receptor for

the Second Messenger c-di-GMP: The PilZ Domain Protein YcgR Controls Motility in Enterobacteria. *Journal of Biological Chemistry* **281**, 30310–30314 (2006).

14. Blair, K. M., Turner, L., Winkelman, J. T., Berg, H. C. & Kearns, D. B. A Molecular Clutch Disables Flagella in the *Bacillus subtilis* Biofilm. *Science* **320**, 1636–1638 (2008).

15. Porter, S. L., Wadhams, G. H. & Armitage, J. P. Signal processing in complex chemotaxis pathways. *Nature Publishing Group* **9**, 153–165 (2011).

16. Hess, J. F., Oosawa, K., Kaplan, N. & Simon, M. I. Phosphorylation of three proteins in the signaling pathway of bacterial chemotaxis. *Cell* **53**, 79–87 (1988).

17. Scharf, B. E., Fahrner, K. A., Turner, L. & Berg, H. C. Control of direction of flagellar rotation in bacterial chemotaxis. *Proc. Natl. Acad. Sci. U.S.A.* **95**, 201–206 (1998).

18. Armitage, J. P. & Macnab, R. M. Unidirectional, intermittent rotation of the flagellum of *Rhodobacter sphaeroides*. *Journal of Bacteriology* **169**, 514–518 (1987).

19. Pilizota, T. *et al.* A molecular brake, not a clutch, stops the *Rhodobacter sphaeroides* flagellar motor. *Proc. Natl. Acad. Sci. U.S.A.* **106**, 11582–11587 (2009).

20. Ely, B. *et al.* General nonchemotactic mutants of *Caulobacter crescentus*. *Genetics* **114**, 717–730 (1986).

21. Nierman, W. C. *et al.* Complete genome sequence of *Caulobacter crescentus*. *Proc. Natl. Acad. Sci. U.S.A.* **98**, 4136–4141 (2001).

22. Wolfe, A. J. & Visick, K. L. Get the Message Out: Cyclic-Di-GMP Regulates Multiple Levels of Flagellum-Based Motility. *Journal of Bacteriology* **190**, 463–475 (2008).

23. Abel, S. *et al.* Regulatory cohesion of cell cycle and cell differentiation through interlinked phosphorylation and second messenger networks. *Molecular Cell* **43**, 550–560 (2011).

24. Galperin, M. Y. Bacterial signal transduction network in a genomic perspective. *Environmental Microbiology* **6**, 552–567 (2004).

25. Bourret, R. B. Receiver domain structure and function in response regulator proteins. *Current Opinion in Microbiology* **13**, 142–149 (2010).

26. Skerker, J. M., Prasol, M. S., Perchuk, B. S., Biondi, E. G. & Laub, M. T. Two-Component Signal Transduction Pathways Regulating Growth and Cell Cycle Progression in a Bacterium: A

System-Level Analysis. *PLoS Biol* **3**, 334 (2005).

27. Macnab, R. M. How Bacteria Assemble Flagella. *Annu. Rev. Microbiol.* **57**, 77–100 (2003).

28. Grunenfelder, B., Gehrig, S. & Jenal, U. Role of the cytoplasmic C terminus of the FliF motor protein in flagellar assembly and rotation. *Journal of Bacteriology* **185**, 1624–1633 (2003).

29. Porter, S. L. *et al.* The CheYs of *Rhodobacter sphaeroides*. *J. Biol. Chem.* **281**, 32694–32704 (2006).

30. Muir, R. E. The trans-acting flagellar regulatory proteins, FliX and FlbD, play a central role in linking flagellar biogenesis and cytokinesis in *Caulobacter crescentus*. *Microbiology* **151**, 3699–3711 (2005).

31. Biondi, E. G. *et al.* Regulation of the bacterial cell cycle by an integrated genetic circuit. *Nature* **444**, 899–904 (2006).

32. McGrath, P. T., Iniesta, A. A., Ryan, K. R., Shapiro, L. & McAdams, H. H. A dynamically localized protease complex and a polar specificity factor control a cell cycle master regulator. *Cell* **124**, 535–547 (2006).

33. Ryan, K. R., Huntwork, S. & Shapiro, L. Recruitment of a cytoplasmic response regulator to the cell pole is linked to its cell cycle-regulated proteolysis. *Proc. Natl. Acad. Sci. U.S.A.* **101**, 7415–7420 (2004).

34. Aldridge, P. & Hughes, K. T. Regulation of flagellar assembly. *Current Opinion in Microbiology* **5**, 160–165 (2002).

35. Obuchowski, P. L. & Jacobs-Wagner, C. PflI, a Protein Involved in Flagellar Positioning in *Caulobacter crescentus*. *Journal of Bacteriology* **190**, 1718–1729 (2008).

36. Levi, A. Y. Genetic dissection of *Caulobacter crescentus* surface colonization. *PhD Thesis, University of Basel, Faculty of Science* (2007).

37. Lee, S. Y. *et al.* Crystal structure of an activated response regulator bound to its target. *Nat. Struct. Biol.* **8**, 52–56 (2001).

38. Dyer, C. M. & Dahlquist, F. W. Switched or not?: the structure of unphosphorylated CheY bound to the N terminus of FliM. *Journal of Bacteriology* **188**, 7354–7363 (2006).

39. Eisenbach, M. Control of bacterial chemotaxis. *Molecular Microbiology* **20**, 903–910

(1996).

40. Appleby, J. L. & Bourret, R. B. Activation of CheY mutant D57N by phosphorylation at an alternative site, Ser-56. *Molecular Microbiology* **34**, 915–925 (1999).

41. Duerig, A. *et al.* Second messenger-mediated spatiotemporal control of protein degradation regulates bacterial cell cycle progression. *Genes & Development* **23**, 93–104 (2009).

42. Ely, B. *Methods in Enzymology*. *Methods in enzymology* **204**, 372–384 (1991).

43. Jenal, U. & Shapiro, L. Cell cycle-controlled proteolysis of a flagellar motor protein that is asymmetrically distributed in the *Caulobacter* predivisional cell. *The EMBO Journal* **15**, 2393–2406 (1996).

44. Christen, M. *et al.* 3.3 DgrA is a member of a new family of cyclic di-GMP receptors and controls flagellar motor functions in *Caulobacter crescentus*. *Mechanisms of Cyclic-di-GMP Signaling*

45. Steiner, S., Lori, C., Boehm, A. & Jenal, U. Allosteric activation of exopolysaccharide synthesis through cyclic di-GMP-stimulated protein-protein interaction. *The EMBO Journal, in revision* (2012).

46. Evinger, M. & Agabian, N. Envelope-associated nucleoid from *Caulobacter crescentus* stalked and swarmer cells. *Journal of Bacteriology* **132**, 294–301 (1977).

47. Aldridge, P. & Jenal, U. Cell cycle-dependent degradation of a flagellar motor component requires a novel-type response regulator. *Molecular Microbiology* **32**, 379–391 (1999).

48. Thanbichler, M., Iniesta, A. A. & Shapiro, L. A comprehensive set of plasmids for vanillate- and xylose-inducible gene expression in *Caulobacter crescentus*. *Nucleic Acids Research* **35**, 137–137 (2007).

Figure Legends

Figure 1: CC3100 binds c-di-GMP specific

(A) UV-cross-linking of purified StrepII-CC3100 with increasing amounts of c-[^{33}P] -di-GMP.

(B) Binding of c-[^{33}P] -di-GMP in the presence of unlabeled nucleotides.

Figure 2: Motility behavior of CC3100 deletion and over-expression mutants on semi-solid agar plates.

(A) CC3100 deletion mutants swarm better. Indicated strains were inoculated on PYE 0.3 % agar plates and incubated for 72 h at 30 °C.

(B) Over-expression of CC3100 render cells non-motile. Indicated strains were inoculated on PYE 0.3 % agar plates containing 0.1 % xylose and Kan and incubated for 72 h at 30 °C; VC: vector control.

Figure 3: CC3100 protein levels are cell cycle regulated.

Immunoblots of synchronized cultures show CC3100 levels during the cell cycle. For detection a α-CC3100 polyclonal antiserum was used. CtrA levels were detected using α-CtrA antibodies to confirm successful synchronization. An unspecific band, detected with the α-CC3100 polyclonal antiserum, is indicated as a loading control.

Figure 4: The flagellum and FliM are required for CC3100 localization

Several strains expressing CC3100-GFP from a vanillate inducible promotor were compared in their ability to localize to the cell poles by fluorescence microscopy.

(A) CC3100 deletion mutant expressing GFP from plasmid pMT745 showed no foci.

(B) CC3100-GFP localized to the poles in a CC3100 deletion mutant.

(C) Deletion of *fliF* resulted in delocalized CC3100-GFP fluorescence signal.

(D) In the absence of FliM no polar localization is observed.

All strains were induced with 1 mM vanillate; PH: Phase contrast

Figure 5: c-di-GMP is required for CC3100 localization

(A) Diffuse fluorescence signal in the rc-di-GMP^0 strain expressing GFP from plasmid pMT745

(B) CC3100-GFP did not localize in the rc-di-GMP^0 strain.

The fusion protein was expressed in the presence of 1 mM vanillate from a vanillate inducible promoter.

Figure 1

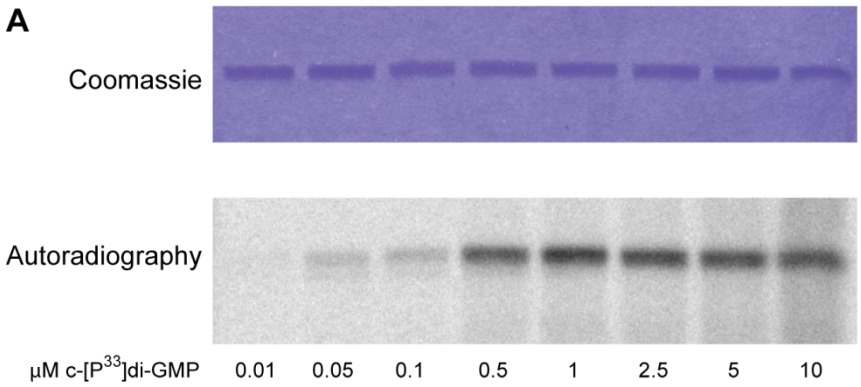
A
Coomassie
Autoradiography
µM c-[P33]di-GMP
0.01
0.05
0.1
0.5
1
2.5
5
10

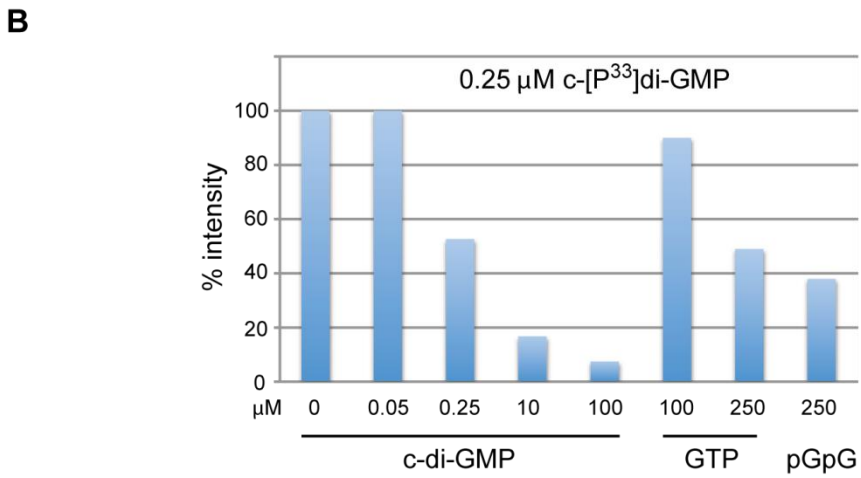
B
0.25 µM c-[P33]di-GMP
% intensity
100
80
60
40
20
0
µM
0
0.05
0.25
10
100
100
250
250
c-di-GMP
GTP
pGpG

Figure 2

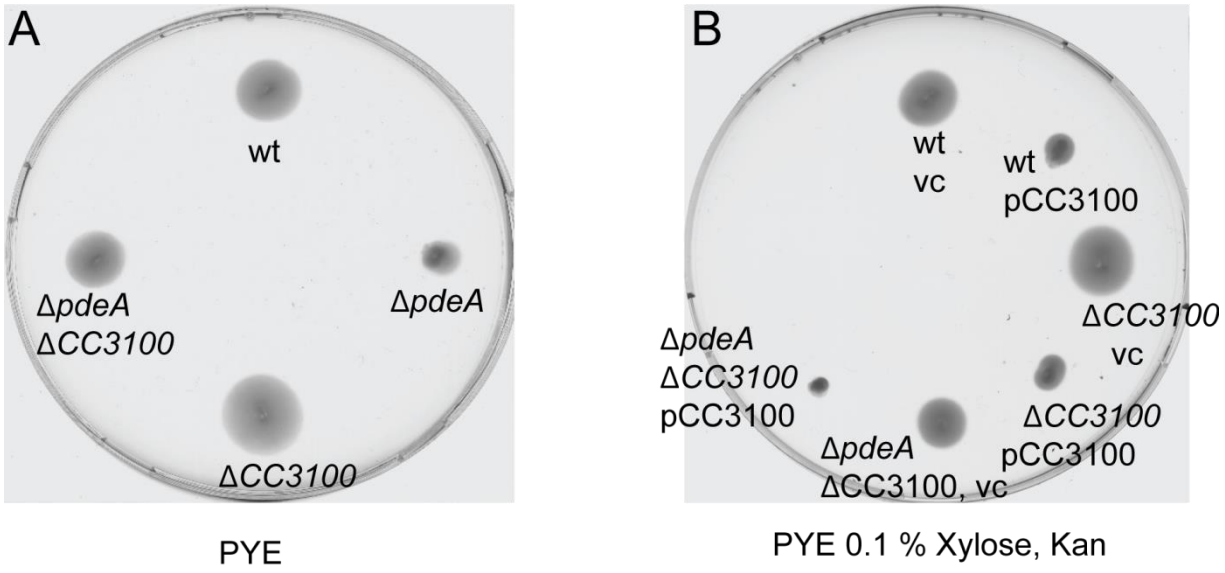

Figure 3

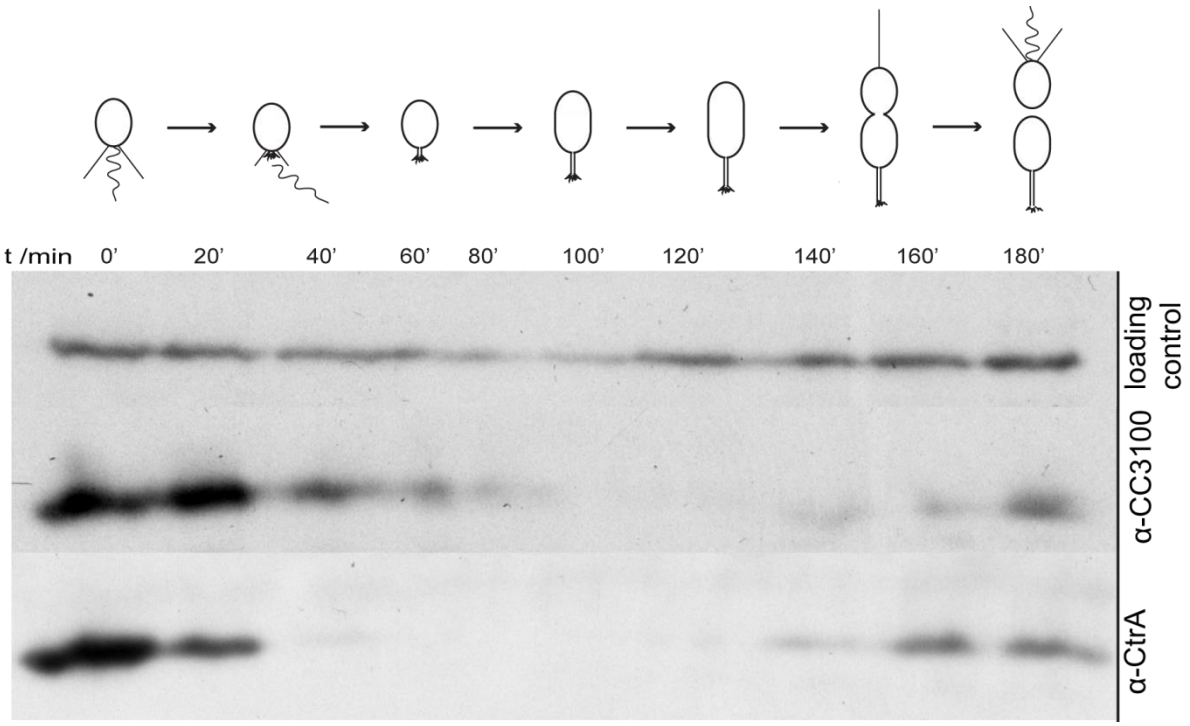

Figure 4

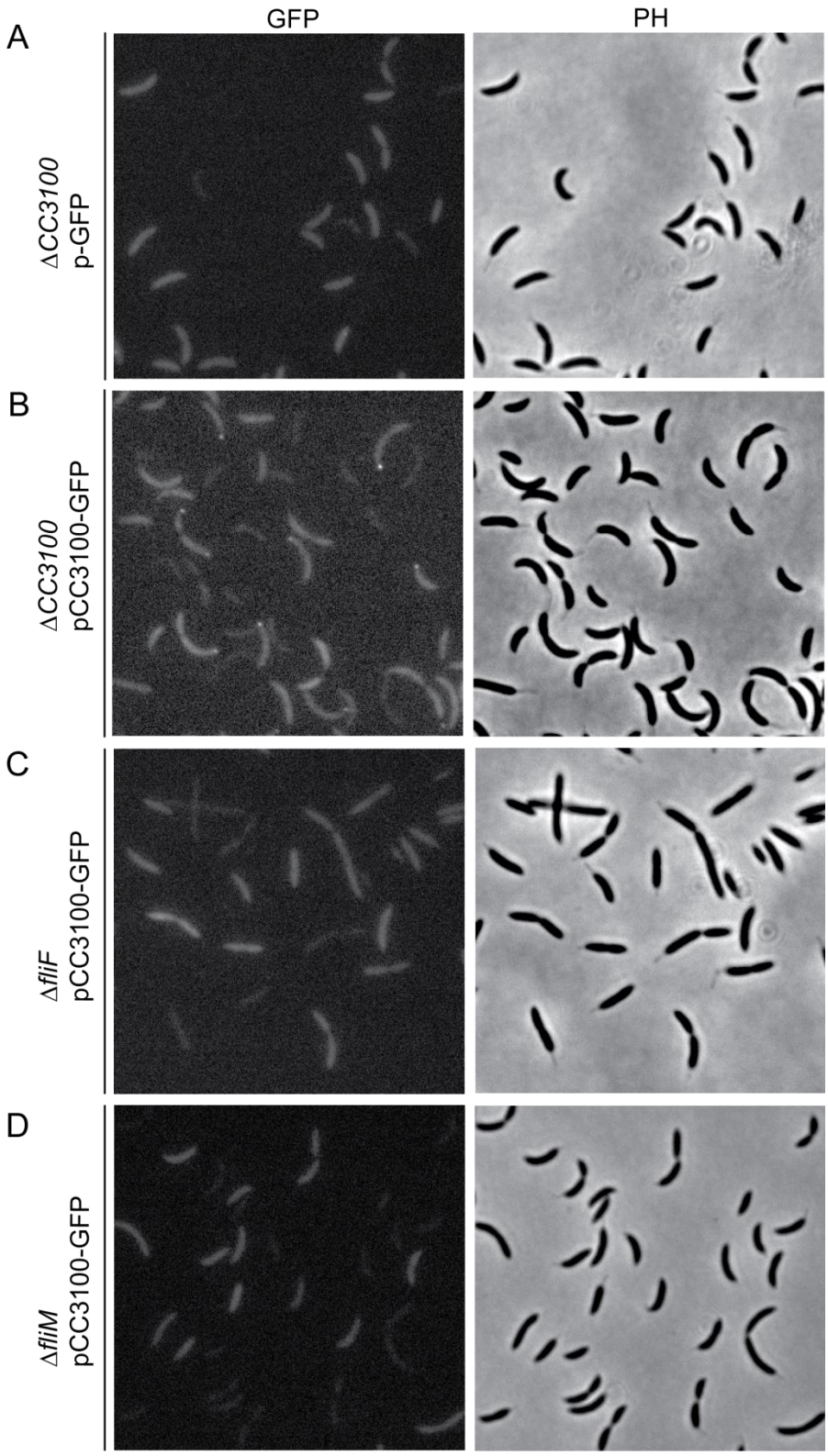
GFP
PH
A
ΔCC3100
p-GFP
B
ΔCC3100
pCC3100-GFP
C
ΔfliF
pCC3100-GFP
D
ΔfliM
pCC3100-GFP

Figure 5

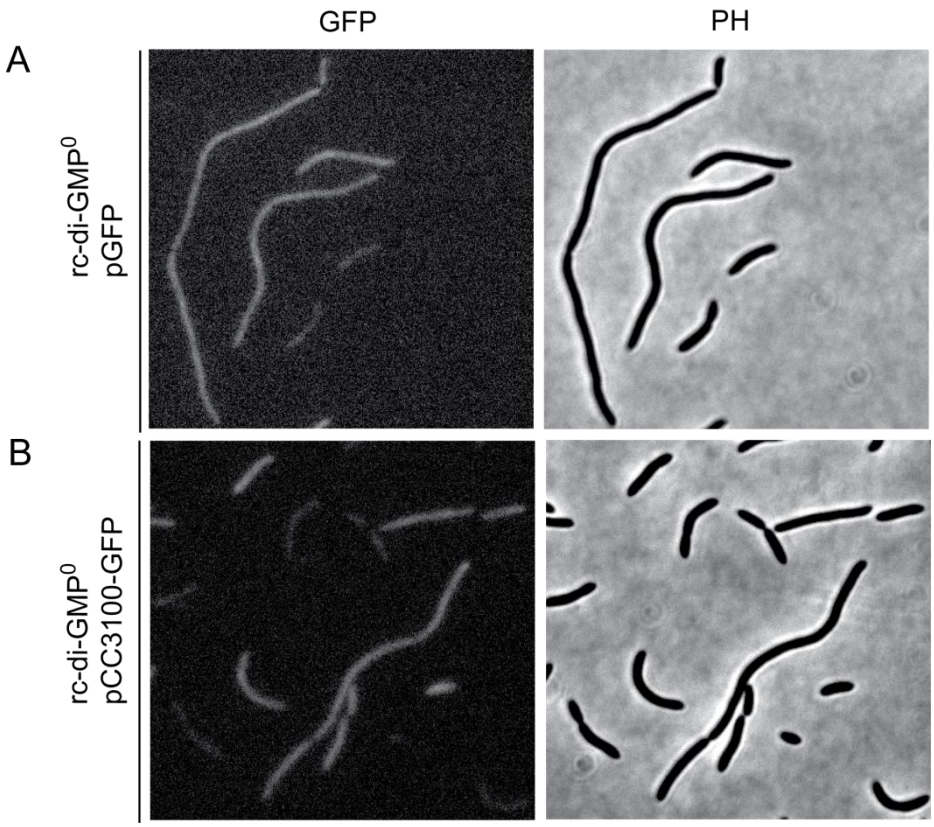

Table 1: RR identified by CCMS

Protein Name	**ID**	**CCMS experiment/CCMS competition[1]** **No of spectral counts of identified peptides**			
Experiment No[2]		1	2	3	4
CheYIII	CC1364	2/0	3/0	1/0	1/0
RR	CC3100	2/0	4/0	6/0	4/0

[1]All competition experiments were performed in the presence of 1 mM c-di-GMP.

[2]Experiment 1 was performed with 10 µM c-di-GMP-CC, experiment 2 with 10 µM c-di-GMP-CC, experiment 3 with 5 µM c-di-GMP-CC, and experiment 4 with 2.5 µM c-di-GMP-CC.

Table 2: Strains used in this study

Name	Genotype and description	Reference
	E. coli strains	
DH10B	F-mcrA D(mrr-hsd RMS- mcrBC) f80dlacZM15DlacX74 endA1 rec1deoR D(ara, leu)7697 araD139 galU nupG rpsL thi prohsd+ recA RP4-2-Tc::Mu-Tn7	[46]
S17.1	F-, lambda (-), thi, pro, recA, restriction (-) modification (+),RP4 derivative integrated into the chromosome with Tet::Mu, Km::T7	[46]
BL21 (DE3)	Expression host for pET21 vectors; genomic integrated T7-RNApolymerase under control of lac promoter; deficient in Lon and OmpT protease	Novagen
	C. crescentus strains	
NA1000	WT; Synchronizable laboratory strain of CB15 (CB15N)	[46]
UJ5065	NA1000 c-di-GMP^0; Markerless in frame deletions of *CC1850*, *CC0740*, *CC0857*, *CC3285*, *CC3094*, *CC0655*, *CC0896*, *CC2462* in NA1000	Micael Nicollier
SoA764	NA1000 rc-di-GMP^0, Markerless in frame deletions of *CC0091*, *CC0655*, *CC0740*, *CC0857*, *CC0896*, *CC1086*, *CC1850*, *CC2462*, *CC3094*, *CC3148*, *CC3285*, *CC3396* in NA1000	Sören Abel
UJ4467	NA1000 Δ*pdeA*; Markerless in frame deletion of *pdeA* in NA1000	[23]
UJ5676	NA1000 Δ*CC3100*; Markerless in frame deletion of *CC3100* in NA1000	This work
UJ5832	NA1000 Δ*pdeA* Δ*CC3100*, Markerless in frame deletion of *CC3100* and *pdeA* in NA1000	This work
LS1218	NA1000 Δ*fliF*	[28]
UJ413	NA1000 *fliM::Tn5*	[47]

Table 3: Plasmids used in this study

Name	Description	Oligos used for cloning	Reference/Source
pMT687	pRXMCS_2; Kan^R, low copy replicating plasmid, xylose inducible promotor		[48]
pMT687-CC3100	pCC3100; pMT687, NdeI-CC3100-KpnI	3615, 3616	This study
pNPTS138	Kan^R, suicide vector with sacB gene and oriT		D. Alley
pNPTS138-ΔCC3100	pNPTS138, HindIII-upstream region of CC3100–BamHI –downstream region of CC3100-EcoRI	3387, 3388, 3389, 3390	This study
pMT745	pGFP; pRVGFPC_6; Cm^R, low copy plasmid for C-terminal GFP fusions, vanillate inducible promotor		[48]
pEF84	pCC3100-GFP; pMT745, NdeI_CC3100_KpnI	4662, 4663	This study
pET28a	Expression vector; T7 promoter; Kan^R,		Novagen
pET28-His-CC3100	pET28a, NdeI-CC3100-HindIII	3615, 3291	This study
pET28-Strep-CC3100	pET28a, NcoI-StrepIItag-BamHI-CC3100-HindIII	3287, 3288, 3290, 3291	This study

Table 4: Oligonucleotids used in this study

Oligo	Sequence[1]	Description
3387	ATATAAGCTTATGGTCGAGGCCTTGCTG	for cloning upstream region of *CC3100* in pNPTS138
3388	TTGGATCCGTTGCCGTCAAACACGAACA	for cloning upstream region of *CC3100* in pNPTS138
3389	TTGGATCCTAGAGCATTTTCCGATCTGT	for cloning downstream region of *CC3100* in pNPTS138
3390	TCAGAATTCCTCGATGGGCGGCTATGT	for cloning downstream region of *CC3100* in pNPTS138
3415	ACATGGGCGGGGGCGGAGCG	for screening of *CC3100* deletion mutants
3416	ACCTTCGCCCTCGCCGGCTT	for screening of *CC3100* deletion mutants
3291	CCGCAAGCTTCTAGGCCGCGCGCCCCCGGT	for cloning of *CC3100* in pET28a
3615	GCGGCAGCCATATGTTCGTGTTTGACGGCAACGT	for cloning of *CC3100* in pET28a
3287	ATATACCATGGGATGGAGCCACCCGCAGTTCGAAAAAGGATCCAAGCTT	for cloning of StrepII tag in pET28a
3288	AAGCTTGGATCCTTTTTCGAACTGCGGGTGGCTCCATCCCATGGTATAT	for cloning of StrepII tag in pET28a
3290	AAGGATCCTTCGTGTTTGACGGCAACGT	for cloning of *CC3100* together with StrepII tag in pET28a
3291	CCGCAAGCTTCTAGGCCGCGCGCCCCCGGT	for cloning of *CC3100* together with StrepII tag in pET28a
3619	GAGACGACCATATGGCGTACGTGGCGAGTTCG	for cloning of *CC3100* in pMT687
3620	GTGGTACCCTAAGCTGCGCGCGGTTTAC	for cloning of *CC3100* in pMT687
4662	AAAGCATATGTTCGTGTTTGACGGCAAC	for cloning of *CC3100* in pRVGFPC_6
4663	TTTAGGTACCGGCCGCGCGCCCCCGGTC	for cloning of *CC3100* in pRVGFPC_6

[1] Restriction sites are underlined

3.2.1 Supplementary material and methods accompanying:

An unorthodox response regulator binds c-di-GMP to control motility in *Caulobacter crescentus*

Jutta Nesper[1], Elvira Friedrich[1], Eric Hajjar[2], Thorsten Schwede[2] and Urs Jenal[1]

Affiliations:

[1]Biozentrum of the University of Basel, Klingelbergstrasse 50, CH-4054 Basel, Switzerland

[2]SIB Swiss Institute of Bioinformatics, Biozentrum University of Basel, CH-4054 Basel,Switzerland

For correspondence: urs.jenal@unibas.ch

Supplementary Data

Supplementary Materials and Methods

Strains, Plasmids, and Oligos

The bacterial strains, plasmids and oligos used are summarized in Supplementary Tables S1, S2, and S3 respectivly.

Bacterial Two-Hybrid Analysis

Proteins of interest were fused in frame to the 3'end of the T25 fragment (pKT25) and to the 3' end (pUT18C) or 5' end (pUT18) of the T18 fragment of the *B. pertussis* adenylate cyclase[1]. pKT25-zip and pUT18C-zip were used as positive controls. The adenylate cyclase deficient *E. coli* strain AB1768 was used to screen for positive interactions. pKT25 derivatives were transformed together with pUT18 or pUT18C derivatives into AB1768 and the transformants selected on LB with ampicillin (100 ug/ml) and kanamycin (50 ug/ml). To screen for protein-protein interaction single colonies were either streaked or overnight cultures were spotted on MacConkey Agar Base plates supplemented with maltose (1%), ampicillin (100 µg/ml) and kanamycin (50 µg/ml).

Phage Sensitivity Assay

C. crescentus overnight cultures (350 µL) were mixed with 2.5 mL of molten 0.5 % PYE top agar and immediately distributed on 1.5 % PYE agar. According to the phage spot assay phage lysates were diluted 10^{-1}-10^{-8} and spotted on the top agar mixture. Plates were incubated at 30 °C for 24 h, until small plaques were visible.

Attachment Assay

The ability to attach to inorganic surfaces was tested in 96-well microtiter plates. Cells were inoculated in PYE and incubated at 200 rpm on a rocking platform for 24 hrs. Planktonic cells were discarded and bacteria attached to the polystyrene surface were stained with crystal

violet (0.3% crystal-violet, 5% isopropanol, 5% methanol). The dye was dissolved in 20% acetic acid and quantified in a photospectrometer (Genesys6, Thermo Spectronic, USA) at 600 nm.

Bioinformatics

The protein sequences of the *C. crescentus* response regulators were retrieved from the KEGG database (http://www.kegg.com/kegg/genes.html). Domain barriers were determined by including all highly conserved residues of the receiver domains[2]. Multiple alignments were performed using the ClustalW server (http://www.ch.embnet.org/software/ClustalW.html) and the Boxshade server (http://www.ch.embnet.org/software/BOX_form.html). The sequence of the CheY protein of *E. coli* was retrieved from the PDB (1F4V).

The phylogenetic tree was generated using the program Phylodendron (http://iubio.bio.indiana.edu/soft/molbio/java/apps/trees/; D.G. Gilbert version 0.8d).

Supplementary References

1. Karimova, G., Pidoux, J., Ullmann, A. & Ladant, D. A bacterial two-hybrid system based on a reconstituted signal transduction pathway. *Proc. Natl. Acad. Sci. U.S.A.* **95**, 5752–5756 (1998).

2. Bourret, R. B., Hess, J. F. & Simon, M. I. Conserved aspartate residues and phosphorylation in signal transduction by the chemotaxis protein CheY. *Proc. Natl. Acad. Sci. U.S.A.* **87**, 41 (1990).

3. Lee, S. Y. *et al.* Crystal structure of an activated response regulator bound to its target. *Nat. Struct. Biol.* **8**, 52–56 (2001).

4. Steiner, S., Lori, C., Boehm, A. & Jenal, U. Allosteric activation of exopolysaccharide synthesis through cyclic di-GMP-stimulated protein-protein interaction.

The EMBO Journal, in revision (2012).

5. Abel, S. *et al.* Regulatory cohesion of cell cycle and cell differentiation through interlinked phosphorylation and second messenger networks. *Molecular Cell* **43**, 550–560 (2011).

6. Jenal, U. & Shapiro, L. Cell cycle-controlled proteolysis of a flagellar motor protein that is asymmetrically distributed in the *Caulobacter* predivisional cell. *The EMBO Journal* **15**, 2393–2406 (1996).

7. Levi, A. Y. Genetic dissection of *Caulobacter crescentus* surface colonization. *PhD Thesis*, University of Basel, Faculty of Science 1-170 (2007).

8. Ohta, N., Swanson, E., Ely, B. & Newton, A. Physical mapping and complementation analysis of transposon Tn5 mutations in *Caulobacter crescentus*: Organization of transcriptional units in the hook gene cluster. *Journal of Bacteriology* **158**, 897–904 (1984).

Supplementary Figure and Legends

Supplementary Figure S1: Multiple alignment and phylogenetic tree of response regulators.

(A) Alignment of the sequences of the 5 response regulators of *C. crescentus* forming a subfamily in comparison with CheY of *E. coli* (CheY_E). Underlined aa indicate the additional homologues region of 29 aa adjacent to the receiver domain. A star above the aa mark the active site residues and the phosphorylation site is indicated by an arrow[2]. A dot below the aa of CheY_E indicate the interaction site with FliM[3].

(B) The phylogenetic tree based on the receiver domains of all RR of *C. crescentus*. CheY and OmpR family type response regulators are indicated.

Supplementary Figure S2: CC3100 is not involved in susceptibility to phages, synchronizability or attachment.

CC3100 was expressed from a xylose inducible low copy plasmid in a ΔCC3100 deletion mutant. A wild-type and a *CC3100* deletion strain containing the empty plasmid (vc) were used as controls. The strains were tested without and with induction by adding 0.1 % xylose.

(A) The susceptibility towards phage ΦCBK that uses pili as a receptor was tested to confirm intact pili formation and flagellum rotation. The plaques correspond to 1:10 dilutions of the phage lysates.

(B) The S-layer of *C. crescentus* was accessible for phage ΦCR30. The plaques correspond to 1:10 dilutions of the phage lysates.

(C) The ability to separate swarmer cells (SW) and stalked cells (ST) in a cell density gradient centrifugation due to proper capsule formation is still retained.

(D) Attachment abilities of *pdeA* and *CC3100* single and double deletion mutants to polystyrene plates. Cells were grown for 24 hrs at 30°C in PYE and attached cells were stained with crystal violet.

Supplementary Figure S3: The C-terminally CC3100-GFP fusion protein is expressed and complements the phenotype of a *CC3100* deletion mutant.

(A) The deletion of *CC3100* causes an increase of the swarm size on semi-solid agar plates. A *pdeA* strain is reduced in size whereas an additional deletion of *CC3100* leads to increase of the swarm size to WT levels. The expression of the CC3100-GFP fusion protein from a vanillate inducible promoter in the different deletion mutants complemented the corresponding phenotypes. The WT and the corresponding deletion strains containing the GFP expressing plasmid (pGFP) were used as controls. The strains were tested without and with induction in the presence of 1 mM vanillate.

(B) α-CC3100 immunoblot to detect expression of the CC3100-GFP fusion protein. The upper band corresponds to levels of the GFP fusion protein and the lower band to the chromosomally native CC3100 protein. The WT and the corresponding deletion strains containing the GFP expressing plasmid were used as controls. The strains were induced with 1 mM vanillate.

Supplementary Figure S4: CC3100 localizes in *motA*, *fliG* and *flbD* deletion strains.

(A) CC3100-GFP forms foci at the poles in a strain that harbors a deletion of the gene coding for the stator protein MotA.

(B) The deletion of the motor switch protein FliG did not abrogate CC3100 localization (indicated by an arrow), however the foci showed a decreased fluorescence intensity.

(C) Polar CC3100 localization was detectable in a *flbD* deletion strain.

Supplementary Figure S5: CC3100 does not interact with MotA or MotB in a bacterial two hybrid assay.

Fusions between CC3100, MotA, MotB and two complementary fragments, T25 and T18, that constitute the catalytic domain of *Bordetella pertussis* adenylate cyclase, were generated in diverse combinations to test for cAMP production on maltose MacConkey agar plates. The combinations used are indicated in the squared box. The two positive controls included formed red colonies when streaked for single colonies; Left rectangle: Interaction between two zipper domains. Right rectangle: Interaction between MotA and MotB.

Figure S1A

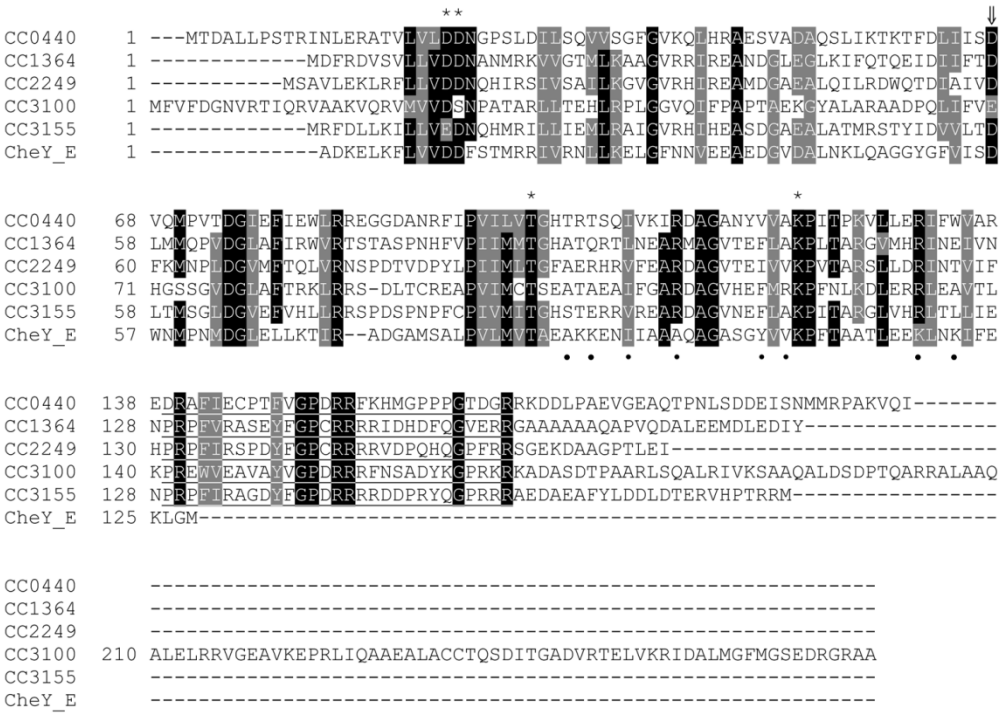

Figure S1B

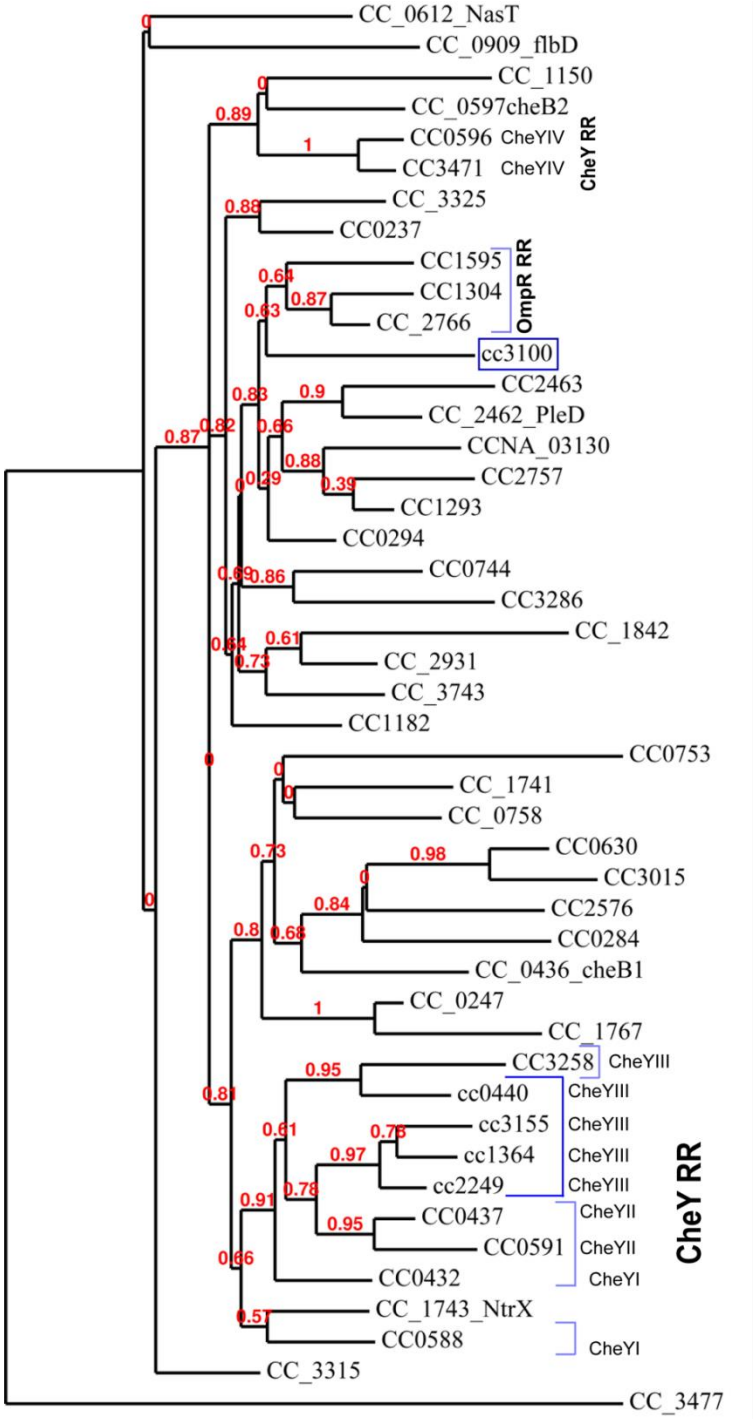
CC_0612_NasT
CC_0909_flbD
CC_1150
CC_0597cheB2
CC0596 CheYIV
CC3471 CheYIV
CheY RR
CC_3325
CC0237
CC1595
CC1304
CC_2766
OmpR RR
cc3100
CC2463
CC_2462_PleD
CCNA_03130
CC2757
CC1293
CC0294
CC0744
CC3286
CC_1842
CC_2931
CC_3743
CC1182
CC0753
CC_1741
CC_0758
CC0630
CC3015
CC2576
CC0284
CC_0436_cheB1
CC_0247
CC_1767
CC3258 CheYIII
cc0440 CheYIII
cc3155 CheYIII
cc1364 CheYIII
cc2249 CheYIII
CC0437 CheYII
CC0591 CheYII
CC0432 CheYI
CC_1743_NtrX
CC0588 CheYI
CheY RR
CC_3315
CC_3477

Figure S2

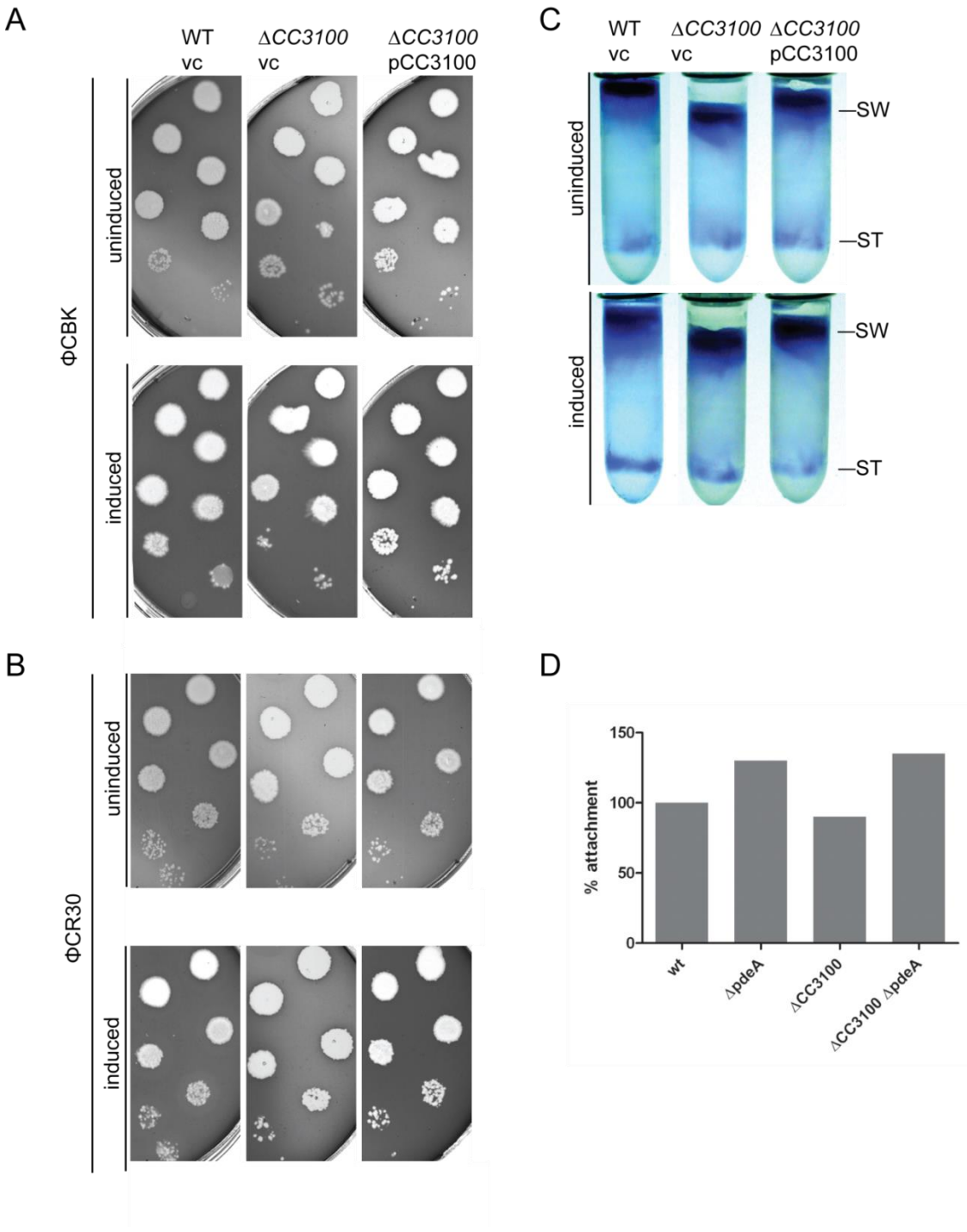
A
WT
vc
ΔCC3100
vc
ΔCC3100
pCC3100
uninduced
induced
ΦCBK
B
uninduced
induced
ΦCR30
C
WT
vc
ΔCC3100
vc
ΔCC3100
pCC3100
uninduced
induced
SW
ST
SW
ST
D
% attachment
150
100
50
0
wt
ΔpdeA
ΔCC3100
ΔCC3100 ΔpdeA

Figure S3

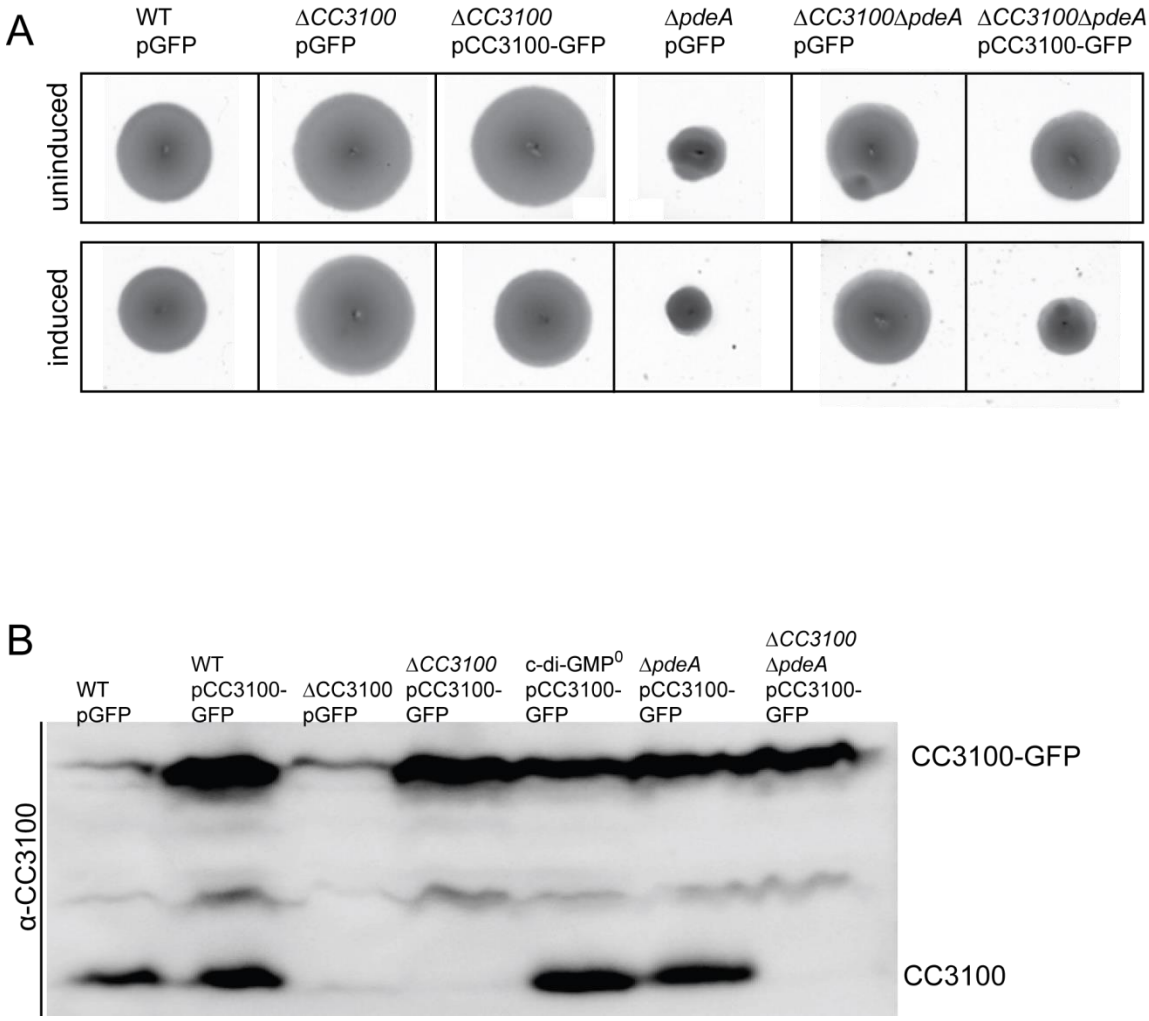
A
WT pGFP
ΔCC3100 pGFP
ΔCC3100 pCC3100-GFP
ΔpdeA pGFP
ΔCC3100ΔpdeA pGFP
ΔCC3100ΔpdeA pCC3100-GFP
uninduced
induced
B
WT pGFP
WT pCC3100-GFP
ΔCC3100 pGFP
ΔCC3100 pCC3100-GFP
c-di-GMP0 pCC3100-GFP
ΔpdeA pCC3100-GFP
ΔCC3100 ΔpdeA pCC3100-GFP
α-CC3100
CC3100-GFP
CC3100

Figure S4

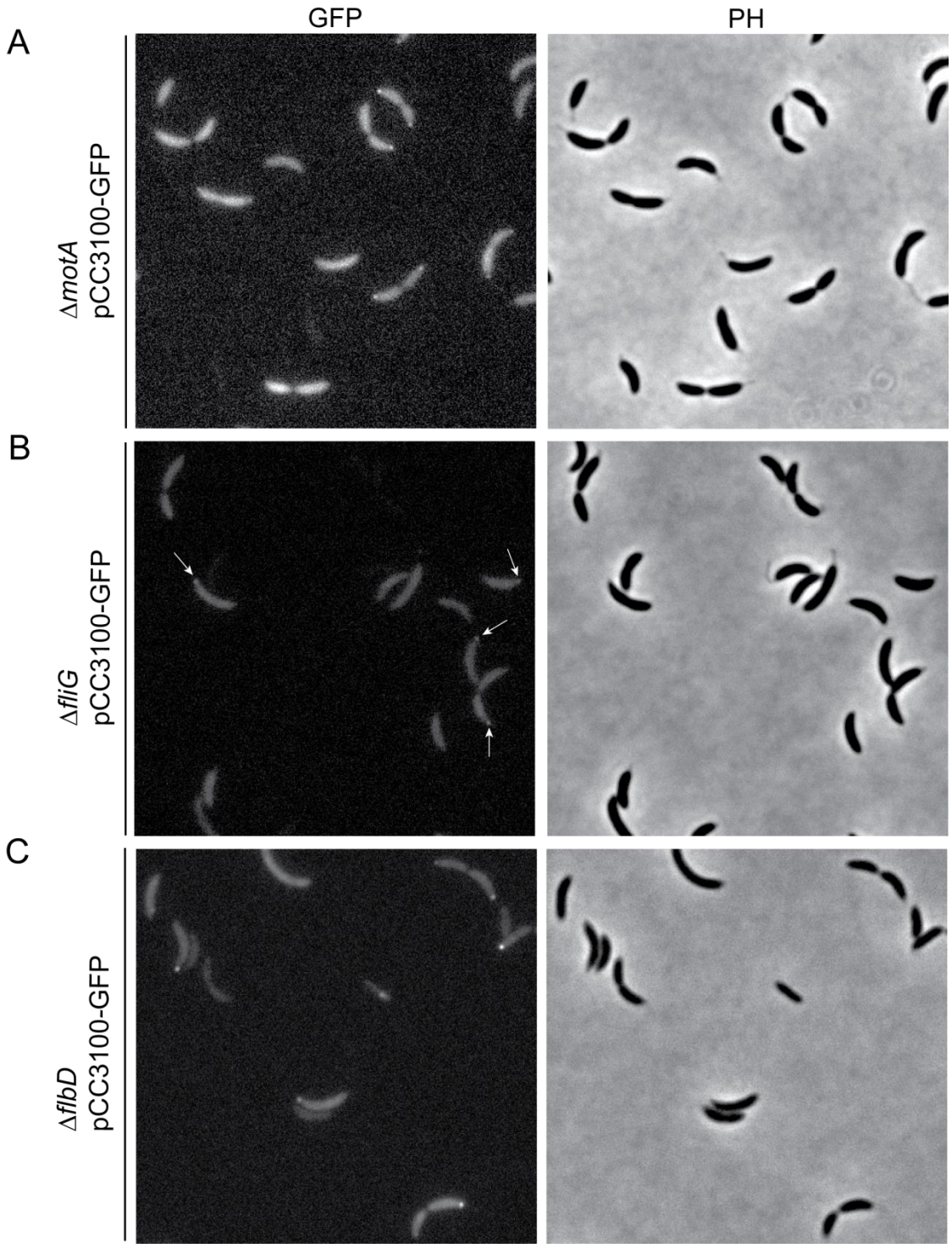
GFP
PH
A
ΔmotA pCC3100-GFP
B
ΔfliG pCC3100-GFP
C
ΔflbD pCC3100-GFP

Figure S5

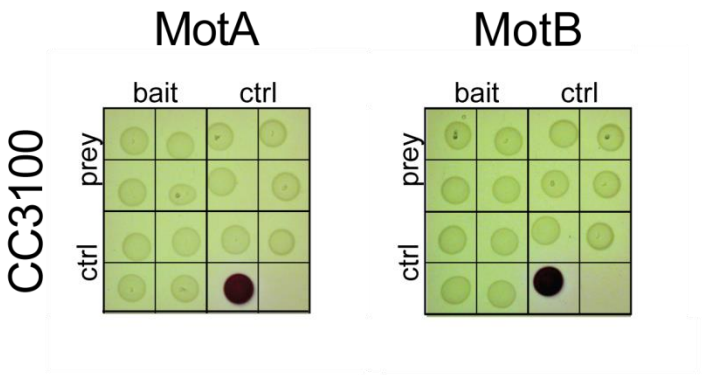

	II		Ctrl I	
I	pKT25-I pUT18-II	pKT25-I pUT18C-II	pKT25-I pUT18	pKT25-I pUT18C
	pKT25-II pUT18-I	pKT25-II pUT18C-I	pKT25 pUT18-I	pKT25 pUT18C-I
Ctrl II	pKT25-II pUT18	pKT25-II pUT18C	pKT25 pUT18	pKT25 pUT18C
	pKT25 pUT18-II	pKT25 pUT18C-II	zip zip	empty

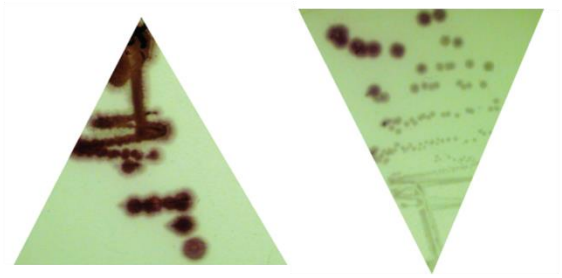

Supplementary Table S1: Strains used in this study

Name	Genotype and description	Reference
	E. coli strains	
AB1768	Δ*cya*::FrT; standard strain for bacterial two-hybrid	[4]
	C. crescentus strains	
CB15	*C. crescentus* wild-type ATCC 19089 *Caulobacter vibrioides* LOT:3967454	
UJ4467	CB15 Δ*pdeA*; Markerless in frame deletion of *pdeA* in CB15	[5]
UJ5692	CB15 Δ*CC3100*; Markerless in frame deletion of *CC3100* in CB15	This work
UJ5831	CB15 Δ*pdeA* Δ*CC3100*, Markerless in frame deletion of *CC3100* and *pdeA* in CB15	This work
LS2356	NA1000 Δ*fliG*	[6]
UJ2591	CB15 *motA::Tn5*	[7]
LS485	SC1032 *flbD198*::Tn5	[8]

Supplementary Table S2: Plasmids used in this study

Name	Description	Oligos used for cloning	Reference or Source
pKT25	P_{lac} T25 Kan^R,pSU40 derivative, used for fusions to the C-terminus of the T25 fragment of CyaA		[1]
pKT25-zip	pKT25 derivative with T25 fused to leucine zipper of GCN4		[1]
pUT18	P_{lac} T18 Amp^R, pUC19 derivative, used for fusions to the N-terminus of the T18 fragment of CyaA		[1]
pUT18c	pUC19 derivative, used for fusions to the C-terminus of the T18 fragment of CyaA		[1]
pUT18-zip	pUT18C derivative with T18 fused to leucine zipper of GCN4		[1]
pKT25-CC3100	pKT25, BamHI-CC3100-EcoRI	4438 and 4439	This study
pUT18c-CC3100	pUT18c; BamHI-CC3100-EcoRI (815 bp fragment from pKT25_CC3100)		This study
pKT25_motA	pKT25::*motA*		Sören Abel
pUT18_motA	pUT18::*motA*		Sören Abel
pUT18c_motA	pUT18c::*motA*		Sören Abel
pkT25_motB	pKT25::*motB*		Sören Abel
pUT18_motB	pUT18::*motB*		Sören Abel
pUT18c_motB	pUT18c::*motB*		Sören Abel

Supplementary Table S3: Oligonucleotides used in this study

Oligo	Sequence[1]	Description
4438	TAGAGGATCCGTTCGTGTTTGACGGCAACGT	for cloning into pKT25
4439	AAGAATTCCTAGGCCGCGCGCCCCCGGT	for cloning into pKT25

[1]Restriction sites are underlined

4 Bibliography

1. Camilli, A. & Bassler, B. L. Bacterial small-molecule signaling pathways. *Science* **311**, 1113–1116 (2006).

2. Hogg, T., Mechold, U., Malke, H., Cashel, M. & Hilgenfeld, R. Conformational antagonism between opposing active sites in a bifunctional RelA/SpoT homolog modulates (p)ppGpp metabolism during the stringent response. *Cell* **117**, 57–68 (2004).

3. Mechold, U., Murphy, H., Brown, L. & Cashel, M. Intramolecular regulation of the opposing (p)ppGpp catalytic activities of Rel(Seq), the Rel/Spo enzyme from *Streptococcus equisimilis*. *Journal of Bacteriology* **184**, 2878–2888 (2002).

4. Potrykus, K. & Cashel, M. (p)ppGpp: still magical? *Annual Review of Microbiology* **62**, 35–51 (2008).

5. Robison, G. A., Butcher, R. W. & Sutherland, E. W. Cyclic AMP. *Annual Review of Biochemistry* **37**, 149–174 (1968).

6. Zubay, G., Schwartz, D. & Beckwith, J. Mechanism of activation of catabolite-sensitive genes: a positive control system. *Proceedings of the National Academy of Sciences* **66**, 104–110 (1970).

7. Kim, Y. R., Kim, S. Y., Kim, C. M., Lee, S. E. & Rhee, J. H. Essential role of an adenylate cyclase in regulating *Vibrio vulnificus* virulence. *FEMS Microbiology Letters* **243**, 497–503 (2005).

8. Botsford, J. L. & Harman, J. G. Cyclic AMP in prokaryotes. *Microbiological Reviews* **56**, 100–122 (1992).

9. Ochoa De Alda, J. A., Ajlani, G. & Houmard, J. *Synechocystis* strain PCC 6803 cya2, a prokaryotic gene that encodes a guanylyl cyclase. *Journal of Bacteriology* **182**, 3839–3842 (2000).

10. Cadoret, J.-C. *et al.* Cyclic nucleotides, the photosynthetic apparatus and response to a UV-B stress in the *Cyanobacterium Synechocystis* sp. PCC 6803. *Journal of Biological Chemistry* **280**, 33935–33944 (2005).

11. Marden, J. N., Dong, Q., Roychowdhury, S., Berleman, J. E. & Bauer, C. E. Cyclic GMP controls *Rhodospirillum centenum* cyst development. *Molecular Microbiology* **79**, 600–615 (2011).

12. Galperin, M. Y., Nikolskaya, a N. & Koonin, E. V. Novel domains of the prokaryotic two-component signal transduction systems. *FEMS Microbiology Letters* **203**, 11–21 (2001).

13. Schirmer, T. & Jenal, U. Structural and mechanistic determinants of c-di-GMP signalling. *Nature Reviews. Microbiology* **7**, 724–735 (2009).

14. Tal, R. *et al.* Three cdg operons control cellular turnover of cyclic di-GMP in *Acetobacter xylinum*: genetic organization and occurrence of conserved domains in isoenzymes. *Journal of Bacteriology* **180**, 4416–4425 (1998).

15. Ausmees, N. *et al.* Genetic data indicate that proteins containing the GGDEF domain possess diguanylate cyclase activity. *FEMS Microbiology Letters* **204**, 163–167 (2001).

16. Tarutina, M., Ryjenkov, D. a & Gomelsky, M. An unorthodox bacteriophytochrome from *Rhodobacter sphaeroides* involved in turnover of the second messenger c-di-GMP. *Journal of Biological Chemistry* **281**, 34751–8 (2006).

17. Jenal, U. & Malone, J. Mechanisms of cyclic-di-GMP signaling in bacteria. *Annual Review of Genetics* **40**, 385–407 (2006).

18. Boehm, A. *et al.* Second messenger signalling governs *Escherichia coli* biofilm induction upon ribosomal stress. *Molecular Microbiology* **72**, 1500–1516 (2009).

19. Malone, J. G. *et al.* YfiBNR mediates cyclic di-GMP dependent small colony variant formation and persistence in *Pseudomonas aeruginosa*. *PLoS Pathogens* **6**, e1000804 (2010).

20. Ouyang, S. *et al.* Structural Analysis of the STING Adaptor Protein Reveals a Hydrophobic Dimer Interface and Mode of Cyclic di-GMP Binding. *Immunity* **379**, 1–14 (2012).

21. Burdette, D. L. *et al.* STING is a direct innate immune sensor of cyclic di-GMP. *Nature* **478**, 515–518 (2011).

22. Römling, U. Great times for small molecules: c-di-AMP, a second messenger candidate in Bacteria and Archaea. *Science Signaling* **1**, pe39 (2008).

23. Woodward, J. J., Iavarone, A. T. & Portnoy, D. a c-di-AMP secreted by intracellular *Listeria monocytogenes* activates a host type I interferon response. *Science* **328**, 1703–1705 (2010).

24. Ryjenkov, D. A., Tarutina, M., Moskvin, O. V. & Gomelsky, M. Cyclic diguanylate is a ubiquitous signaling molecule in bacteria: insights into biochemistry of the GGDEF protein domain. *Journal of Bacteriology* **187**, 1792–1798 (2005).

25. De, N., Navarro, M. V. a S., Raghavan, R. V. & Sondermann, H. Determinants for the activation and autoinhibition of the diguanylate cyclase response regulator WspR. *Journal of Molecular Biology* **393**, 619–633 (2009).

26. Christen, M., Christen, B., Folcher, M., Schauerte, A. & Jenal, U. Identification and characterization of a cyclic di-GMP-specific phosphodiesterase and its allosteric control by GTP. *Journal of Biological Chemistry* **280**, 30829–30837 (2005).

27. Paul, R. *et al.* Cell cycle-dependent dynamic localization of a bacterial response regulator with a novel di-guanylate cyclase output domain. *Genes & Development* **18**, 715–727 (2004).

28. Pei, J. & Grishin, N. V. GGDEF domain is homologous to adenylyl cyclase. *Proteins* **42**, 210–216 (2001).

29. Sinha, S. C. & Sprang, S. R. Structures, mechanism, regulation and evolution of class III nucleotidyl cyclases. *Reviews of Physiology, Biochemistry and Pharmacology* **157**, 105–140 (2006).

30. Hengge, R. Cyclic-di-GMP reaches out into the bacterial RNA world. *Science Signaling* **3**, e44 (2010).

31. Merkel, T. J., Barros, C. & Stibitz, S. Characterization of the bvgR locus of *Bordetella pertussis*. *Journal of Bacteriology* **180**, 1682–1690 (1998).

32. Schmidt, A. J., Ryjenkov, D. A. & Gomelsky, M. The ubiquitous protein domain EAL is a cyclic diguanylate-specific phosphodiesterase: enzymatically active and inactive EAL domains. *Journal of Bacteriology* **187**, 4774–4781 (2005).

33. Minasov, G. *et al.* Crystal structures of YkuI and its complex with second messenger cyclic Di-GMP suggest catalytic mechanism of phosphodiester bond cleavage by EAL domains. *Journal of Biological Chemistry* **284**, 13174–13184 (2009).

34. Barends, T. R. M. *et al.* Structure and mechanism of a bacterial light-regulated cyclic nucleotide phosphodiesterase. *Nature* **459**, 1015–1018 (2009).

35. Rood, K. L., Clark, N. E., Stoddard, P. R., Garman, S. C. & Chien, P. Adaptor-dependent degradation of a cell-cycle regulator uses a unique substrate architecture. *Structure* **20**, 1223–1232 (2012).

36. Ryan, R. P. *et al.* Cell-cell signaling in *Xanthomonas campestris* involves an HD-GYP domain protein that functions in cyclic di-GMP turnover. *Proceedings of the National Academy of Sciences of the United States of America* **103**, 6712–6717 (2006).

37. Lovering, A. L., Capeness, M. J., Lambert, C., Hobley, L. & Sockett, R. E. The structure of an unconventional HD-GYP protein from *Bdellovibrio* reveals the roles of conserved residues in this class of cyclic-di-GMP phosphodiesterases. *mBio* **2**, (2011).

38. Baraquet, C., Murakami, K., Parsek, M. R. & Harwood, C. S. The FleQ protein from *Pseudomonas aeruginosa* functions as both a repressor and an activator to control gene expression from the pel operon promoter in response to c-di-GMP. *Nucleic Acids Research* 1–12 (2012).

39. Sudarsan, N. *et al.* Riboswitches in eubacteria sense the second messenger cyclic di-GMP. *Science* **321**, 411–413 (2008).

40. Boehm, A. *et al.* Second messenger-mediated adjustment of bacterial swimming velocity. *Cell* **141**, 107–116 (2010).

41. Lee, V. T. *et al.* A cyclic-di-GMP receptor required for bacterial exopolysaccharide production. *Molecular Microbiology* **65**, 1474–1484 (2007).

42. Newell, P. D., Boyd, C. D., Sondermann, H. & O'Toole, G. A c-di-GMP effector system controls cell adhesion by inside-out signaling and surface protein cleavage. *PLoS Biology* **9**, e1000587 (2011).

43. Amikam, D. & Galperin, M. Y. PilZ domain is part of the bacterial c-di-GMP binding protein. *Bioinformatics* **22**, 3–6 (2006).

44. Habazettl, J., Allan, M. G., Jenal, U. & Grzesiek, S. Solution structure of the PilZ domain protein PA4608 complex with cyclic di-GMP identifies charge clustering as molecular readout. *Journal of Biological Chemistry* **286**, 14304–14314 (2011).

45. Christen, M. *et al.* DgrA is a member of a new family of cyclic diguanosine monophosphate receptors and controls flagellar motor function in *Caulobacter crescentus. Proceedings of the National Academy of Sciences* **104**, 4112–4117 (2007).

46. Duerig, A. *et al.* Second messenger-mediated spatiotemporal control of protein degradation regulates bacterial cell cycle progression. *Genes & Development* **23**, 93–104 (2009).

47. Navarro, M. V. A. S., De, N., Bae, N., Wang, Q. & Sondermann, H. Structural analysis of the GGDEF-EAL domain-containing c-di-GMP receptor FimX. *Structure* **17**, 1104–16 (2009).

48. Kazmierczak, B. I., Lebron, M. B. & Murray, T. S. Analysis of FimX, a phosphodiesterase that governs twitching motility in *Pseudomonas aeruginosa*. *Molecular Microbiology* **60**, 1026–1043 (2006).

49. Newell, P. D., Monds, R. D. & O'Toole, G. A. LapD is a bis-(3',5')-cyclic dimeric GMP-binding protein that regulates surface attachment by *Pseudomonas fluorescens* Pf0-1. *Proceedings of the National Academy of Sciences* **106**, 3461–3466 (2009).

50. Navarro, M. V. a S. *et al.* Structural basis for c-di-GMP-mediated inside-out signaling controlling periplasmic proteolysis. *PLoS Biology* **9**, e1000588 (2011).

51. Mettke, I., Fiedler, U. & Weiss, V. Mechanism of activation of a response regulator: interaction of NtrC-P dimers induces ATPase activity. *Journal of Bacteriology* **177**, 5056–61 (1995).

52. Arora, S. K., Ritchings, B. W., Almira, E. C., Lory, S. & Ramphal, R. A transcriptional activator, FleQ, regulates mucin adhesion and flagellar gene expression in *Pseudomonas aeruginosa* in a cascade manner. *Journal of Bacteriology* **179**, 5574–5581 (1997).

53. Hickman, J. W. & Harwood, C. S. Identification of FleQ from *Pseudomonas aeruginosa* as a c-di-GMP-responsive transcription factor. *Molecular Microbiology* **69**, 376–389 (2008).

54. Poindexter, J. S. The *Caulobacters*: ubiquitous unusual bacteria. *Microbiological Reviews* **45**, 123–179 (1981).

55. Merker, R. I. & Smit, J. Characterization of the adhesive holdfast of marine and freshwater *Caulobacters*. *Applied and Environmental Microbiology* **54**, 2078–2085 (1988).

56. Levi, A. & Jenal, U. Holdfast formation in motile swarmer cells optimizes surface attachment during Caulobacter crescentus development. *Journal of Bacteriology* **188**, 5315–5318 (2006).

57. Marczynski, G. T. Chromosome methylation and measurement of faithful, once and only once per cell cycle chromosome replication in *Caulobacter crescentus*. *Journal of Bacteriology* **181**, 1984–1993 (1999).

58. Cooper, S. & Helmstetter, C. E. Chromosome replication and the division cycle of *Escherichia coli*. *Journal of Molecular Biology* **31**, 519–540 (1968).

59. Ackermann, M., Stearns, S. C. & Jenal, U. Senescence in a bacterium with asymmetric division. *Science* **300**, 1920 (2003).

60. Ackermann, M., Schauerte, A., Stearns, S. C. & Jenal, U. Experimental evolution of aging in a bacterium. *BMC Evolutionary Biology* **7**, 126 (2007).

61. Jacobs-Wagner, C. Regulatory proteins with a sense of direction: cell cycle signalling network in *Caulobacter*. *Molecular Microbiology* **51**, 7–13 (2004).

62. Abel, S. *et al.* Regulatory cohesion of cell cycle and cell differentiation through interlinked phosphorylation and second messenger networks. *Molecular Cell* **43**, 550–560 (2011).

63. Laub, M. T., Chen, S. L., Shapiro, L. & McAdams, H. H. Genes directly controlled by CtrA, a master regulator of the *Caulobacter* cell cycle. *Proceedings of the National Academy of Sciences* **99**, 4632–4637 (2002).

64. Curtis, P. D. & Brun, Y. V. Getting in the loop: regulation of development in *Caulobacter crescentus*. *Microbiology and Molecular Biology Reviews* **74**, 13–41 (2010).

65. Domian, I. J., Quon, K. C. & Shapiro, L. Cell type-specific phosphorylation and proteolysis of a transcriptional regulator controls the G1-to-S transition in a bacterial cell cycle. *Cell* **90**, 415–424 (1997).

66. Jenal, U. The role of proteolysis in the *Caulobacter crescentus* cell cycle and development. *Research in Microbiology* **160**, 687–695 (2009).

67. Biondi, E. G. *et al.* Regulation of the bacterial cell cycle by an integrated genetic circuit. *Nature* **444**, 899–904 (2006).

68. Solano, C. *et al.* Genetic reductionist approach for dissecting individual roles of GGDEF proteins within the c-di-GMP signaling network in *Salmonella*. *Proceedings of the National Academy of Sciences* **106**, 7997–8002 (2009).

69. Bucher, T. C-di-GMP is a key regulator of *Caulobacter crescentus* flagellum biosynthesis. *Master Thesis, University of Basel, Faculty of Science* (2011).

70. Nicollier, M. The influence of the bacterial second messenger c-di-GMP on cell cycle and pole development in *Caulobacter crescentus*. *Master Thesis, University of Basel, Faculty of Science* (2009).

71. Levi, A., Folcher, M., Jenal, U. & Shuman, H. A. Cyclic diguanylate signaling proteins control intracellular growth of *Legionella pneumophila*. *mBio* **2**, e00316–10 (2011).

72. Huitema, E., Pritchard, S., Matteson, D., Radhakrishnan, S. K. & Viollier, P. H. Bacterial birth scar proteins mark future flagellum assembly site. *Cell* **124**, 1025–1037 (2006).

73. Abel, S. & Jenal, U. The role of cyclic di-GMP in *Caulobacter crescentus* development and cell cycle control. *ASM books* **9**, 1–35 (2009).

74. Ferreira, R. B. R., Antunes, L. C. M., Greenberg, E. P. & McCarter, L. L. *Vibrio parahaemolyticus* ScrC modulates cyclic dimeric GMP regulation of gene expression relevant to growth on surfaces. *Journal of Bacteriology* **190**, 851–860 (2008).

75. Bharati, B. K. *et al.* A full length bifunctional protein involved in c-di-GMP turnover is required for long term survival under nutrient starvation in *Mycobacterium smegmatis*. *Microbiology* 1-31 (2012).

76. Gupta, K., Kumar, P. & Chatterji, D. Identification, activity and disulfide connectivity of C-di-GMP regulating proteins in *Mycobacterium tuberculosis. PloS One* **5**, e15072 (2010).

77. Levet-Paulo, M. *et al.* The atypical two-component sensor kinase Lpl0330 from *Legionella pneumophila* controls the bifunctional diguanylate cyclase-phosphodiesterase Lpl0329 to modulate bis-(3'-5')-cyclic dimeric GMP synthesis. *Journal of Biological Chemistry* **286**, 31136–31144 (2011).

78. Suzuki, K., Babitzke, P., Kushner, S. R. & Romeo, T. Identification of a novel regulatory protein (CsrD) that targets the global regulatory RNAs CsrB and CsrC for degradation by RNase E. *Genes & Development* **20**, 2605–2617 (2006).

79. Hazelbauer, G. L., Falke, J. J. & Parkinson, J. S. Bacterial chemoreceptors: high-performance signaling in networked arrays. *Trends in Biochemical Sciences* **33**, 9–19 (2008).

80. Kentner, D. & Sourjik, V. Dynamic map of protein interactions in the *Escherichia coli* chemotaxis pathway. *Molecular Systems Biology* **5**, (2009).

81. Blair, K. M., Turner, L., Winkelman, J. T., Berg, H. C. & Kearns, D. B. A molecular clutch disables flagella in the Bacillus subtilis biofilm. *Science* **320**, 1636–8 (2008).

82. Brown, M. T., Delalez, N. J. & Armitage, J. P. Protein dynamics and mechanisms controlling the rotational behaviour of the bacterial flagellar motor. *Current Opinion in Microbiology* **14**, 734–740 (2011).

83. Pilizota, T. *et al.* A molecular brake, not a clutch, stops the *Rhodobacter sphaeroides* flagellar motor. *Proceedings of the National Academy of Sciences* **106**, 11582–11587 (2009).

84. Amsler, C. D., Cho, M. & Matsumura, P. Multiple factors underlying the maximum motility of *Escherichia coli* as cultures enter post-exponential growth. *Journal of Bacteriology* **175**, 6238–6244 (1993).

85. Ryjenkov, D. a, Simm, R., Römling, U. & Gomelsky, M. The PilZ domain is a receptor for the second messenger c-di-GMP: the PilZ domain protein YcgR controls motility in enterobacteria. *The Journal of Biological Chemistry* **281**, 30310–30314 (2006).

5 Curriculum Vitae

Contact Information

Name:	Elvira Friedrich
Contact:	Winkelriedstrasse 58
	CH-6003 Lucerne
Nationality:	German

Education

09/2008 – 09/2012	PhD in Microbiology/Biochemistry in the lab of Prof. Urs Jenal, Biozentrum Basel, Switzerland
10/2002 – 03/2008	Study of Chemistry at the Albert-Ludwigs-University of Freiburg, Germany Emphasis on Biochemistry Diploma thesis topic: On the role of the [Fe-S]-cluster N1a from *Escherichia coli* complex I (NADH:Ubiquinone Oxido-reductase) for its mechanism
09/1993 – 06/2002	Abitur at the Hochrhein-Gymnasium Waldshut, Germany Focus subjects: Chemistry, English

Scholarship

10/2005 - 02/2006	SOKRATES (education program of the European Union), University of East Anglia, Norwich, England

Additional Activities

05/2011 – 09/2012	PhD Representative at the Biozentrum Basel
10/2007 – 02/2008	Work as a tutor for the lecture “Organic Chemistry I” for chemists
09/2006 – 02/2007	Voluntary tuition for pupils with learning disability
02/2005 – 04/2005	Supervision for the chemical laboratory for biologists, physicists and geologists

Skills

Workshop:	Intervision for cooperative coaching
Computer	MS-Office 2010, Adobe Illustrator CS3, Adobe Photoshop CS3
Language	German (native), English (fluent), French (basic), Russian (good)

6 Acknowledgments

I would like to express my gratitude to all those who gave me the possibility to complete this thesis.

In the first place, I want to thank Prof. Urs Jenal, my supervisor, for giving me as chemist the opportunity to work on an exciting biological research project and for lots of very fruitful scientific discussions in our biweekly meetings. I also want to thank my PhD committee, Prof. Tilman Schirmer and Prof. Christoph Dehio for their interest in my work and for scientific advices not only during the annual PhD meetings.

I want furthermore to thank Dr. Claudia Massa and Dr. Jutta Nesper with whom I share parts of the manuscript for their help, advice and collaboration.

I would like to give my special thanks to Fabienne Hamburger for her help in cloning and thousands other things, that made my lab life easier and who always had something sweet for me.

I wish to thank my colleagues from the Microbiology Department of the Biozentrum in Basel who supported me in my research work by providing a very nice working atmosphere and gave me input for my thesis: Sören Abel for his great ideas regarding my project and his proof-reading of the manuscript from across the ocean, Imke de Jong for her endless help at the microscope and providing me a sleeping place whenever it got late in Basel, Tina Jäger for always giving me a good advice and for her proof-reading, Alberto Reinders and Raphael Boos for helping me whenever I had problems with my PC, Lucie Hosch for going with me to the gym, Samuel Steiner for working next to me and sharing scientific ideas, Christian Lori for his M&Ms, Benoit-Joseph Laventie for sharing his office bench with me, Annina Moser for having nice chats, Marco Lüthi, Isabelle Hug, Kathrin Sprecher, Shogo Ozaki, Ursula Broder, Janiv Cohen and Antje Hempel.

Franziska Zähringer I want to thank for her biochemical advice and sharing good and bad news at the very important 3 pm meetings and for her encouraging and catching laugh.

Nicht zuletzt und besonders herzlich möchte ich mich bei meinen Eltern Lydia und Artur Friedrich bedanken, die mich mein Leben lang in jeder Situation liebevoll unterstütz haben.

Meiner Schwester Olga und meinem Schwager Tobias Tröndle danke ich für ihre Freundschaft und ihre uneingeschränkte Hilfsbereitschaft.

Zudem möchte ich Brigitte und Wolfgang Bodien danken, die mich so manches Wochenende fürsorglich aufgenommen haben und auf die ich mich immer verlassen konnte.

Der Schluss der Arbeit gehört dem Menschen, dem ich am meisten danken möchte. Jemand, der mit mir durch alle Phasen meiner Promotion gehen musste, der mich aufgebaut und motiviert hat, der mir niemals seine Hilfe entzogen hat und auf dessen Liebe ich immer bauen konnte. Mein besonderer Dank gilt dir, Volker Bodien.